Measurement, Control and Enhancement of Friction/Traction in a Simulated Wheel/Rail Contact

Stephen Robert Lewis

July 2011

Thesis submitted for the Degree of Doctor of Philosophy

Department of Mechanical Engineering
University of Sheffield

Measurement, Control and Enhancement of Friction/Traction in a Simulated Wheel/Rail Contact

Stephen Robert Lewis

Summary

The focus on rail transportation has shifted in recent years to be a viable alternative to road based means of travel and freight distribution. With a finite stockpile of the world's natural hydrocarbon based fuels and ever increasing road congestion, rail research has become a prime topic of late. In this thesis the focus has been upon the wheel/rail contact and the measurement of railhead friction.

The initial project was the development of an alternative technique to measure railhead friction. Adhesion loss is a major problem on railways around the world and is common during the autumn, at times for no obvious reason. Currently there are hand-pushed Tribometers which are used by rail networks to periodically measure and record friction on their rails. These devices however, are large bulky items and due to their design can only measure friction over a relatively large distance. However, most adhesion loss problems are caused by localised phenomena. A pendulum tester was chosen as a potentially viable alternative to the Tribometer as it could measure over shorter lengths of track (i.e. 13 cm compared to 3 m as in the case of the Salient Systems Tribometer). The pendulum is also relatively small and hence is convenient to transport. After a series of laboratory and field based tests the pendulum has been shown to match very well with Tribometer and twin-disc data.

Friction modifiers are commonly used on railways around the world and are promoted to have many benefits such as reduced fuel consumption, reduced wear and damage to wheels and rails and reductions in operating noise. These products have been adopted in many different countries. It was noticed in the literature that very little study had been done on how the performance of these products is affected by varying atmospheric conditions or levels of railhead contamination. Another aspect of this thesis has been the measurement of one of the leading brands of top of rail friction modifier using a pin-on-disc tester with attached atmospheric chamber. It was found that humidity and the presence of iron oxide have a far greater effect on the friction modifier than temperature.

In the final two chapters a study was carried out to measure the performance of traction enhancing products. These are intended to restore traction in cases of adhesion loss from, for example, leaves on the line. It is critical that correct levels of adhesion/traction are maintained for braking and acceleration purposes. A twin-disc tester was used in this study and a technique for forming a crushed leaf layer on the discs was developed. The traction enhancers consist of sand particles of uniform size suspended in a water based gel. There were four products tested each using a different sand grain size. The first series of tests measured the performance of each product in terms of traction compared to that of a leaf layer alone. It was found that the smaller particles showed the best performance by restoring the traction to uncontaminated levels in the shortest time. The second series of tests focused on the impact these products had on wheel and rail wear and track signalling. Wear was also measured in terms of mass lost from the discs. An A.C. circuit operating at 2 kHz was used to simulate a TI21 track circuit which is used in the UK as part of the signalling system. Impedance caused by each product was measured and compared to impedance levels for uncontaminated discs. It was found that the impedance of a leaf layer plus the product was lower than the impedance of the leaf layer alone. There also seemed to be no correlation between particle size and impedance. The impedance levels seen with the products were not deemed to be enough to cause a significant issue to the signalling system.

Contents

Abbreviations

Abbreviation	Meaning	Units
AC	Alternating Current	Amperes
C	Capacitance	Farads
CAE	Computer Aided Engineering	
CMC	Carboxymethylecelulose	
COF	Coefficient of Friction	
EDS	Energy-dispersive X-ray Spectroscopy	
EHL	Elastohydrodynamic Lubrication	
F	Tangential Force	Newton
F_T	Tractive Force	Newton
f	Frequency	Hertz
FM	Friction Modifiers	
GDOES	Glow Discharge Emission Spectroscopy	
HCFM	High Coefficient Friction Modifier	
HDL	Hydrodynamic Lubrication	
HPFM	High Positive Friction Modifier	
I	Current	Amperes
IRHD	International Rubber Hardness Degrees	
KTH	Royal Technical Institute, Stockholm, Sweden	
L	Inductance	Henry
LCFM	Low Coefficient Friction Modifier	
MPa	Mega Pascal's	
MPV	Multi Purpose Vehicle	
P	Normal Load	Newton
POD	Pin-on-disk	
R	Resistance	Ohms
R_a	Roughness Average	
RCF	Rolling Contact Fatigue	
RH	Relative Humidity	%
RPM	Revolutions Per Minute	
SEM	Scanning Electron Microscope	
SRV	Slip Resistance Value	
SUROS	Sheffield University Rolling Sliding Machine	
T	Torque	Newton Meter
TORFM	Top of Rail Friction Modifiers	
V	Body Velocity	Meters Per Second
V_T	Tangential Velocity	Meters Per Second
X	Reactance	Ohms
Z	Impedance	Ohms
μ	Coefficient of Friction	
μ_T	Traction Coefficient	

Acknowledgements

The author would like to express his thanks to Dr Roger Lewis for his unfaltering guidance and advice throughout this project. Thanks also to Professor Mark Rainforth for allowing access to the twin-disc rig which has formed a vital part of this thesis.

The author would also like to extend their gratitude towards Professor Ulf Olofsson for their accommodation and allowing access to specialist equipment.

Recognition also goes to Dave Butcher and Chris Grigson for their help on technical issues.

Finally I wish to express my gratitude to my parents John and Carol for their support and encouragement without which this project would not have been completed.

Chapter 1: Introduction

1.1 Statement of the Problem

Modern railways utilising diesel and electric locomotives differ from their steam powered equivalents in more than just their method of propulsion. New electrified trains are much lighter and faster, less maintenance intensive with wheels and rails constructed of vastly superior grades of steel. However, despite all this, railways have become subject to new problems. These range from adhesion loss to wheel and rail failure by fatigue. There are also less well understood phenomena such as corrugation, which plague the modern rail network. The rail system is also an open system which means it is not easily defended from sources of contamination such as rain water, oil, grease and leaves. Such seemingly insignificant substances can have considerable effects on the operation (in terms of performance and safety) and maintenance of today's rail network.

There are two problems which this thesis will deal with. One is the measurement and the other is the control of friction on the rail head and within the wheel/rail contact.

There are two methods by which friction at the wheel/rail contact/rail head can be studied. These are by using field or laboratory based measurements. Both of these techniques have their respective benefits. In the case of the field there are instrumented trains which can measure the friction/traction in the wheel/rail contact directly. Although this method offers the ultimate in terms of direct measurement of the wheel/rail contact there are obvious practicality issues. The alternative in terms of field measurement is the hand-pushed Tribometer which is widely used by railway maintenance personnel. Although this is not measuring the actual wheel/rail contact it offers a far better solution in terms of practicality and accuracy. The alternative to field testing is laboratory based testing. Laboratory tests generally offer greater controllability of test parameters than field tests at the sacrifice of representation of the actual wheel/rail contact. Such examples include twin-disc and pin-on-disc testing. Twin-disc testing offers one of the closest representations of the actual rolling/sliding contact. A pin-on-disc test, even though not an ideal representation, offers much more controllability. None of these tests can be transferred between lab and field and

hence cannot be directly compared with each other. There is therefore a call for a quick reliable measurement technique which can be used both in the lab and field.

Friction/traction at the wheel/rail contact is very rarely constant and can vary from dry levels, nominally 0.6, to below 0.1 [Nagase, 1989]. Low levels of friction cause significant safety issues concerning braking, and even signalling. Timetables can also be effected by low friction as trains cannot accelerate adequately and wheel spins also cause significant damage to both wheels and rails. Conversely, fiction levels which are too high can also cause problems in terms of wear, fuel consumption and noise. It is therefore beneficial to control the level of railhead friction within a defined range which is not too low as to affect braking, but low enough to achieve optimum fuel consumption and wear levels. This level is considered to be approximately 0.3-0.35 [Lu, 2005]. Top of rail friction modifiers (TORFM's) are designed to keep the friction within this range. TORFM's are commercially available in either liquid or solid form. The liquid product is usually delivered directly to the rail via a trackside pump. The solid version however is loaded against the wheels of the rail vehicle and thus transferred to the track. TORFM's can also promote other benefits such as reducing wear, fuel consumption and noise amongst others. Thus the definition of a friction modifier is not necessarily to reduce friction, but to control it within an optimum range. This differs from a lubricant where the main purpose is to reduce friction as low as possible. There have been many studies on friction modifiers and their influence on factors such as noise and wear/fatigue [Eadie, 2003 and Fletcher, 2000a]. However, there has been no such research into the effects of changes in atmospheric conditions upon the performance of friction modifiers. This seems an important issue as friction modifiers are used in different climates around the world. More so FM's are also being used in tunnels which can be subject to vastly different operating conditions than in the open air regardless of outside climate.

There are cases however, of extremely low friction on the railhead where a friction modifier may not be enough to solve the problem. These cases of extremely low adhesion occur mainly due to leaf fall on wet tracks. With friction levels below 0.1 this represents a significant safety hazard not just in terms of braking, but also in terms of signalling. This is because leaves can cause significant obstruction to the flow of electrical current. As signalling systems work on electrical circuits, this can be a major problem. A track circuit, as shown in Figure 1, is typical of many signalling circuits used throughout the world. Lengths

of track will be divided into isolated sections each with their own track circuit. When a section of track is free 100% of the signal from the transmitter will be received at the detector, thus showing a green light. However, if that section of track becomes occupied the vehicle's axles will short the circuit and only a very small proportion of the signal will reach the detector. In this case a red light will be displayed.

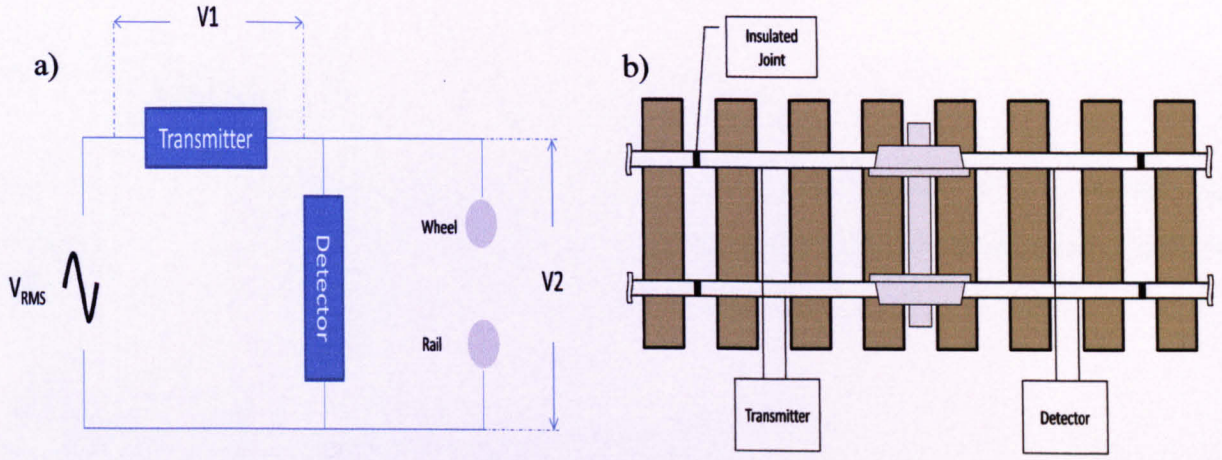

Figure 1 a) TI21 track circuit diagram b) track circuit schematic

Every autumn, leaves fall from trackside trees and gather near the rail. The aerodynamics of a modern rail vehicle is such that its turbulence will pick up these leaves causing some of them to land directly on the rail head [Johnson, 2006]. The leaves are then rolled over by the multiple wheels of a passing locomotive. The leaf is then subject to a unique set of conditions such as extreme pressure and high flash temperatures. This results in the leaf chemically bonding with the rail [Cann, 2006]. This forms a thin "Teflon like" film on the track which is extremely hard wearing and difficult to remove. The very low friction caused by this film poses problems for locomotives with large costs due to network disruptions and damage to rolling stock. Current methods used to combat leaf layers include rail grinding, high pressure water jetting, laser removal and Sandite® application. Sandite® is a suspension of sand within a paste and is used extensively on the UK rail network. Although Sandite® seems to tackle the issue of low adhesion satisfactorily competitors have started to emerge offering very similar products at lower cost and improved performance. One such product is currently under development and is intended to utilise a more uniform size of sand particle. There is little scientific knowledge available on performance of these products and there is no standard test which they need to pass before they are put on the rails. Therefore, for this thesis, a twin-disc testing machine was utilised in order to closely measure the performance

of both these products in terms of friction/traction and also in terms of wear and electrical impedance. A method of generating a leaf layer on the discs of the machine was also developed. The low friction of this leaf layer could then be used as a benchmark to assess the performance of the products. This leaf layer was analysed using a Scanning Electron Microscope, SEM and Energy-dispersive X-ray Spectroscopy, EDS to measure its chemical content.

1.2 Aims

The overall aim of this project is to improve the understanding of the control and enhancement of railhead friction/traction and develop a new method for measuring railhead friction. This thesis can be broken down into three sections:

1. **Railhead Friction Measurement**
   This part of the project involved the investigation of an alternative method for measuring railhead friction. A pendulum tester was chosen as a viable alternative to the currently used Tribometer due to its compactness and suitability of measuring localised friction problems. Tests were performed in the laboratory and compared with twin-disc data to validate the suitability of the pendulum for rail application. The pendulum was then taken into the field and the results compared with Tribometer data.

2. **Effects of Atmospheric Conditions and Contamination on Friction Modifier Performance**
   A pin-on-disc test machine with attached atmospheric chamber was used for this study. Temperature, relative humidity (RH) and iron oxide were all varied in this experiment. Iron oxide was used to simulate the oxide layer which is present on top of the rail head. The atmospheric conditions were varied to simulate a range of conditions (10 to 20°C and 40 to 90% RH). Within this range were typical tunnel conditions (typically 10°C and 70% RH) which were of particular interest.

3. **Performance of traction enhancing products within a wheel/rail contact**
   This series of tests was carried out on a twin disc test machine and aimed to measure the performance of traction enhancers. In the first part of this test a technique was developed

to produce a realistic leaf layer on the discs. A controllable method of delivering the traction enhancer to the contact was also designed. The performance of the products was measured in terms of traction. In the second part of this work a simulated track circuit was used to measure the impedance at the contact caused by the products. In this second part wear due to the products was also measured.

1.3 Thesis Layout

A review of the effects of contaminants within the wheel/rail contact is presented in chapter 2. This chapter is a collation of past and present studies into how factors such as friction, wear, rolling contact fatigue and isolation are affected by contaminants including: water, oil and leaves on the railhead. The chapter also includes current understanding of friction modifiers, their usage and their benefits.

In chapter 3 an alternative method for measuring railhead friction was developed using a pendulum tester. The pendulum rig was tested in the laboratory and compared with twin-disc data. It was then tested in the field alongside a hand pushed Tribometer. In this chapter a section of rail with leaf layer which had been removed from the field was tested in the lab.

The next two chapters of this thesis report on the testing and analysis of a range of traction enhancing products. The testing in both of these two chapters was carried out using a twin-disc test machine. Chapter 4 outlines work in which the performance of each of the products was assessed in terms of friction/traction and developed a standard test method for use in chapter 5. Chapter 5 reports on further testing of the products in which wear of the test discs and isolation due to each of the products was measured.

Effects of atmospheric conditions and levels of iron oxide on the performance of top of rail liquid friction modifiers were tested in chapter 6. A pin-on-disc tester with attached climate chamber was utilised for this work. Surface chemical analysis was also performed on post test discs using Glow Discharge Optical Emission Spectroscopy, GDOES.

Chapter 2: Review of Third Body Effects in the Wheel/Rail Contact

2.1 Introduction

Today's rail infrastructure is subject to increasing demands from its operators. Trains have to be faster, more reliable, carry greater pay loads, have reduced stopping distances and further more rails and wheels are expected to last longer between regrinding and replacements [Ward, 2002]. However, these changes are coming in tandem with increasing load in the wheel/rail contact. The wheel/rail contact has been the vital part of rail systems since the invention of the steam locomotive. It is the point at which all forces are transferred between the vehicle and the ground. It provides directional control, friction for acceleration and braking and a source of electrical contact for railway signalling systems. The contact itself is roughly the size of a £1 coin. Figure 2 shows the complex range of factors which need to be taken into account in order to maintain and increase profitability of a rail network.

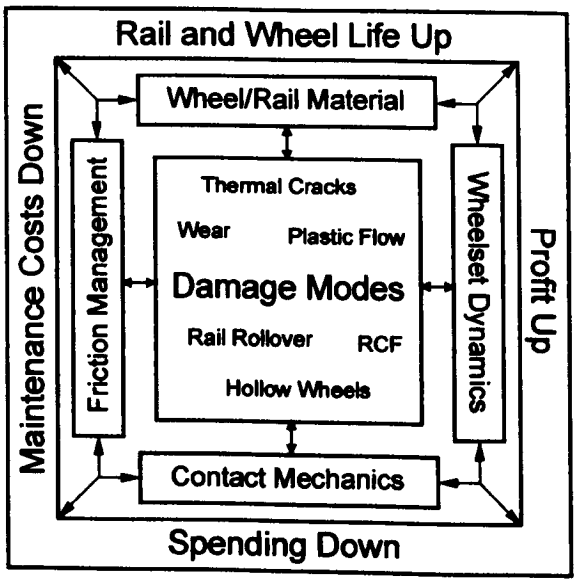

Figure 2 systems approach to wheel/rail interface management and research [Kalousec, 1997]

Although the wheel/rail system can be compared to that of a gear tooth or rolling bearing, it has one main difference in that it is an open system. This means that it is susceptible to contamination such as rain, falling leaves (during the autumn) or oil/grease dropped from stationary locomotives. With the greater loads on the modern day rail network; these contaminants are imposing greater influence on ultimate performance of the rail network.

These foreign bodies can be divided into two areas: Climatic and Operational, as defined by Descartes et al [2005]:

- *Climatic bodies* can be: water, leaves, and the oxide layer which builds up on the rail surface.

- *Operational bodies* (Contaminants), include oil, grease (deposited by passing trains) and rail ballast.

There are also products which are intentionally placed on the rail to alter the friction, wear and noise/vibration levels generated during use. These are commonly known as; Friction Modifiers, FM's.

All of the above will increase or decrease: adhesion between the wheel and the rail, their respective wear rates and fatigue life and also the conductivity between the wheel and rail which is vital in train detection, signalling and safety.

The aim of this review is to explore previous research on the wheel/rail tribosystem, with particular attention on the effects of third bodies upon it. This will allow the identification of what has been done and what is still yet unexplored. This study will include previous measurements which have been made in this field under different contamination conditions.

2.2 Wheel/Rail Contact

When a train is running on a straight section of track; contact will occur between the wheel tread and the rail head on the low rail as shown in Figure 3. However, as a train enters a curve the contact will shift to a position between the wheel flange and the rail gauge corner on the high rail. The position and size of the contact between the wheel and the rail is constantly varying, even when running on a straight section of track. These two factors will depend on the speed of the train, whether it is on straight track or a curve and the profile of the wheel and rail. Typical contact areas are in the region of 1 cm^2 on straight track [Lewis, 2006a]. However, if there is contact between the wheel flange and rail gauge (i.e. during curving) then this contact reduces in size and higher stresses, slips and wear rates will prevail. Sinclair

[2004] shows the ideal friction coefficients that should be seen in each contact case. In a low rail situation a friction coefficient between 0.25 and 0.4 is ideal for safe braking and adequate acceleration. When the contact shifts to the high rail position, however, the friction coefficient needs to be kept as low as possible to avoid excess wear, noise and vibration. This level, however, is dangerously low and can have severe impacts on braking. It is thus important that the friction on the rail head never sees this low level and is still maintained within the 0.25-0.4 region to maintain safe vehicle control. Within the wheel tread/rail head contact there will be a region of adhesion and a region of sliding. Under curving the contact patch between the rail gauge and wheel flange will consist of pure sliding.

Researchers have also tried to assess the level of stress in the contact zone. The level of contact pressure will change with the change in profile as the wheel and rail wears. Pressure will also be dependent on train mass. Kalousek et al [1985] showed that contact stresses can vary between 830-3000 MPa.

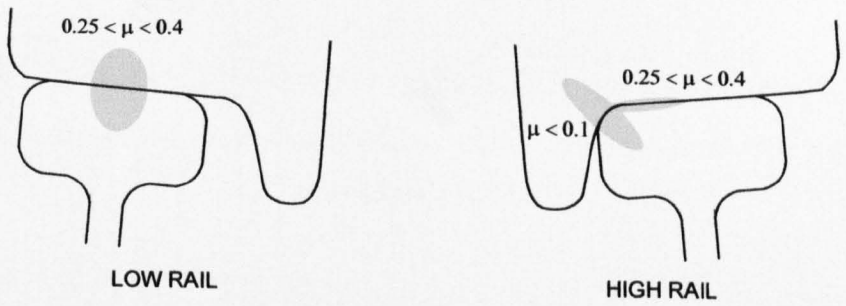

Figure 3 cross section of wheel and rail; showing contact position and ideal friction coefficient [Sinclair, 2004]

Most of the work looking into the size and pressure of the wheel/rail contact has been theoretical, based on Hertzian models and more sophisticated CAE models. Marshall [2004], used ultrasonic scanning as an experimental method for determining the wheel/rail contact geometry. The technique used an ultrasonic signal incident to two hydraulically loaded wheel/rail profiles. Using the principle that where contact is made the ultrasound wave will be transmitted through the material and where there is a gap the wave will be reflected; a map of the contact was made. Figure 4 shows the results from [Marshall, 2004] at various contact loads. A Hertzian solution is superimposed over the top of the ultrasound scan showing good agreement between the two methods. The ultrasonic method, however, reveals the contact in

much greater detail as it is able to capture the effects of surface roughness and minor profile deviations, i.e. due to damage or machining inconstancies for example. Contact pressure was also determined by relating the interfacial stiffness of the contact to the reflected signal. Results gave a maximum contact pressure of 1200 MPa, comparable to analytically derived values.

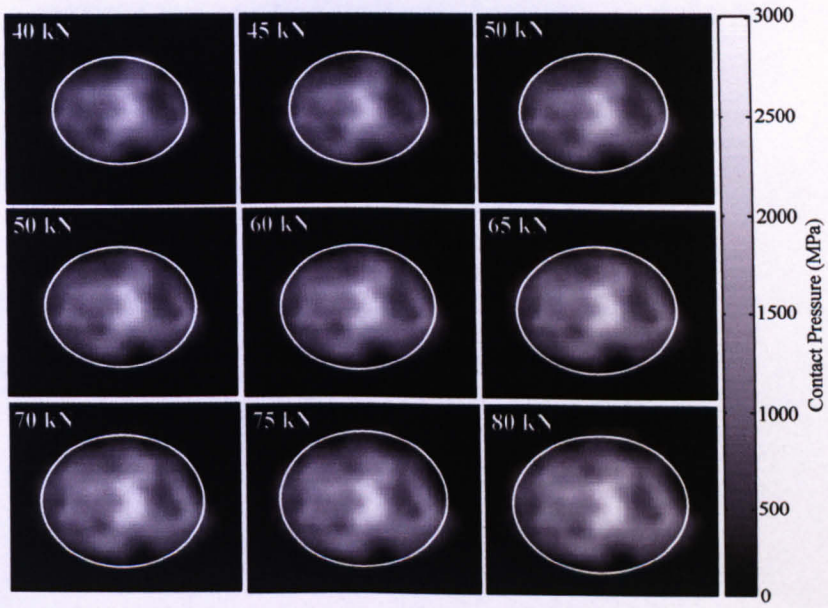

Figure 4 ultrasonic scan of wheel/rail contact under varying load with superimposed Hertzian solution [Marshall, 2004]

2.3 Testing

Extensive testing has been carried out to gain a better understanding of the interaction of the bodies within the wheel-rail contact. Various laboratory investigations have been employed to try and simulate the contact such as, Tribometer [Beagley, 1975b], twin disc tests, Rolling Disc MTM test device as used in [Cann, 2006], pin-on-disc [Olofsson, 2004] and a full scale Roller Rig, using an actual bogie wheel set [Zhang, 2002]. A number of researchers have also performed tests on sections of active track using rail mounted push Tribometers [Beagley, 1975a] and instrumented trains [Nagase, 1989]. The Tribometer is a hand pushed device used to measure friction on the rail head or gauge. It interfaces with the rail via a small steel wheel. Load is applied to the rail through the wheel via a user-adjustable clamping screw [Harison, 2002]. The wheel is connected to a magnetic clutch and as the user commences the measurement, i.e. by pushing the device along the rail, the wheel will roll along the rail freely i.e. the clutch is disengaged. Slowly and gradually the clutch is engaged subjecting the wheel

to a gradually increasing braking force. As the tangential force on the wheel approaches the limit of friction the wheel will slip. At this point the Tribometer's on board computer can calculate the friction using the maximum torque at which the wheel slipped and the normal force on the wheel. The device needs a working length of 3 metres for enough braking torque to build up on the wheel between each measurement.Twin disc testing offers more controllable, less expensive and more convenient alternative to full scale or field testing. Although this approach may not fully simulate the actual wheel/rail contact (i.e. it is a line contact), parameters such as speed, slip and load are more controllable than in full scale field tests. The disc machine can also be used to carry out a number of tests including: adhesion loss, rolling contact fatigue, wear and isolation.

Author	Test Apparatus	Load/Contact Pressure	Rolling Speed (km/h)	Test Conds.	Peak μ	Slip at Peak μ (%)	Stable μ (5% slip)
Zhang [2002]	Full-scale roller rig (using an actual bogie)	44kN	10-70	Dry	0.57-0.5	2	0.57-0.5
		67kN	10-70	Dry	0.55-0.44	1-2	0.52-0.44
		44kN	120-240	Wet	0.13-0.07	0.5-1	0.12-0.065
		67kN	80-240	Wet	0.11-0.05	0.5-1	0.105-0.05
Jin [2004]		67kN	140-300	Oil	0.055-0.045	1	0.052-0.044
		135kN	140-300	Oil	0.05-0.04	1	0.048-0.037
Harrison [2002]	Triborailer (used on actual track)			Dry	0.52	1	0.5
	Push Tribo-meter			Dry	0.7	2-5	0.7
Nagese [1989]	Instrumented bogie on test vehicle (run on test track and actual routes)	Variable	Variable	"Dry"	Range of μ: 0.2-0.4		
				Wet	Range of μ: 0.05-0.2		
				Oil	Range of μ: 0.05-0.07		
				Leaves	Range of μ: 0.025-0.10		
Gallardo [2008]	Twin Disc	1500MPa/ 7.7kN	3.54	Dry	0.6	2	0.54
			3.54	Wet	0.2	1	0.17
			3.54	Oil	0.07	1	0.06

Table 1 matrix of field and laboratory testing showing friction/traction coefficients obtained [Gallardo-Hernandez, 2008]

Table 1 was constructed by Gallardo-Hernandez & Lewis [2008] and shows various field tests comparing them to twin-disc testing under cases of dry, water and oil contamination. This shows good correlation between different testing methods. However, a compromise exists between field and laboratory tests. Field tests will offer the best measurement of the actual wheel/rail contact, and thus data from this type of testing will be more reliable. Field test can be full scale such as the instrumented bogies used in Zhang et al, [2002] and Nagase, [1989], however, such instruments can be costly as locomotives have to be modified to accommodate new hardware and instrumentation. They can also be time consuming as drivers, technicians and time-tables will have to be organised and the number of tests which can be done in a fixed period will be limited. Controllability of test parameters is also restricted due to the size of test components involved. The alternative is to uses hand pushed Tribometers such as in [Harrison, 2002]. Tibometers on the other hand will only measure friction on the rail head. The contact loads and pressures of the Tribometer will be insignificantly small with no controllability. Even so Table 1 shows there is good correlation with other test methods, however the Tribometer is more suited as a maintenance tool where technical crews can gather data on the rail network during downtime rather than for pure research. Laboratory tests can offer greater controllability of test parameters, significantly less lead time, and much superior test/time efficiency. Twin-disc testing as in [Gallardo-Hernandez, 2008] is a widely accepted method to research the wheel/rail contact due to its range of parameters which can be controlled and its ability to recreate the immense contact pressures seen in the actual wheel/rail contact. Pin-on-disc testing is an alternative laboratory based technique for researching the wheel/rail contact which offers even greater controllability in comparison to twin-disc testing. Even atmospheric conditions such as temperature and humidity can be controlled as in [Olofsson, 2004]. However, this increased controllability is at a compromise to the extent at which pin-on-disc tests represent the actual wheel/rail contact as pin-on-disc will be a pure sliding scenario; the wheel/rail contact is a rolling sliding contact. Therefore a compromise can be imagined between representation of the wheel/rail contact and controllability/efficiency of the test. It is thus at the discretion of the researching body/product developer as to the best means of gathering test data regarding time and funds available.

There are an increasing number of products being placed on our railways, yet none of them are required to pass any standard test before they can be introduced. Product approval is by

an approach of observing effects that they have on the rail, but no real understanding of the mechanical change to the system is gained in this way. It is suggested that a product approval scheme be introduced whereby the product is initially tested small scale with high controllability (e.g. twin-disc). Once certain parameters (i.e. creep, traction, wear, isolation etc.) are understood then field trials could begin.

2.4 Traction

Figure 5 illustrates the difference between friction and traction. In Figure 5 (a) we can imagine a block sliding at velocity, v along a stationary plane surface. The block is subject to a normal force, P (the weight of the block). The horizontal force which opposes the motion of the block when kept at a constant velocity is deemed the friction force and the relationship between the friction force and the normal force is referred to as the friction coefficient (equation 1). Figure 5 (a) presents a case of pure sliding and the friction coefficient will vary depending on the combination of materials in contact and their combined surface roughness.

$$\mu_f = \frac{F}{P} \tag{1}$$

Figure 5 b) shows a case of rolling/sliding and is analogous to the case of a driven wheel rolling along a rail. The wheel is subject to normal force, P and travels along the rail at velocity, v. The wheel is subject to torque, T which maintains the surface velocity of the wheel at V_t. The tangential velocity at the wheels surface, V_t, for a driven wheel will always be greater than its body velocity, V, during acceleration or when maintaining a constant speed due to the inertia of the wheel and vehicle. Under braking the body velocity will become greater than the tangential velocity. The difference between the tangential velocity of the wheel, V_t and the body velocity, v, is referred to as creep or slip and is usually given in terms of percentage. The reaction force seen at the rail is known as the tractive effort/traction F_T. This force can also be termed adhesion. This is ultimately what will propel the wheel along the rail. The relationship between traction and the normal force is known as the traction coefficient (equation 2). As can be seen in Figure 6 the traction coefficient is dependent on the rate of creep up until saturation.

$$\mu_T = \frac{F_T}{P} \qquad (2)$$

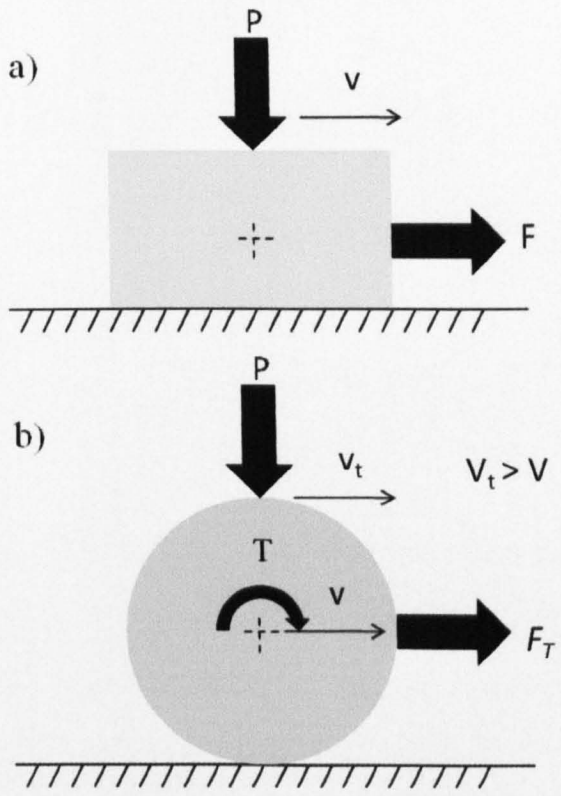

Figure 5 illustration of a) pure sliding contact b) rolling/sliding contact under acceleration

The level of friction at the wheel/rail interface has implications for the performance of trains and the whole network. Under braking, the level of traction determines the stopping distances. It is also important for acceleration. A good level of traction while pulling away from a station, for example, reduces wheel spins, maintaining the timing of service. The amount of creep within the wheel/rail contact will depend on the normal load on the wheel, the amount of torque applied to the wheel (powered wheels) and the friction coefficient.

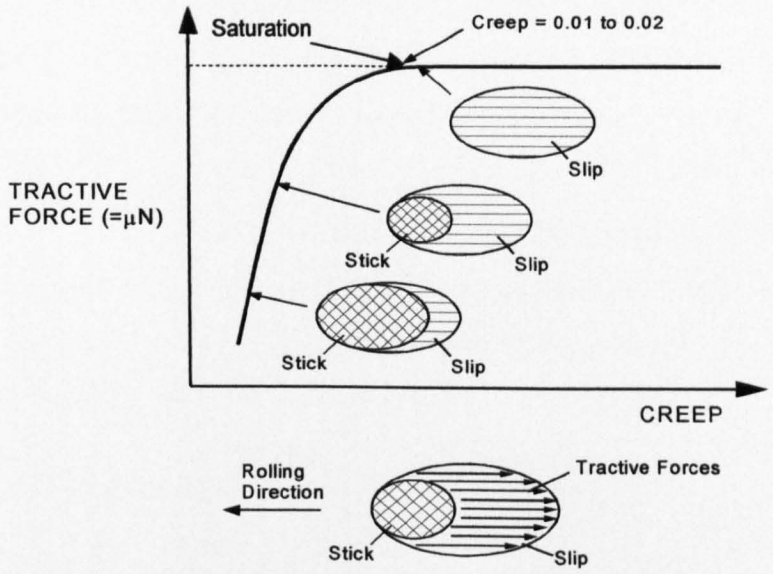

Figure 6 typical creep curve under dry, un-contaminated conditions

Figure 6 shows a typical creep curve, for a three dimensional i.e. elliptical contact, and it can be seen that as the tractive effort is increased so too is the creep (i.e. difference in tangential speeds of the wheel and rail) and hence the amount of slip in the contact also increases. The initial relationship is linear up until approximately 1% creep. At this point there is full slip in the contact and this is known as the saturation point. At this point the tractive force will be equal to the friction force of two identical bodies sliding against one another under identical contact conditions. The form of the creep curve is thus dependent on the underlying friction level on the rail. After the saturation point traction usually declines for contaminated/uncontaminated contact conditions, due to heat generated within the contact. At levels of creep approaching zero it is assumed that the traction becomes zero i.e. passes through the origin of Figure 6. However, traction at these ultra-low levels of creep is hard to measure.

For two dimensional contacts such as in twin-disc testing, where there is a line contact, the stick and slip zones will be different from those in Figure 6. Creep curves generated by Gallardo-Hernandez and Lewis [2008] using a twin-disc tester (see Figures 8 and 9) are of a similar form to that in Figure 6.

For dry rails, the operational coefficient of friction between the wheel and the rail is in the region of 0.5 - 0.7 [Beagley, 1975b]. These measurements were taken with the naturally occurring oxide layer on the head of the rail, as would be found in practice.

The level of adhesion in the wheel/rail interface can be greatly affected by the presence of a third body. Contaminants such as oil, water and leaves are known to reduce the coefficient of traction as low as 0.03 (in the case of leaves), as reported in [Beagley, 1975b]. The following section looks at the effect of third bodies on traction in more detail.

2.5 Effect of Contaminants

2.5.1 Leaves

Leaves present a major problem to the rail network every autumn. Leaves on the line cause adhesion and isolation issues which result in delays and signalling issues. The cost to networks around the world in terms of removal and service delays is very high, typically £50 million per year in the UK alone [Vasić, 2008].

In the early years of steam powered railways, leaves did not present such a concern. With high temperature exhaust gasses line side trees were a potential fire hazard so were regularly cut back. Rail steels were also of poorer quality, and locomotives had larger diameter driving wheels with a larger area of contact giving higher wear rates. Thus track replacement was more frequent and any leaf layer which did form on the rail would be quickly worn away.

Dead leaves will fall from track-side trees during the autumn. These leaves can then be picked up by the turbulence of a passing train, and due to its aerodynamics, are drawn directly into the wheel/rail contact [Johnson, 2006]. The leaf will then be crushed as it is rolled over by each consecutive wheel pass. Patches of crushed leaves can be seen on railheads as a Black "Teflon Like" Film [Cann, 2006] which is strongly bonded to the rail surface [Olofsson, 2004]. This dark patch was originally thought to be charring of the leaf material as it is repeatedly crushed. However, in [Cann, 2006] this transformation of the leaves was re-created in the laboratory. The leaves were observed to transform into this black matter at a high rate. This has led current researchers to believe that this may be a result of a chemical reaction between the leaf residue and the rail steel.

The first problem caused by crushed leaf layers on the rail is that of traction loss. In [Cann, 2006] friction coefficients as low as 0.03 have been reported; this was also reported by Broster et al [1974]. However, Nagase [1989] reported coefficients of around 0.01 using an instrumented bogie on an actual section of commuter track and similar levels were seen during twin-disc tests [Gallardo-Hernandez, 2008]. Levels as low as this represent a major loss of traction, causing wheel spins/skids and braking issues leading to train delays platform overruns and signals passed at danger.

Chemical analysis of leaf layers was initially performed by Fulford, [2004] and taken from field and laboratory samples. Results showed the layer contained a mixture of iron, iron oxide, water, cellulose and oil. Cann [2006] later used Fourier Transform Infra Red (FTIR) spectroscopy to analyse laboratory generated leaf layers. This analysis showed that the layers contained cellulose and pectin. Li [2009] performed FTIR analysis on twin-disc generated leaf layers highlighting a further constituent of the leaf layer, lignin. Measurements of the layer thickness was also gathered in [Li, 2009] and shown to be between 10-100 μm which is greater than the surface roughness of the discs used in that test; nominally 1μm R_a.

2.5.2 Water

Friction can also be greatly reduced by water on the rail. Work carried out by British Rail Research [Beagley, 1975b; Beagley, 1975a; Broster, 1974; Beagley, 1975c] in the 1970's showed that water on its own reduced the coefficient of friction to 0.3 from its dry level of between 0.5-0.7. However as reported in [Beagley, 1975a] the friction can be reduced even further depending on the level of debris (iron oxide, brake block dust etc) in the contact. However, this debris on its own (i.e. dry) has little effect on the overall levels of adhesion [Broster, 1974]. It was shown in the laboratory that when the ratio of water to debris is low then friction levels can drop to 0.05. When this debris mixes with low amounts of water a high viscous paste is formed [Beagley, 1975a; Jenks, 1997].

Results of tests carried out by Olofsson & Sundval [2004] show that humidity also has a large effect on the coefficient of friction for a dry rail as shown in Figure 7. However when the test was contaminated with leaves, humidity had little effect on the already reduced friction. Other laboratory tests [Beagley, 1975a] have also reported humidity as influencing friction in

the wheel/rail contact. However, this has not been reported in field or full scale tests due to the uncontrollability of atmospheric humidity.

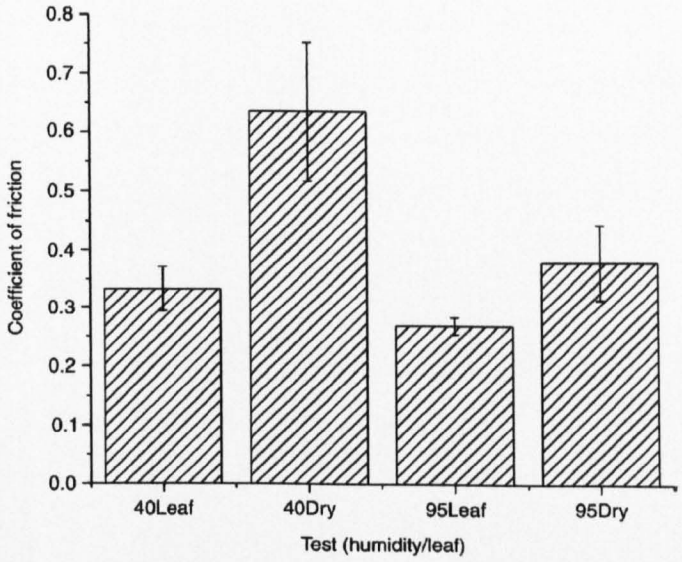

Figure 7 chart showing influence of humidity (40% and 95%) on a dry and leaf contaminated rail

[Olofsson, 2004]

Water is also known to increase the rate of rolling contact fatigue. It does this by a mechanism known as 'fluid crack pressurisation'. Water on the rail head is rolled over by the wheel of a passing locomotive and is subject to a very large pressure by way of this. This high pressure forces the water into any small cracks on the rail surface. This pressurised fluid then intensifies the Mode I stress intensity at the crack tip (opening the crack) leading to an increase in crack propagation rate [Bower, 1988; Fletcher, 2006]. A secondary effect that can occur is that the water lubricates the crack faces intensifying the Mode II (shear) stress intensity again leading to increased propagation.

2.5.3 Oil

Oil has also been observed to reduce the levels of friction at the wheel/rail interface. The main reason that the levels of friction vary on a dry rail are down to the tiny deposits of oil on the railhead [Beagley, 1975a]. Oil can be dropped by passing trains and then transferred over larger areas as it is rolled over. Grease is also used as a lubricant on tight curves where Gauge/flange contact occurs. This grease could potentially find its way up onto the rail head.

Gallardo-Hernandez & Lewis, [2008] used a twin-disc tester to develop creep curves for various contamination conditions including oil. Figure 8 shows that traction coefficients under oil contamination are very low and in the range of 0.04-0.06. Field testing by Beagley & Pritchard, [1975a] showed that oil is quickly removed as it is rolled over by passing trains and hence any effects that it may have on friction levels are short-lived. One reason for the discrepancies between field and laboratory testing in this area, may be that in the twin disc tests, the contaminant will cling to disc and hence the removal, as seen in the field, will not be observed in the lab.

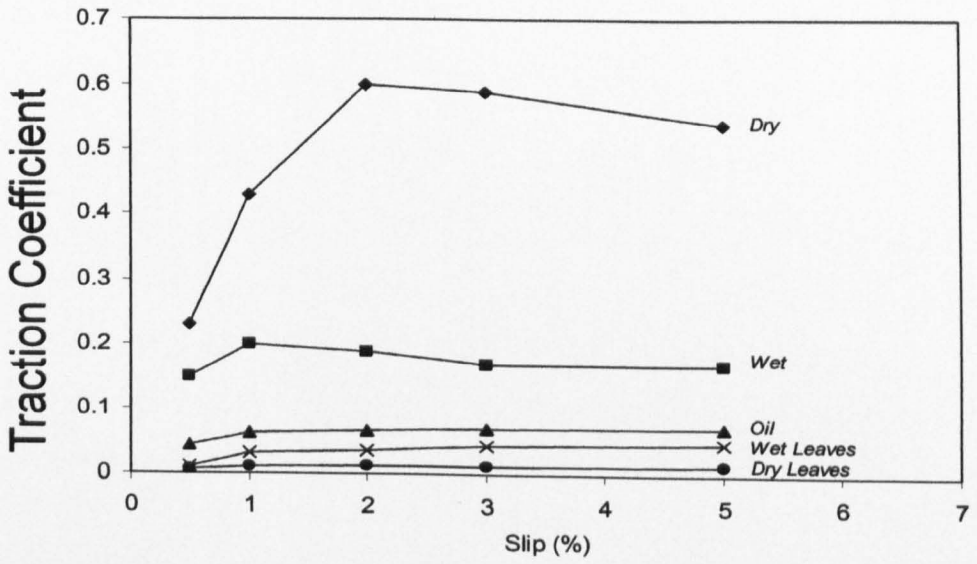

Figure 8 creep curves generated by twin-disc testing [Gallardo-Hernandez, 2008]

Lewis et al, [2009b] also tested oil and water mixtures using a twin-disc tester. These were compared with pure water and pure oil. Tests were performed at a range of different slips to create creep curves as shown in Figure 9.

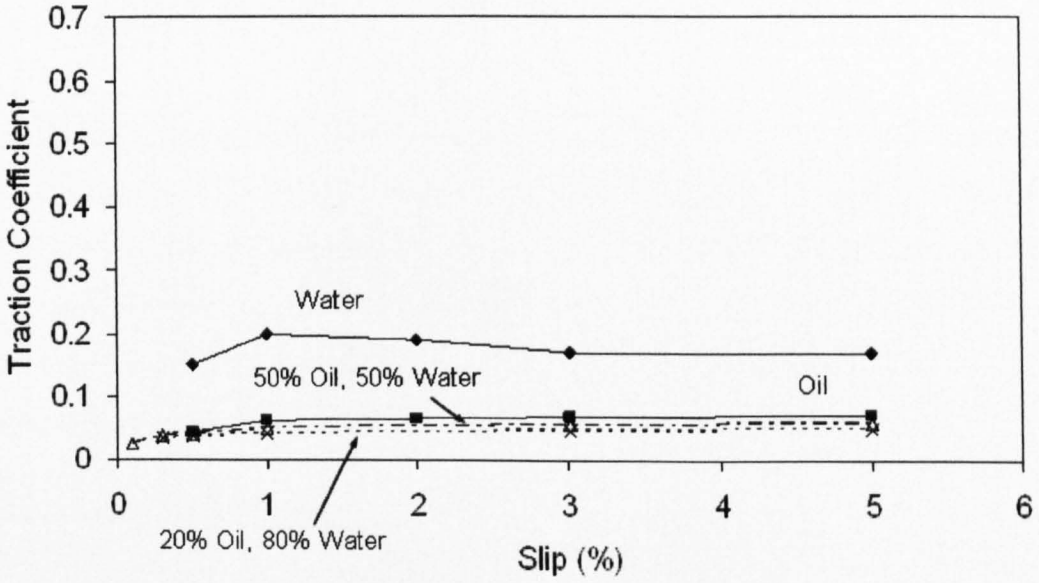

Figure 9 creep curves generated for oil and water mixtures [Lewis, 2009b]

Figure 9 shows that the oil in the oil/water mixture dominates the traction by bringing it down to a level just below the pure oil creep curve. This effect seems to be independent of the amount of oil in the mixture as the 20% oil is in the same region as the 50% blend. What is also interesting is that both the oil/water blends reduce traction levels below that of pure oil. Figure 9 also shows that the lesser the oil in the mixture the lower the friction.

Oil also effects rolling contact fatigue, RCF in the same way as water [Kaneta, 1985], see above. Although the mechanism is the same ('fluid crack pressurisation'), oil can affect RCF in a different way. Research [Eadie, 2006; Fletcher, 2000a] has shown that how oil affects RCF depends upon how frequently the oil is applied. When lubrication is applied intermittently crack growth rate dramatically increases. Conversely, higher frequency lubrication will slow crack growth rate or halt it entirely This seems to suggest that as oil has a greater surface tension than water it takes longer for it to seep into a crack. Meaning that if there is a small amount of oil on the rail with a high frequency of wheels passes over it, it will not have time to enter the crack before it is squeezed out of the contact. If lubricant is left on the rail for longer, then there may be sufficient time for the oil to seep into the crack before it is rolled over by the wheel.

2.5.4 Other Contaminants

Full scale testing, by Nagase, using an instrumented bogie fitted to a commuter train also showed sharp decreases in adhesion coefficient at the sites of level crossings. The severity of the drop seemed to be proportional to the number of road vehicles using the crossing [Nagase, 1989]. Later inspection of these crossing showed that there was mud present on the rail; transferred from tyre to rail by passing cars [Nagase, 1989]. There also maybe an alteration of the track surface by the passing cars, i.e. wear or chemical.

2.5.5 Traction Enhancers

There are other bodies which are intentionally placed into the wheel/rail contact in order to increase traction when it is needed i.e. under emergency braking. They may also be used to restore adhesion under situations of low friction such as leaf or oil contamination.

2.5.5.1 Sand

Sand is commonly used on the British rail network to counteract the low adhesion problems presented by oil, water and leaves. Sand is supplied from a hopper below the train directly into the wheel/rail interface with compressed air. It is delivered automatically when the emergency brakes are applied, or can be applied at the driver's discretion during acceleration. It has been shown that when sand is entrained into the wheel/rail contact it is crushed, and in twin disc tests this crushing causes some particles to be ejected from the contact [Lewis, 2005]. It was also shown in [Lewis, 2006b] that when the interface is contaminated with water the addition of sand to the contact can actually restore the levels of adhesion back to those seen under dry conditions. However, scaling of the contact or sand feed rate, was not used in these experiments as in [Kumar, 1986]. It was also shown when sand is used in the presence of leaves; adhesion is restored to levels before the leaves were added [Gallardo-Hernandez 2008]. Tests also showed that when sand is used in dry conditions the coefficient of friction is actually reduced slightly, see Figure 10. This was thought to be due to the crushed sand particles sliding over one another and acting, essentially, as a poor solid lubricant. Crushed railway ballast (granite) has also shown the same effects under dry conditions as reported in [Lewis, 2006b]. The results of tests done with sand by Descartes et al. [Descartes, 2005] showed that sand increased the friction coefficient from 0.4 (no sand) to

0.55. The test in [Descartes, 2005] was carried out with a disc on flat rail as opposed to twin-disc. Arias-Cuevas et al, [2010b] also performed dynamic tests with sand and showed that small sand grains in the region of 0.06-0.6 mm would cause friction to drop when entrained within a dry twin-disc contact. The level at which the friction is reduced was most pronounced with the smallest sand grains and at the lowest slip rate. The fall in friction was also proportional to the sand feed rate. At the highest feed rate (7.5 g/m) friction dropped to below 0.1 after the application of sand from a level of approximately 0.4 before the sand was applied. The larger (elliptical) contact in [Descartes, 2005] could account for the discrepancies between the findings in that test and those from [Lewis, 2006b]. However, tests by Kumar et al, [1986] also showed that sand can increase traction in the wheel/rail contact. What is interesting here is that the feed rate used in [Kumar, 1986] was below any used in [Arias-Cuevas, 2010b]. Hence, is possible that a transition in sand feed rate could exist. Any feed rates below this transition would increase traction and any in excess of it will reduce friction.

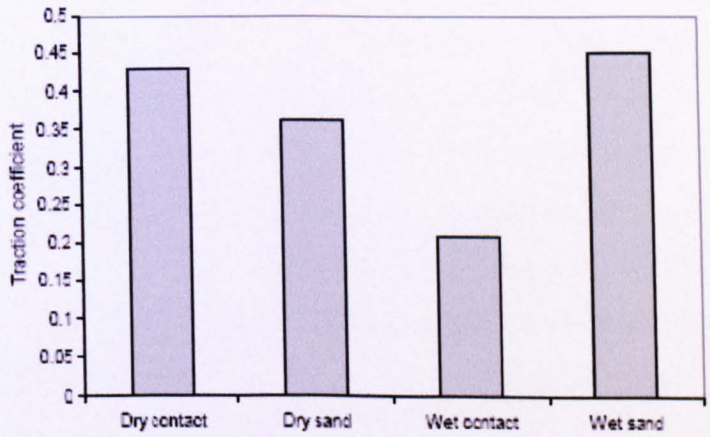

Figure 10 results of experiments carried out in [Lewis, 2005]

2.5.5.2 Other Friction Enhancers

There are a number of alternative friction enhancing products available and one such product was tested by Li et al, [2009] using a twin-disc tester. The traction enhancer is referred to by its commercial name Sandite®. Sandite® is widely used by the British rail network to combat low adhesion problems caused by leaf fall. The product contains a mixture of sand grains, gel and steel shot particles. The gel acts as a suspending matrix which holds the sand and steel particles in a uniform distribution on the rail head. The steel shot is used to guarantee good

electrical conductance between the wheel and rail for signalling purposes. The product uses a range of different particle sizes and is usually dispensed from maintenance vehicles at specific sites where low adhesion problems prevail. The main advantage of Sandite® over pure sand is that it can be left on the railhead to increase friction levels at specific sites and will restore adhesion for a specific period before it needs to be re-applied. Sand on the other hand is dispensed from locomotives usually at the drivers discretion and will only remain useful for an instant i.e. once the sand has passed through the wheel/rail contact most of it will dissipate. Sandite® was shown to perform well in both dry and wet conditions by Arias-Cuevas et al, [2010b].

2.5.6 Friction Modifiers

Sand is one of the original solutions to the adhesion loss problem in rail applications. However, even though sand is good at restoring adhesion in wet or oily conditions, it is not the most practical solution. Sand in the wheel/rail contact increases wear and can cause complete isolation, having implications on train detection. This has lead to the development of artificial products known as Friction Modifiers (FM's). These can be in the form of liquid or solid products which are traditionally placed on the rail via automatic trackside applicators. However, recent developments are allowing these products to be placed on the rail from the vehicle [Tomeoka, 2002, Suda, 2005]. These, vehicle applied, FM's are usually in solid form and are applied to the wheel by spring loading a solid stick of the FM directly to the wheel tread. This solid stick is abraded by the rotating wheel causing a film to be generated. This film is then transferred to the rail.

It should be noted that friction modifiers are vastly different from flange lubricants. A lubricant is primarily intended to give the lowest possible friction as a way of combating excessive wear. A friction modifier on the other hand is designed to bring friction within a controlled range of 0.3 – 0.35. This level has been shown to reduce wear but not affect braking or acceleration [Lu, 2005]. Twin-disc tests with solid variants of friction modifier [Lewis, 2009a] showed traction levels of approximately 0.3 at 3% slip and 0.25 for 1% slip. This shows FM's ability to control friction within a tighter range as dry tests from [Lewis, 2009a] showed traction coefficients of 0.55 and 0.4 at 3% and 1% slip respectively. The main distinguishing feature between Friction Modifiers and traditional lubricants is that they

provide a controllable friction level within the contact once full slip conditions are reached [Egana, 2005]. It was also shown by Eadie et al. [2006] that friction modifier can vastly reduce wear rates. However this may have adverse effects on the RCF rate. Firstly lower wear rates mean lower crack truncation rates as newly formed fatigue cracks from the ratcheting process will not be worn away and thus left to propagate; Friction modifiers can be classified into two sections:

- Low Coefficient Friction, LCFM also termed lubricants
- High Coefficient Friction, HCFM or HPFM

Friction Modifiers are classified as to their effect on the coefficient of friction (COF) once saturation has been reached in the contact (i.e. full slip). If the effect of a FM is to reduce the coefficient of friction after saturation then it is classified as a LCFM. LCFM's are typically applied to the wheel flange / rail gauge interface. If friction increases after saturation then this is a HPFM. See Figure 11. LCFM is used an in situations of high slip i.e. curving where high slip rates occur between the wheel flange and rail gauge. HPFM's can be used in situations of adhesion loss such as sections of track affected by leaf-fall.

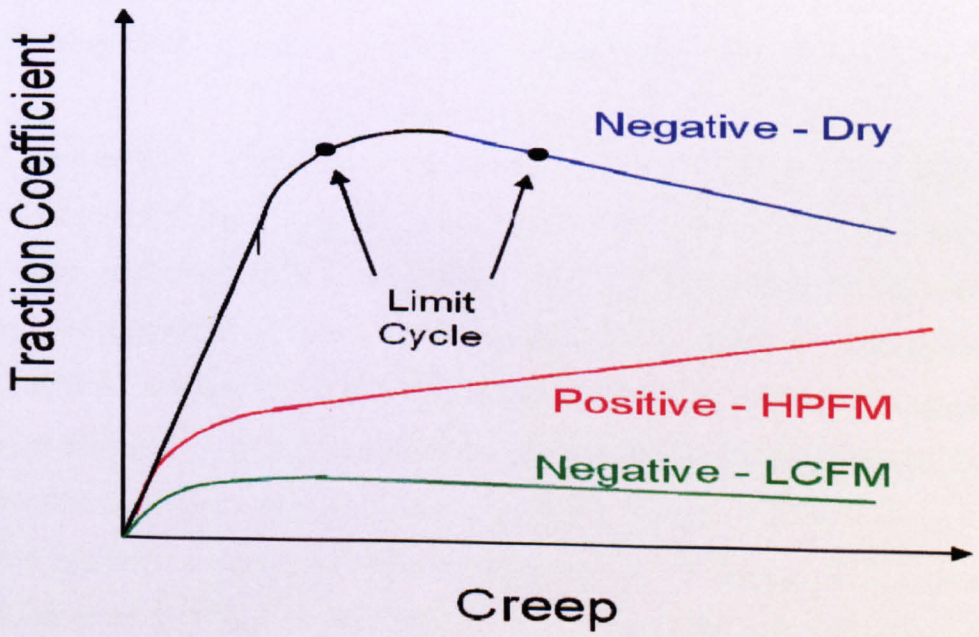

Figure 11 illustration of Friction Modifier effects on Creep Curve

Top of rail friction modifiers (TORFM's) are designed to provide a positive friction characteristic to the wheel/rail contact [Egana, 2005]. As can be seen in Figure 11 a HPFM will achieve the positive attribute by lowering the general traction level. A dry rail with nominal oxide layer will typically exhibit a negative creep curve, Figure 11. This means that as saturation is reached traction levels will start to decrease with increasing creep i.e. light curving. This can cause a noise problem as creep exceeds saturation a limit cycle is created meaning creep alternates between two points where the traction level is the same. This stimulates a resonant frequency in the wheel web resulting in a high pitched squeal [Eadie, 2002]. This can also cause a wear phenomenon of the rail in the form of corrugation. By providing positive friction this limit cycle is eliminated, hence noise and rail damage are reduced [Eadie, 2006]. In serious noise affected areas sound pressure levels can be reduced by up to 21dB with an average reduction of 10-15dB [Eadie, 2003]. Figure 11 also shows that LCFM reduces general traction levels to levels lower than the dry and HPFM cases while also introducing a negative curve.

2.6 Rolling Contact Fatigue

Rolling contact fatigue, RCF, like any other form of metal fatigue, is caused by the development and growth of cracks in materials under cyclic contact. It is common in bearings, gear teeth and wheels and rails. However, in RCF, crack nucleation is by a different mechanism because cyclic compressive stresses dominate the loading as opposed to tensile.

RCF failure can occur by a variety of different mechanisms, however, the two most common are described here. In the first instance, cracks may develop below the surface where stress is at its peak. These cracks will grow to the surface causing a small amount of material to break away (pitting). In the second process, the high stresses in the wheel/rail contact cause a thin layer of the railhead material to yield. Repeated loading by the passing of multiple wheels causes an incremental flow of plastic material at the rail surface. Eventually the ductility of the metal in this region is exhausted and a crack will form. This process is known as ratcheting and can lead to complete structural failure of the rail [Bower, 1991]. As this is the more severe cause of RCF it has been focused on in a great deal in the literature. There are three stages to this type of RCF crack growth as shown below (Figure 12) [Kapoor, 2003].

1. At this initial stage, the crack will grow rapidly at a shallow angle (15°) in the direction of motion of the wheel. As the crack lengthens the high growth rate is retarded [Smith, 2004]. Depending on the stress conditions at the surface of the rail the crack will either stop growing or develop into the next stage of growth. These cracks are driven by the ratchetting process [Descartes, 2005].
2. If the crack is not arrested at stage one then the crack will develop into the second stage, driven by contact stresses in the rail. Again at the beginning of this stage, growth rate is high but then slows as the crack length increases [Smith, 2004].
3. At this stage the crack will branch either upward toward the surface of the rail or downward at a steep angle. The way in which the crack grows at this stage is dependent on a large range of contact parameters and is not entirely understood. If the crack grows upward then it will eventually meet the surface and a small flake of material will be lost from the surface. However if the crack turns downward then this can lead to catastrophic failure of the rail [Smith, 2004]. Crack propagation is driven by the bending stresses in the rail.

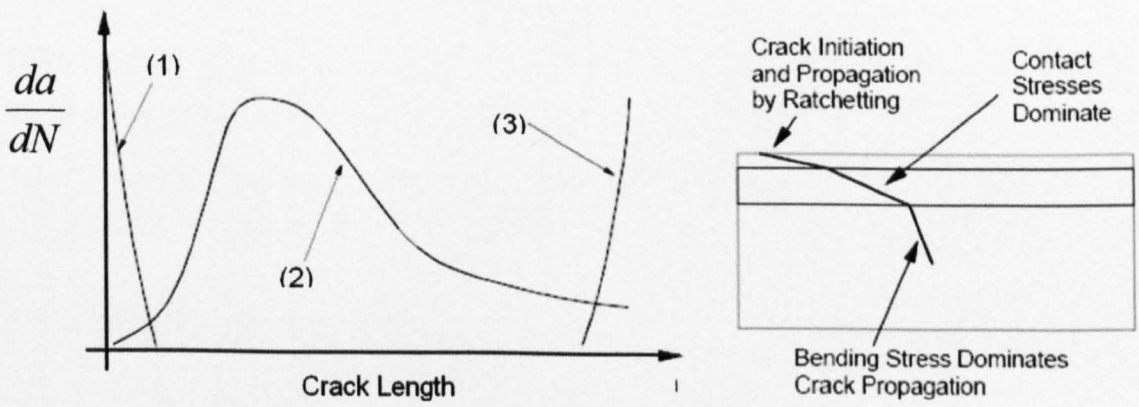

Figure 12 stages of RCF crack growth [Kapoor, 2003]

2.6.1 Interaction of Fatigue and Wear

In the rolling/sliding contact conditions which are typical of the wheel/rail contact wear and fatigue will occur simultaneously. (This is unlike most other engineering components where only one mechanism is expected to dominate.) Thus we need to take care that by reducing one we are not increasing the other. For example, oil may be used to treat wear problems; however, such fluids can penetrate fatigue cracks, increasing their rate of propagation [Kapoor, 2003]. Wear of the material at the railhead will (depending on crack length)

eliminate or shorten growing fatigue cracks. This is known as crack truncation. Ideally we would want the wear rate to be at a level where fatigue cracks are just worn away, ensuring that the rail life is determined by wear and not fatigue which is much less predictable. The two loci in Figure 13 [Kapoor, 2003] indicate the life of the rail due to wear, and the life due to fatigue with material removal rate.

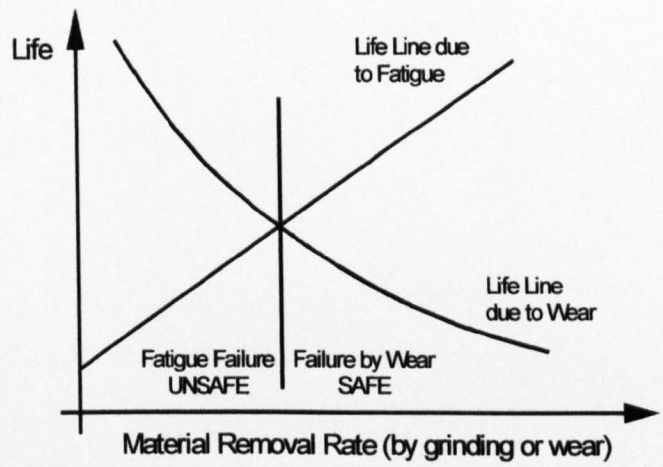

Figure 13 Illustration of effects of crack truncation [Kapoor, 2003]

It can be seen from Figure 13 that a compromise between the wear rate and fatigue life is found where the two loci cross. However, as will be seen in the next chapter wear is not easily manageable due to its dependence on a large range of factors and hence a point just to the right of where the fatigue and wear lines intersect is set, ensuring that rail life is dominated by wear and not fatigue [Kapoor, 2003].

2.6.2 Contamination and RCF

This is currently an important area of research as an increasing number of products (liquid and solid) are being placed on the rail gauge/head to help with adhesion problems. However more understanding is needed about how they affect other parameters such as rolling contact fatigue.

Water is known to increase the rate of rolling contact fatigue. It does this by a mechanism known as 'fluid crack pressurisation' [Way, 1935]. Water on the rail head is rolled over by the wheel of a passing locomotive and is subject to a very large pressure as a result. This high pressure forces the water into any small cracks on the rail surface. This pressurised fluid then intensifies the Mode I stress intensity at the crack tip (opening the crack) leading to an

increase in crack propagation rate [Bower, 1988; Fletcher 2006]. A second effect that can occur is that the water lubricates the crack faces intensifying the Mode II (shear) stress intensity again leading to increased propagation.

It had been well noted by researchers [Littmann, 1968; Rowe, 1982] that the presence of lubricants in a rolling sliding contact had significant effect on the fatigue life of components. Although Way [1935] had put forward his "hydraulic pressure effect" for pitting of rolling bearings half a century earlier, it wasn't until the work of Kaneta et al, [Kaneta, 1985; Kaneta, 1987], which led to the increased research into the fluid penetration of surface cracks within the wheel/rail contact.

Fletcher & Beynon, [2000a] investigated the effect of intermittent lubrication using a chemical solution similar to a commercially available wheel flange lubricant. Again a twin-disc testing method was used. Fletcher & Beynon [2000a] showed in these tests that when the lubricant was re-applied after a short pause: rapid fatigue failure of the disc surfaces occurred. This effect was not seen with water. Eadie et al [2006] also performed tests using a water-based friction modifier. A full scale test rig was used for the investigation with the FM sprayed onto the rail head and gauge with varying application rates. No cracks were detected under high frequency application (equal to approximately 1 application every 3 and 15 train passes). However, under the lower application rate (application after every 30 train passes) cracks were observed. Cracks were also observed under dry conditions. Cracks formed under FM application showed a greater average crack length but a lower number of cracks per length of rail tested. The results in [Eadie, 2006] show that if frequent application of FM is maintained, this can retard or prevent crack formation compared to dry conditions. When FM application rate is low, cracks do form, seemingly under dry running, and crack growth rate is higher than that for un-lubricated running; this correlated with what Fletcher observed in [Fletcher, 2000a] for intermittent lubrication.

Work has also been carried out to investigate solid contaminants on RCF. Dwyer-Joyce et al, [2003a] carried out tests using crushed ballast (granite) and sand, two types of solid contaminant commonly found on the railways. The experiment was conducted using a twin-disc test. Ballast did not seem to have an effect on fatigue although it did introduce a third-

body abrasion mechanism; however, sand increased the fatigue rate vastly [Dwyer-Joyce, 2003].

2.7 Wear

Over time wear can change the profile of wheels and rail. This change in profile adversely affects the performance of the wheel/rail contact and leads to costly maintenance measures, such as rail grinding and wheel turning. Wear and adhesion are proportional to each other [Hou, 1997], i.e. sand application will increase wear and adhesion simultaneously. Highest wear rates occur between the wheel flange and rail gauge during curving due to high slip and load. Measures to combat wear include application of lubricating oils or specifically formulated "friction modifiers", which can be in either liquid or solid form. These lubricants are primarily intended to reduce friction in between the flange and gauge in order to minimise wear rates but are also being used to reduce noise i.e. wheel squeal. In [Eadie, 2006] full scale laboratory testing showed a significant reduction in wear rate with FM application, however, these tests were performed at a much lower speed than seen in practice.

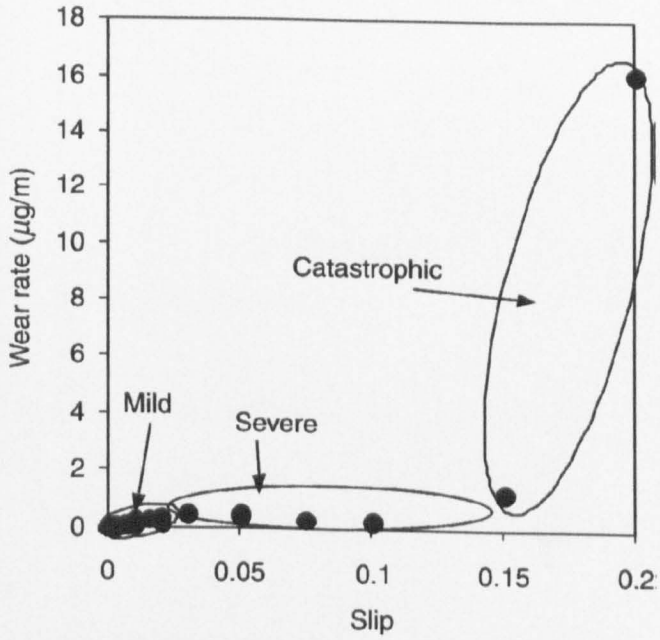

Figure 14 results of twin disc testing [Lewis, 2004] showing three wear regimes

Bolton and Clayton [1984] performed tests on an AMSLER (twin-disc) wear testing machine and identified three wear regimes in wheel/rail applications. These have been designated,

Mild, Severe and Catastrophic. The particular regime of wear at any time is largely dependent on the amount of slip in the contact and is shown in
Figure 14. Within each wear regime there is an associated wear mechanism. It was concluded in [Bolton, 1984] that the Mild regime, which occurs under low contact stress and speed, is associated with an oxidative wear mechanism. This has also been shown by Lewis and Dwyer-Joyce [2004] where discs run under low speed and load form a dark brown film on the surface; characteristic of oxidative wear. As slip and load are increased further so does wear rate (severe regime). Wear surfaces for the second regime are described in [Bolton, 1984] as having ripple like features with much smaller wear debris seeming to emanate from the troughs. Under the third regime (catastrophic) very high wear rates were seen [Bolton, 1984; Lewis, 2004] with much rougher wear surfaces than in either mild or severe. There was also evidence of abrasive wear seen as large scratches on the surfaces. It is not exactly clear what occurs in the contact to cause the transition between severe and catastrophic wear. In [Bolton, 1984] it was suggested that it may be due to high temperatures created in the contact causing changes in material properties. Gallardo-Hernandez et al [2006] used an analytical approach to determine the temperatures caused in a twin-disc contact. This was done alongside analysis using a thermal imaging camera. Analytically determined temperatures were in good agreement with those gained by thermal camera and showed that high temperatures in the range of 280°C – 700°C are generated at high slip values. Evidence of high temperature can be seen in the field as wheel and rail spalls. These spalls are areas of Martensite formation and are thought to occur due to very high temperatures generated by pure sliding [Sawley, 2007]. As martensite is a very hard yet brittle phase of steel; cracks form and wheel flats or out of roundness occurs which can accelerate wear.

Various wear models have been created by researchers in the past such as [Kalker, 1991; Lewis, 2003b]. Generally these models are used to predict changes in wheel and rail profile over time. More sophisticated modelling software such as ADAMS/Rail is allowing researchers to refine bogie design to achieve optimum wheel/rail performance as in [Stanca, 2001].

Models have also been developed to closer understand the wear mechanisms and explore factors such as changes in material properties, work hardening and tribological layers on the rail head. Such models can be found in [Kapoor, 2000; Franklin, 2001] where the rail surface

is modelled as a series of thin layers. The layer closest to the surface is subject to shear stresses from the passing wheel and will accumulate strain until failure which is determined by the yield stress of the material. This model was updated to try and predict wear and crack growth rate in rails in order to refine rail grinding sequences [Franklin, 2006].

However, none of these models incorporate contamination and therefore cannot include their effects in their outputs.

2.7.1 Wear and Contamination

As with fatigue, wear can also be greatly affected by the presence of contaminating media within the wheel/rail contact. The level and type of contamination can vary with location. For example a sidings where there is not a lot of traffic large amounts of oxidation can be found on the rail, or leaked oil and grease from standing locomotives. However, if we look at part of a busy main-line then the level of oxidation will decrease but we may find other contaminants such as water, leaves or sand.

The most commonly found contaminant on the rail is rust or oxidation. It has been shown that this oxide layer is the largest sole influence on wear and adhesion combined. If there is sufficient oxidation build up then this can not only increase adhesion but also reduce wear [Hou, 1997].

Sand is one of the most common products put down on the rail in order to increase adhesion. However, it has been shown [Kumar, 1986; Jenks, 1997] that presence of sand within the contact can vastly increase wear rates by 10-100 times. It is also noted in [Jenks, 1997] that sand does not only cause damage to rails and wheels, but also damages bearings, causes drain blockages and contaminates track ballast. However, work done in the above only quantified wear rates and further work was done in [Grieve, 2001; Lewis, 2005] to investigate the wear mechanisms due to sand contamination. It is general expectation that only solid contaminants will lead to higher wear rates due to abrasive action. It was also shown in [Eadie, 2006] that the application of liquid friction modifiers to the track, although increasing rolling contact fatigue, virtually eliminated wear.

As solid particles such as sand or granite are entrained into the wheel/rail contact they are crushed as shown in Figure 15.

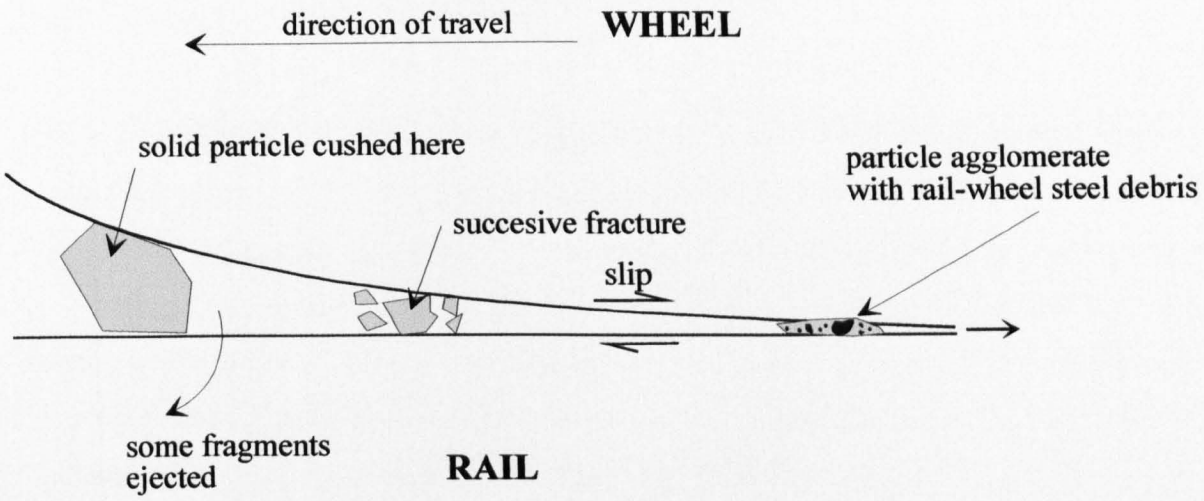

Figure 15 illustration of successive fracture of a solid particle on entry into the wheel/rail contact [Grieve, 2001].

Contact pressures are so high that the particles are broken down to very small fragments. Twin disc testing [Lewis, 2006b] showed that this breaking up of the particles causes some of the sand to be ejected from the contact unless the contact is wet in which case most of the sand will be entrained as in Figure 16.

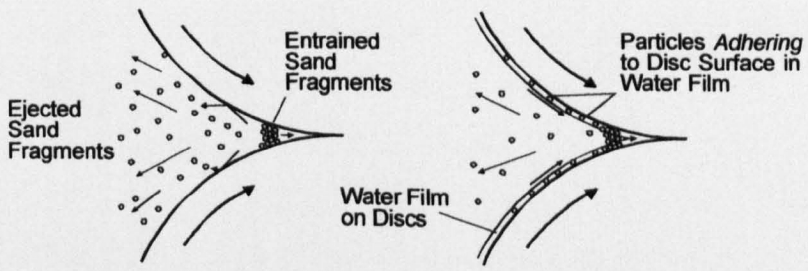

Figure 16 ejection of sand particles from a twin disc contact [Lewis, 2006b]

Granite, the material used as railway ballast could also be found on the rail head. Grieve et al. [2001] performed static tests, assessing the surface damage caused to wheel and rail by sand and ballast. The railway ballast was loaded between two hydraulically pressed wheel and rail platens, and showed that solid particles were crushed in the contact by the extreme pressures. This crushing caused a small indentation on the surface of the softer wheel material approximately 1-2μm deep, however, this depth of indentation was found to be very small

compared to the amount of plastic strain which accumulates during dry running, and hence was not thought to be the main cause of wear. However, sand resulted in much greater damage to the wheel with indentations up to 100 μm. A small amount of indentation on the rail was also found.

Dynamic laboratory tests by Kumar et al[1986] and Jenks [1997] showed that sand can increase wear rates by 10-100 times over that of uncontaminated conditions. This wear mechanism was shown to be 'three body abrasion' [Rabinowicz, 1961]. As sand particles enter the wheel/rail contact, high pressure causes crushed fragments of the particles to be indented into the softer wheel surface. The artificially roughened wheel will then abrade the harder rail surface due to the localised micro-slip in the contact patch. In such cases the harder material, in this case the rail, wears faster than the softer one.

However, in [Lewis, 2006b] three body abrasion was not observed, during testing with sand. Results showed that it was actually the softer wheel that wore fastest. In this case what was happening was low cycle fatigue had been initiated in the wheel disc by the sand particles being indented into it. This caused large fragments of wheel material to be lost as wear debris. It must be noted however, that much more severe contact conditions were used and an apparent shift in wear regime had occurred. Either way it is clear that the presence of sand in the wheel/rail contact is detrimental to the life of the railway system. Grieve et al, [2001] devised a model to predict the three body abrasion process in the wheel/rail contact. The model calculates material removal rate assuming that an embedded particle removes a volume of material equivalent to its cross-sectional area.

Results from twin disc testing [Lewis, 2006b] are shown in Figure 17 and show wear rates under uncontaminated, dry sand and wet sand contamination. The difference in wear rates between the rail and wheel can be as much as 2.5 times [Lewis, 2006b]. In this case sand had caused much greater surface damage during the static tests. What is interesting is that with wet sand total wear rates are almost an order of magnitude higher. There are probably two mechanisms at play here. Firstly when wet, more sand will be entrained into the contact meaning more damage can occur. Secondly sand will act as an initiation for fatigue cracks. With the presence of water the growth of these cracks will be accelerated via the 'fluid crack

pressurisation' mechanism. This is a cause for concern especially as sand is most likely to be found on the rail in low adhesion situations i.e. wet rails [Lewis, 2006b].

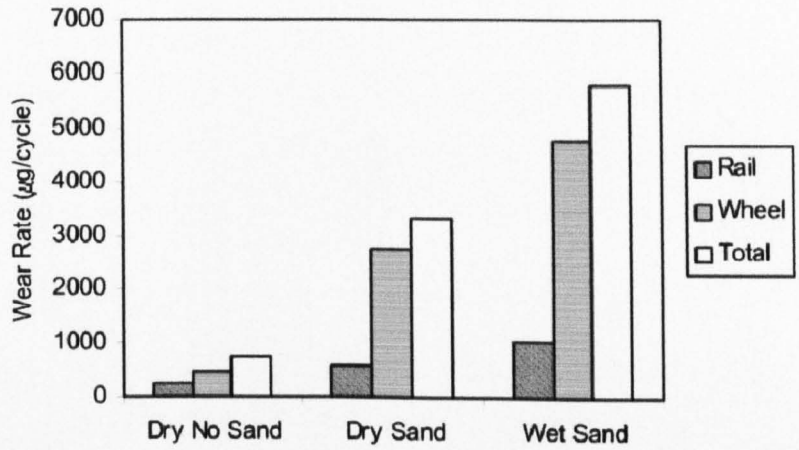

Figure 17 wheel and rail wear rates under for sand contamination; twin disc testing [Lewis, 2006b]

Another interesting phenomenon seen in this investigation showed that traction direction (i.e. accelerating, braking) had no effect on the wear rates.

2.8 Isolation

On the UK main-line train detection is by an electrical isolation method. Detection is a major operational and safety measure. An electrical current is passed through a section of track at one end and detected at the other end by relay, as shown in Figure 18. When no train is present in a particular section the full current will flow through the track to the detector. As a train moves into the electrified section it will short the circuit and a low or zero reading will be observed by the detector. This will indicate that a train is present in that section.

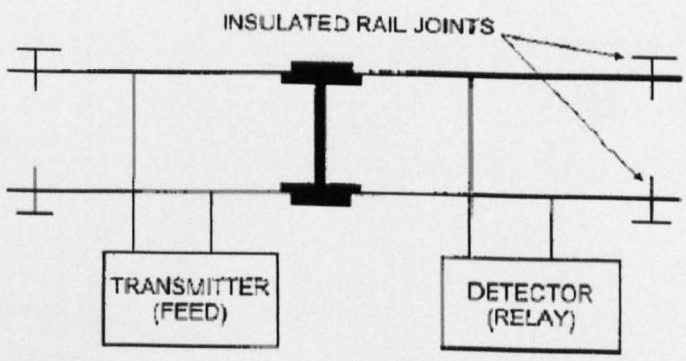

Figure 18 Schematic of detection system [Lewis, 2006c]

2.8.1 Effect of Contamination on Isolation

It can be foreseen that the presence of a foreign body within the wheel/rail contact could potentially form an insulating layer, and in a worst case scenario would cause an occupied section of track to appear vacant. It is clear from the literature that there has been little work carried out in this area of research. With an ever increasing range of products being put on to our rail network and greater amounts of traffic, it is felt that this is currently an important area of research.

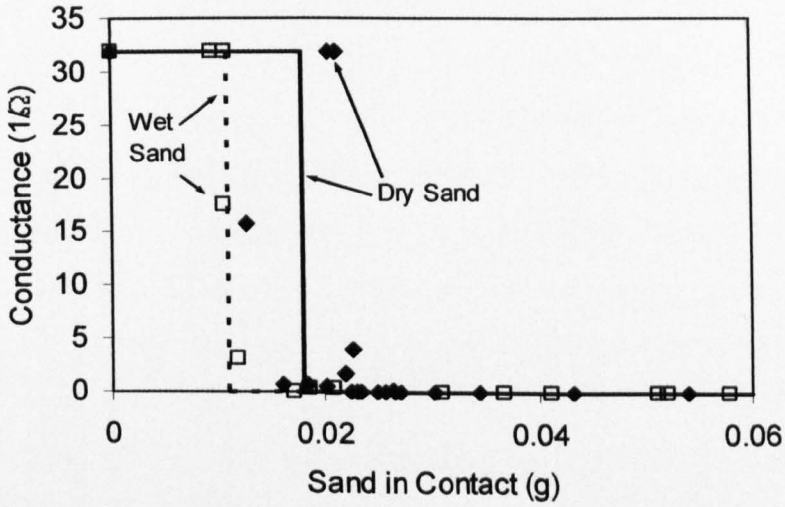

Figure 19 wheel/rail isolation caused by sand in the contact; static tests [Lewis, 2006c]

In [Lewis, 2006c] Lewis and Masing conducted experiments using contaminants sandwiched between two hydraulically loaded wheel and rail platens. The platens were sections of full-scale wheel and rail with contact patch assumed to be in the order of that measured by Marshal et al [2004] in figure 4. Contaminants used were sand and leaves. Tests with sand showed a critical mass of sand in the contact of 0.018g above which there was complete isolation. Interestingly the addition of water to the contact decreased this critical mass to 0.011g as in Figure 19. Dynamic tests [Lewis, 2003a] also confirmed the above findings. However, these values represent very high sand flow rates and are higher than those employed on the British rail network. Although this could become an issue at lower train speeds.

Arias-Cuevas et al, [2010b], studied the electrical isolation caused by sanding using a twin-disc tester. In this research two different types of sand were used. Silica sand which was

sieved to give 3 different particle sizes and filter sand which is typically used on railways in the Netherlands. The testing showed that the smaller particles could not only act as lubricants, significantly reducing friction, but could also cause complete isolation [Arias-Cuevas, 2010b].

Leaves showed good conductivity providing that they were broken down properly in the contact. Fresh leaves showed good conductance. However, dead leaves (most likely to be found on the rail) did show isolation problems due to lack of moisture. A mixture of sand and leaves was also tested. However, the sand lowered conductance levels and it was unclear [Lewis, 2006c] as to whether the low voltage could be properly received by the detector. Dynamic testing of sand with relation to isolation was also tested using a twin-disc machine [Lewis, 2003a]. As in [Lewis, 2006c] a transition exists in the sand flow rate into the contact where complete isolation is seen. This value is, however, higher than rates currently used in practice. Static laboratory tests [Lewis, 2006c] have shown that fresh leaves conduct current after they have been crushed by the wheel. Figure 20 shows the loads (18 – 30 kN) at which various types of leaves are crushed and metal to metal contact happens allowing conductance. However, dead leaves showed some isolation. As sand application is a common treatment for leaves on the line, a mixture of sand and leaves was also tested. This showed that adding sand to the contact increases the load required for complete conduction from 18-30 kN as in Figure 20 to approximately 50 kN. This severely increases the chances of isolation occurring when leaves and sand are both present in the wheel/rail contact.

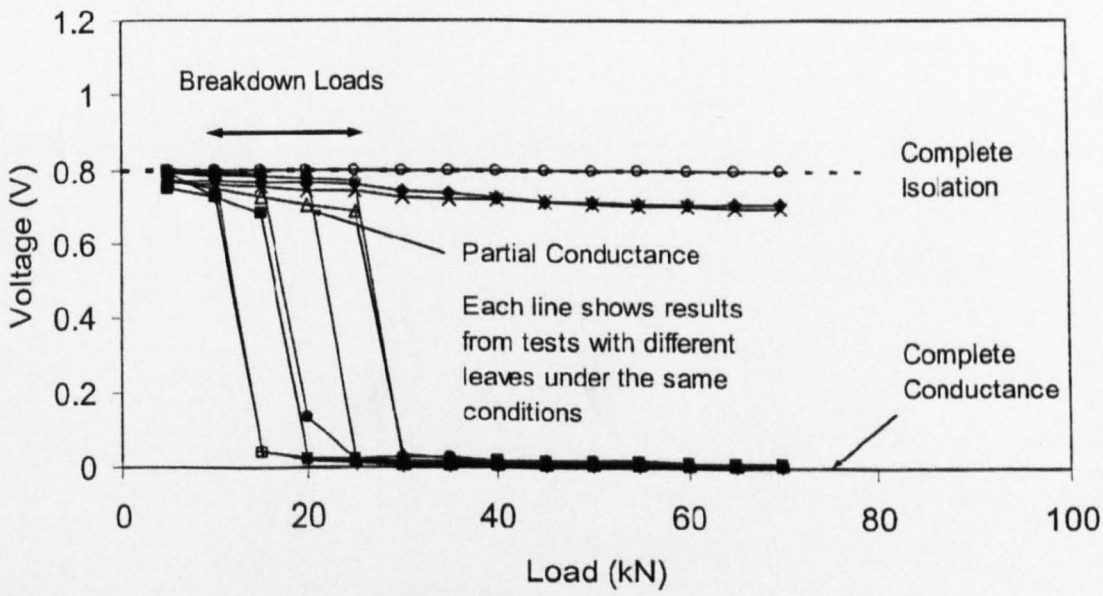

Figure 20 Isolation caused by leaves and the relationship between contact load and voltage across the contact [Lewis, 2006c]

Lewis et al, [2009a] studied the effects of friction modifiers on wheel/rail isolation. A twin-disc method was used with the solid HPF friction modifier. It was shown in dynamic and static conditions that the application of HPF had no influence on impedance levels as in Figure 21. This finding is understandable as solid friction modifiers do not cover the whole of the contact meaning there is still metal to metal contact. However, there are many liquid friction modifiers which are also used. A review of the literature shows that there has been little study on the isolation properties of liquid friction modifiers.

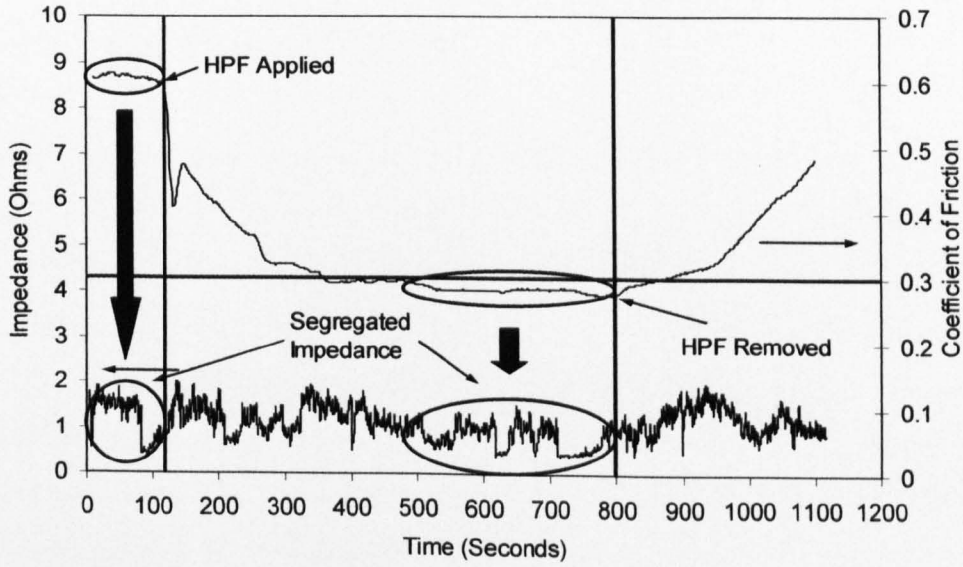

Figure 21 impedance at a twin disc contact when solid friction modifier is used [Lewis, 2009a]

2.9 Discussion

Contaminants in the wheel/rail contact affect the performance of the whole rail network by causing surface damage to the wheel and rail, altering friction levels sometimes beyond safe limits, causing wear, initiating rolling contact fatigue and causing signalling problems.

When high viscosity liquid contaminants or lubricants become entrained into the wheel/rail contact an Elastohydrodynamic (EHL) film will be formed between the two interfaces. This mechanism will reduce traction levels to below 0.1. This is beneficial during curving, when the contact will shift to the rail gauge / wheel flange where high wear rates may otherwise result. However, if such traction coefficients are present on the rail head then significant safety issues arise. It has also been observed that liquids can accelerate the rate of fatigue in

rails by a mechanism of 'fluid crack pressurisation' [Way, 1935]. There has been field and laboratory testing on this topic [Eadie, 2006; Fletcher, 2000a; Fletcher 2006]. However, the mechanism of 'fluid crack pressurisation' is complex and can be better understood by using modelling techniques such as fracture mechanics or numerical modelling [Kaneta, 1985; Bogdanski, 1998].

Modelling of solid particulate contaminants can be even more complex. The effects of the particles on friction/traction, wear and fatigue highly depend on how the particles break down as they are subject to the immense pressures of the contact. This in turn will depend on the size and mechanical properties of the particles.

There are two main methods of testing: field and laboratory. Field testing is the most useful as it is an exact representation of the issue, however, it is expensive and parameters such as slip and speed do not have the same controllability of laboratory based testing. Field trials are reported in [Broster 1974; Nagase, 1989]. Laboratory based testing can be split into two areas. These are full scale such as [Fletcher 2006; Eadie 2006] which provide a good approximation of the wheel/rail contact, but tend to be slow to run. The alternative is small scale testing which offers the greatest level of controllability, however, it does not replicate the actual wheel/rail contact to the greatest of accuracy. Examples of this small scale testing are [Cann, 2006; Oloffson, 2004; Lewis, 2005]. Twin-disc testing is a widely used example of small scale testing and due to its level of controllability can be used to run tests with variable: materials, contact pressure, slip and contamination types.

Data has been gathered from twin-disc testing [Lewis, 2005] to illustrate the relationship between traction coefficient and wear rate under the different types of contamination condition discussed in this chapter. Figure 22 shows the findings with Table 2 showing the test conditions of each contamination case. There is a clear trend of wear rates increasing with higher traction coefficients. Obviously the values of these wear rates will differ from ones which may be seen in the field. Thus, Figure 22 is intended as an illustration of the effects of different contaminant types. No data for wear rates seen under leaf contamination has been reported; however, damage caused by leaf stalks being entrained into contact has been reported but has not been quantified. It is important to notice that the wear axis in Figure 22 has a logarithmic scale and that the wear rate caused by oil is virtually negligible

compared to that of other contaminants. It can be seen in Table 2 that the tests with sand were performed under much more severe conditions than the other tests. It was reported in these tests [Lewis, 2006b] that a fatigue process was dominating over any wear process. It is thought that under comparable conditions the wear rates seen under sand contamination would be lower than those reported but still higher than dry wear rates.

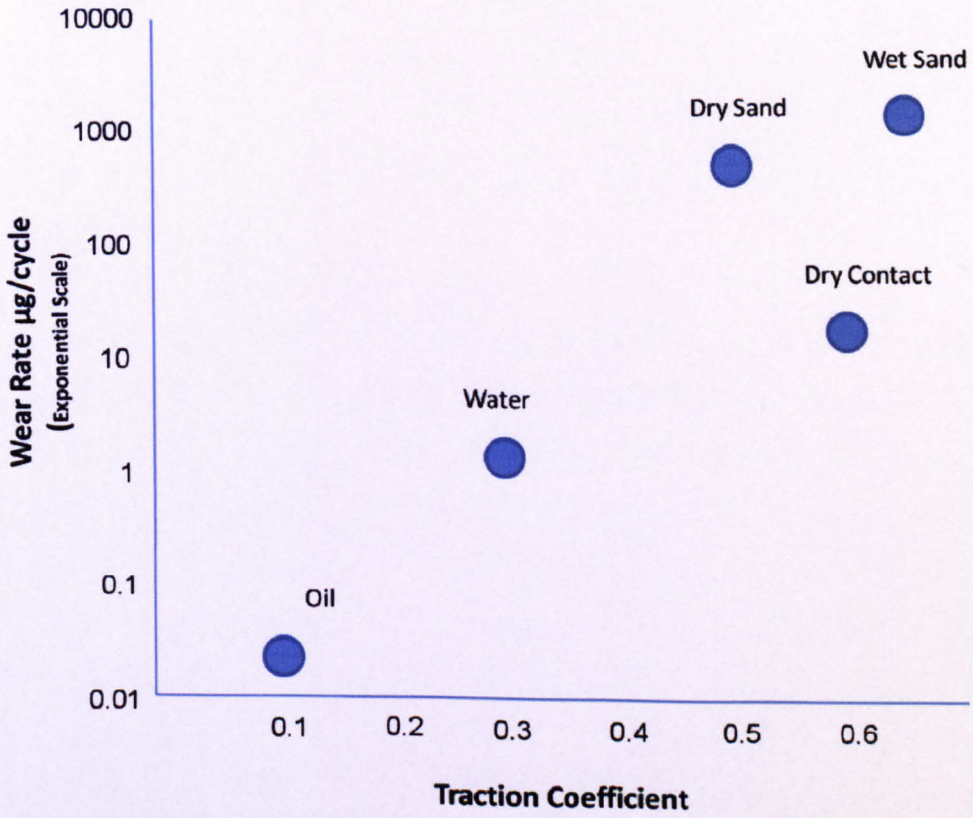

Figure 22 relationship between wear and traction coefficient under various contamination conditions

	Wear Rate (µg/cycle)	Test Conditions
Dry	21	400 RPM 1% Slip, 1500 MPa
Water	1.23	400 RPM, 1% Slip, 1500 MPa
Dry Sand	614.5	400 RPM, 20% Slip, 1500 MPa
Wet Sand	1082.8	400 RPM, 20% Slip, 1500 MPa
Oil	0.02	400 RPM, 1% Slip, 1500 MPa

Table 2 Wear data and test conditions (data from [Lewis, 2006b])

Managing the wheel/rail contact is of increasing importance. Friction/traction levels need to be controlled so that they are high enough to provide adequate acceleration and braking; but

also low enough as to avoid excessive wear. Wear can never be eliminated since there will always be metal to metal contact between the wheel and rail. However, it has been shown that wear can be a useful tool in the combat of rolling contact fatigue. Therefore a balance needs to be struck where the wear rate dominates over the much more un-predictable and far more catastrophic fatigue rate. A case in point would be the Hatfield rail disaster of 2000, where the rail failed due to unmanaged fatigue cracks.

Chapter 3: Development and Testing of an Alternative Technique for the Measurement of Railhead Friction

3.1 Introduction

For the optimum operation of a rail network, friction must be kept at correct levels. Friction must be high enough in times of acceleration and deceleration while at the same time low enough to give acceptable efficiency. Incorrect levels of friction not only lead to line delays and passenger inconvenience but can also lead to severe damage of rolling stock and infrastructure through wheel spins and skids.

Assessing the level of adhesion on live sections of rail can be impractical, requiring the use of large, cumbersome apparatus, and strict safety regulations to be followed. Furthermore, costs of full scale tests with instrumented trains [Nagase, 1989] can lead to large amounts of money wasted if developed or prototype products fail to perform. As a result, most testing is now done in the laboratory with methods such as: pin-on-disc [Olofsson, 2004], ball-on-disc [Cann, 2006] and twin-disc [Lewis, 2006b]. All of these tests offer a great deal of controllability of test parameters such as contact pressure, speed and slip, something not achievable in the field. However, field testing is still of great importance in order to validate laboratory tests. A tool which can be reliably used in either situation would be of great benefit to this field of research.

Friction on actual railway lines can vary widely often with no obvious cause. Of primary concern is when the friction level drops to dangerous levels below 0.1. These sites of low friction are often very localised and conditions can change rapidly back to safe levels of friction. Current methods for assessing railhead friction can often not be deployed quickly enough to assess the situation.

There is a requirement for a quick railhead adhesion level test method, which is portable and can be used either in the laboratory or out in the field. The test method described in this chapter utilises a pendulum slip resistance meter, as shown in Figure 23. The device was originally developed for measurement of road friction and currently used for the assessment

of flooring and pedestrian slips [Mills, 2009; HSE, 2004]. This is not the first time that such an instrument has been used to asses levels of railhead adhesion. In 2003, during trials performed in collaboration between Network Rail and ARUP [Brooks, 2003], such a rig was used on a section of MOD rail in Bicester in work to develop a stimulant leaf layer. However, limited testing was carried out and testing was not taken any further.

A variety of third bodies which are commonly found on Britain's rails were tested. These include: water, oil, leaves, leaf residue and friction modifiers. Friction results from these experiments are in good agreement with twin disc testing performed in [Gallardo-Hernandez, 2008].

3.2 Test Apparatus and Parameters

The pendulum rig was designed in the 1940's and widely used today as a road surface friction assessing tool in the cases of accidents or experimental road surfaces [BS EN 1306-4:2003]. The test is also used as a standard method of assessing slip resistance of flooring [AN/NZS 4586:2004].

The rig's mode of operation is described below; with reference to Figure 23.

1. the pendulum swing arm is held at its start in position (as in Figure 23) it is then released.
2. it then swings through a radius of arc equal to length (b)-(d).
3. the rubber slider (d) will strike the test specimen as it approaches 90° and will then slide in contact with it for 12.7 cm.
4. the pendulum is pivoted at point (g). The slider is mounted on a constant force spring, which runs up the hollow aluminium swing arm (c), ensuring a uniform normal reaction between the slider and specimen throughout the 12.7 cm contact period.
5. potential/kinetic energy of the pendulum will be lost as work done, as the slider rubs against the test surface. This is measured on scale (a) as the arm comes to rest on its upstroke.

A formula, derived by the pendulum manufacturer [BS 7976-1:2002], is then used to convert this "energy loss" into a friction coefficient. This formula has been derived for a contact

length, (the length that the rubber slider is in contact with the test surface) of 12.7cm (5 inches):

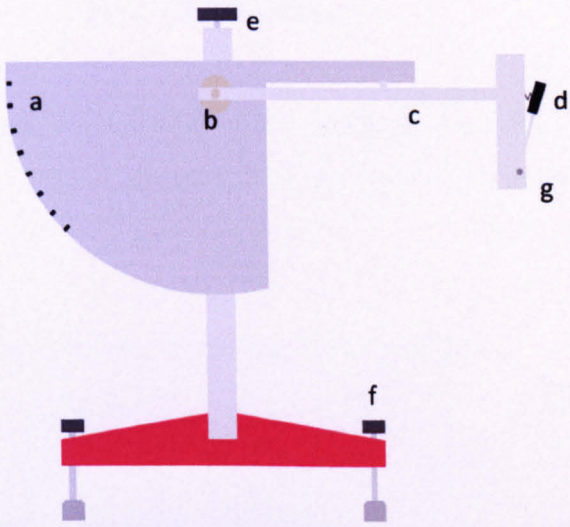

Figure 23 pendulum rig: (a) SRV scale; (b) height-adjustable pivot; (c) pendulum swing arm; (d) spring mounted slider (rubber pad attached here); (f) height adjustable feet

The Slip Resistance Value (SRV) can be converted into a friction coefficient using the following formula which has been specified by the pendulum manufacturer [BS 7976-1:2002].

$$\mu = \left(\frac{110}{SRV} - \frac{1}{3}\right)^{-1} \quad (3)$$

where μ is the friction coefficient and SRV is the slip resistance value as read from the scale on the rig.

The formula above has been derived specifically for a contact length, between the rubber pad and test surface, of 127mm (5 inches):

The rig uses two different types of rubber pad: Four-s and TRL. The, Harder, Four-s type rubber represents the heel of the average shoe and the TRL (softer pad) represents the heel of a foot. Rubber hardness is measured using the International Rubber Hardness Degrees, IRHD system. The harder rubber has an IRHD value of 96, and the softer 55 [BS 7976-1:2002]. The hardness test used in the IRHD differs from hardness tests on other materials like metals and

ceramics which measure the ability of the material to withstand plastic deformation i.e. indentation. Instead it measures the modulus of the rubber using a spherical indenter and observes the depth of indentation with a given force [BS ISO 48:2007]. The IRHD scale ranges from 0 (no modulus) to 100 (infinite modulus).

The majority of experiments described in this chapter all used the harder, Four-s type rubber, representing the heel of a shoe. However, tests were carried out with the softer pad for comparison purposes.

All tests have been performed at the following parameters:

- Strike length 127 mm
- Rail used was premium pearlitic rail steel

The section of rail was mounted under the path of the pendulum at a height sufficient to maintain a contact length of 127 mm. The rail was cleaned with acetone prior to each test and pad was cleaned and reconditioned using P400 paper. This ensured no transfer of material between each test.

3.3 Laboratory Pre-Tests

The aim of the pre-tests was to distinguish if the pendulum was suitable for testing on rail. It was also to determine optimum methods for application of contaminants, such as oil, water, leaves and friction modifiers for tests carried out in the laboratory.

The rig was used to measure friction coefficients for the above mentioned contaminant conditions. These were compared with data from twin disc tests carried out in similar conditions.

3.3.1 Application of Liquid contaminants

At first liquid contaminants (water, oil) were spread across the rail at a constant volume. This provided inconsistent results as some water would run off the rail (Figure 24a, b). More

consistent results were obtained by marking the contact area onto the rail head and distributing the contaminants within this area as shown below (Figure 24c, d). At this stage the time that the pad was in contact with the rail and the contact area between the rail and pad were determined

These preliminary tests also helped determine the volume of liquid to disperse within the marked contact. Water was syringed into the contact at 4ml and oil 3.5ml. These volumes equated to the amount of the specific contaminant which would fill the marked contact area. The differences in volume are due to the difference in density between oil and water. Friction modifiers were applied to the rail with a spatula as they were too viscous to syringe. Although this method of application gave little controllability in terms of mass of product applied; as there was a fixed contact length (127 mm), changes in how much product may have been squeezed between the slider and rail will have been small.

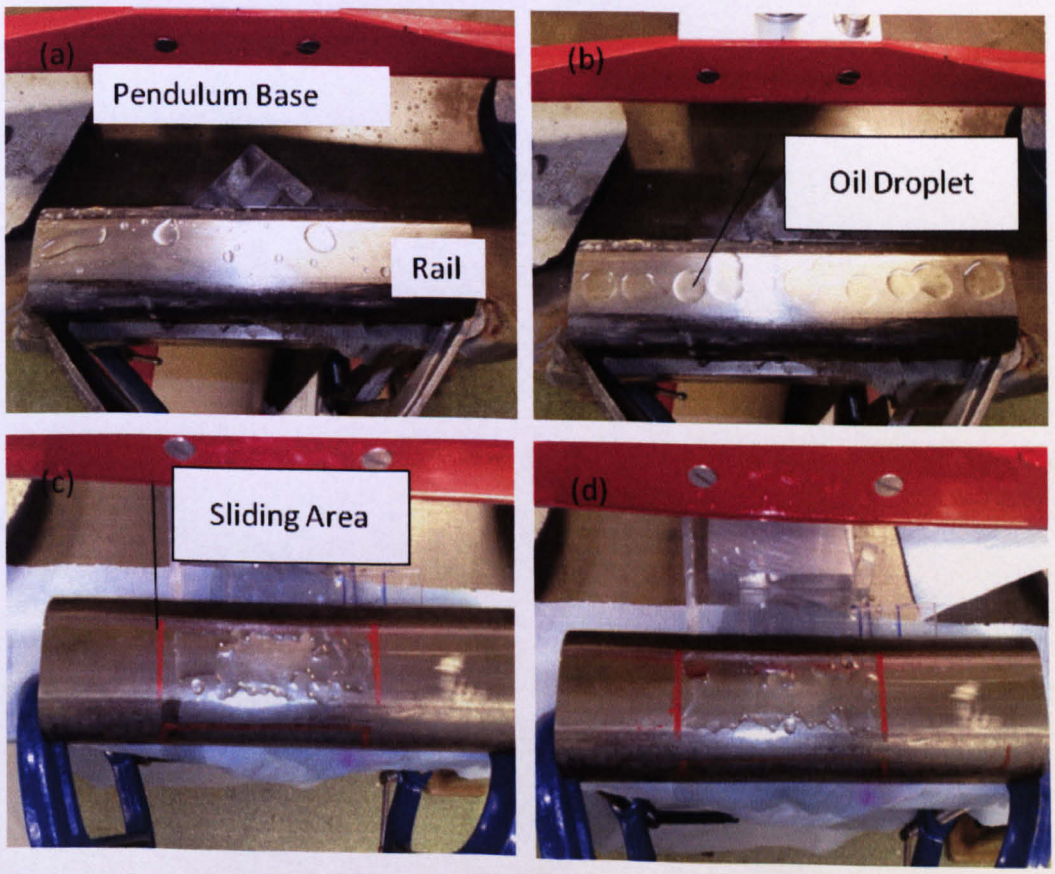

Figure 24 a) water spread along rail, b) oil dispersed along rail, c) water dispersed within marked contact area, d) oil dispersed within contact

Initially inconsistent results were obtained when testing with leaves depending on where the leaf was placed in the contact. Greater consistency was shown when the leaf was placed at the start of the contact. This ensured that the leaf was in contact with the rubber pad throughout the whole contact stroke. This method greatly increased consistency of the results.

3.3.2 High Speed Analysis

A high speed camera was used to observe the interaction between the contaminants and the pendulum. The setup of the camera is shown in Figure 25.

Figure 25 setup of high-speed analysis

The camera trigger was controlled via a laptop computer just out of view in Figure 25. Artificial lighting was used to increase the contrast and clarity of the video capture. The camera lens had a very narrow focal area and hence, captured only the part of the swing in which the pad and rail were in contact.

Observations of the interaction between slider and contaminant were also made using the high-speed footage. Footage of water and leaf contamination revealed quite interesting observations. It was shown that the leaf was swept along the rail by the pendulum with water being extracted from the leaf towards the end of the stroke, as shown in Figure 26. This helped to explain why there was more water left on the track after the pendulum swing than before the test. Footage of wet tests showed that the water gathered in front of the slider pad, creating a bow wave. Footage with water also showed that water would flow out from the open ends of the pad/rail contact toward the end of each stroke.

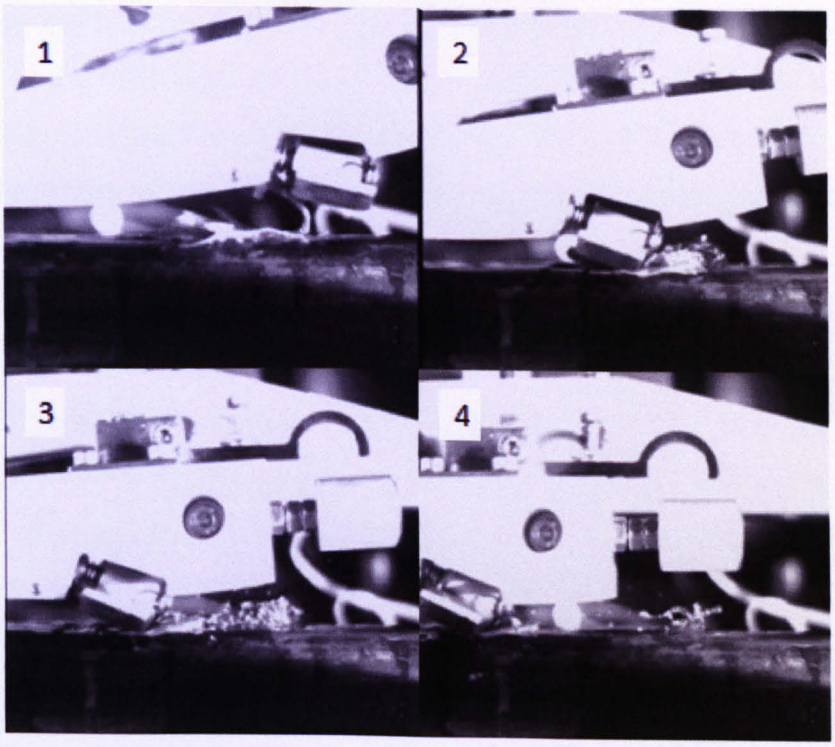

Figure 26 sequence of high-speed video with leaf and contaminant

3.3.3 Determining Dry Friction Levels

Humidity and temperature were measured during the initial tests and related to dry friction values. The changes in humidity were large enough over the period tested that a relationship could be detected and is shown in Figure 27. This clearly shows an inverse relationship between friction and relative humidity. This effect has been noted before in other research [Olofsson, 2004]. Variations in temperature measurements were not significant enough to affect friction readings.

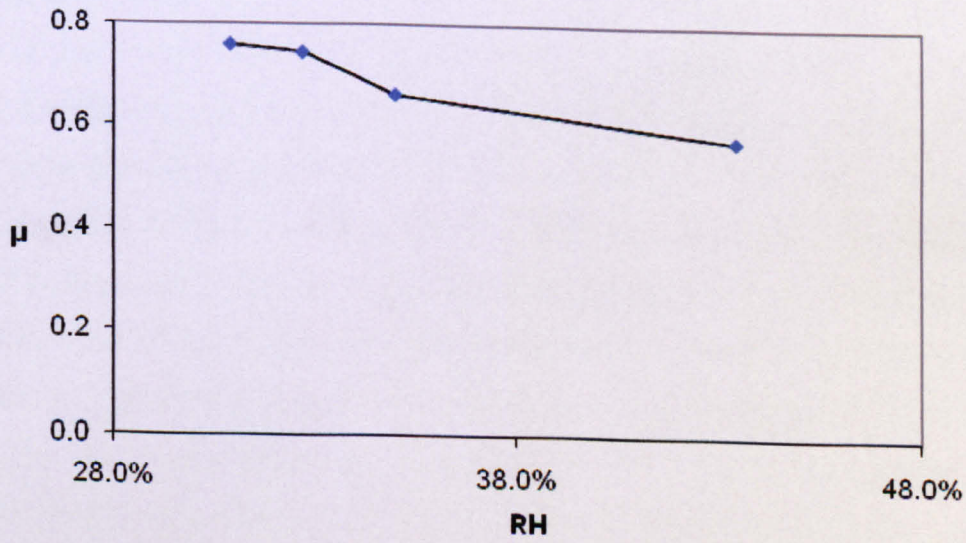

Figure 27 variation of dry friction readings with changes in relative humidity

Typical humidity levels in the laboratory are around 40% RH yielding friction coefficients in the range of 0.5 to 0.6. This compares very well with friction levels seen at the saturated slip region of dry creep curves developed during twin disc testing [Gallardo-Hernandez, 2006]. It is, at first, surprising that rubber-on-steel gives the same level of friction/traction as steel-on-steel. However, reference must also be given to the type of contact in both cases. In the case of the pendulum we have a pure sliding contact and a rolling/sliding contact. The traction value that has been used from the testing done by Gallardo-Hernandez et al [2006] to compare with the pendulum is from the saturation point of the creep curve. This is the point where full slip is established in the contact and thus equals the friction coefficient of steel sliding on steel (presuming identical contact parameters: speed, contact pressure etc). It is thus coincidence that the fiction of rubber sliding on steel is in the same region as steel sliding on steel for the contact parameters in both tests.

3.3.4 Comparison of Harder and Softer Pad

Table 3 illustrates the main differences in friction coefficient in tests comparing the hard and soft slider.

	C.O.F.	
	Four-s	TRL
Dry	0.67	1.2
Wet	0.25	0.14

Table 3 comparison of two rubber pad types under wet and dry conditions

The pendulum is designed to work with two types of slider; the harder Four-s and the softer TRL. It was obvious before testing that the TRL pad would give greater friction just by touch. The average dry friction coefficient yielded by the TRL slider was 1.2, approximately twice the average value yielded by the Four-s slider (0.67, new pad). A TRL slider was also tested on a wet rail and gave a friction coefficient of 0.14. This was lower than that yielded from the Four-s pad for the same conditions (0.25). The higher reading for a dry test with the TRL slider could be expected due to the greater hysteresis of the soft rubber compound used. The softer rubber will deform more easily and hence assist in the creation of a hydrodynamic lubrication film. For the reference dry conditions the Four-s slider gave friction readings closer to those seen in twin-disc tests. Therefore, this was the pad chosen for the main tests.

3.3.5 Worn versus New Pads

The pad does not strike the rail parallel i.e. face to face, instead it strikes at an angle (roughly 45°), with the trailing edge of the pad in contact with the rail. The rubber slider will wear when tested and this leads to a chamfer developing on the trailing edge of the pad. The manufacturer of the rig suggests that the pad be replaced when the chamfer reaches a length of 2 mm, as in Figure 28. Tests were carried out using both a worn and a new pad and data is shown in Figure 29. As the chamfer develops, the area of rubber in contact with the rail increases. It can be seen in the dry case that friction is higher for the old pad.

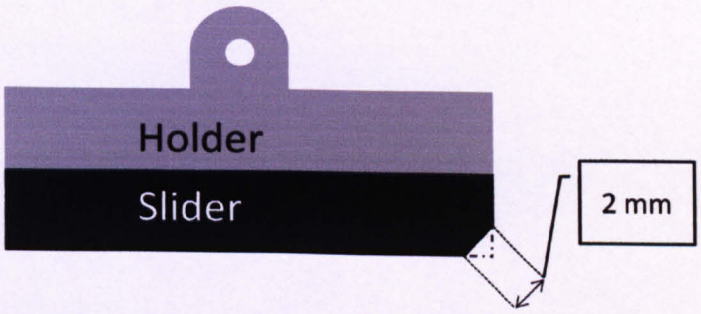

Figure 28 schematic of worn pendulum slider

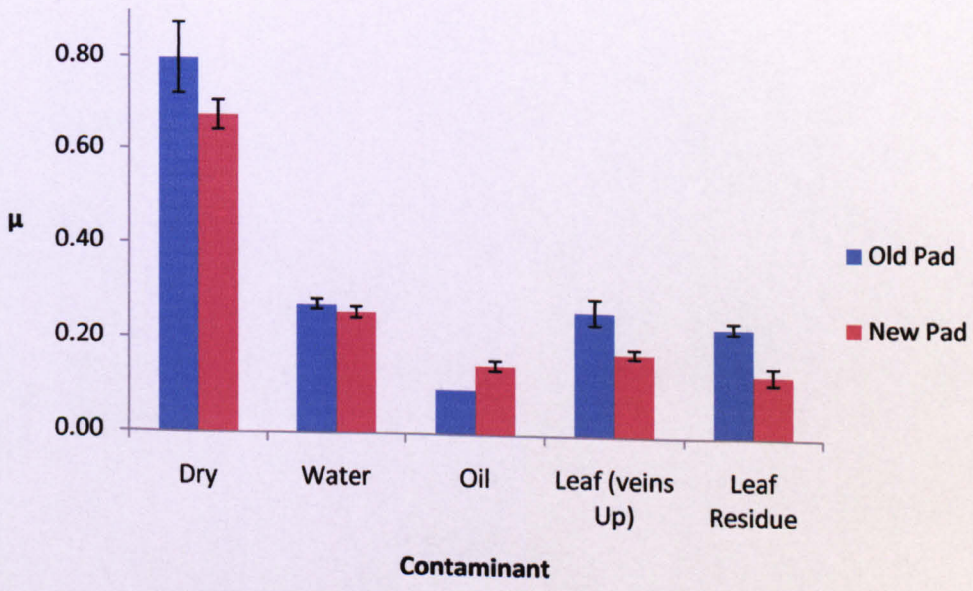

Figure 29 comparison of old and new pad data

This is true for all but the oil contaminated case where the trend is reversed as shown in Figure 29. It also shows that a new pad under the dry condition gives a friction coeficient closer to that seen for twin disc testing. This is of major significance for field testing where

testing is going to be mostly under dry conditions as any contamination will have been subject to the high pressure, temperature and sliding when rolled over passing trains. Thus if there is contamination present it will be in thin film form and moisture should be minimal.

3.4 Laboratory Test Methodology

Each test was carried out to the following procedure determined during the pre-test outlined in section 3.3. Firstly the rail was cleaned with acetone to remove any unintentional contamination. A new rubber pad was used and also reconditioned with P400 (abrasive) paper to ensure a consistent contact profile. This also acted to remove contamination from the pad. Contaminants were then dispersed into the contact as uniformly as possible. The pendulum was then allowed to swing and energy loss was recorded from the scale on the upward part of the swing. Before each test a dry control (no contaminants) reading was taken. This control value varied depending on the day and time that the tests were performed. Table 4 shows details of tests carried out including type and amount of contaminant used.

Test No.	Contaminant	Type	Amount	Proportion	No of Repeats
1	Dry	-	-	-	6
2	Water	Tap	4 ml	-	6
3	Oil	10W40 Motor Oil	3.5 ml	-	6
4	Oil Water Mix	10W40 + Tap Water	1 ml	0.5:0.5 ml	6
5	Oil Water Mix	10W40 + Tap Water	1 ml	0.25:0.75 ml	6
6	Oil Water Mix	10W40 + Tap Water	1 ml	0.75:0.25 ml	6
7	Trackside Transit Dry	Friction Modifier	-	-	6
8	Trackside Transit Wet	Friction Modifier	-	-	6
9	HIRAIL Dry	Friction Modifier	-	-	6
10	HIRAIL Wet	Friction Modifier	-	-	6
11	VHPF Dry	Friction Modifier	-	-	6
12	VHPF Wet	Friction Modifier	-	-	6
13	Sandite® Dry	Friction Modifier	-	-	3
14	Leaf	Sycamore (veins down)	-	-	6
15	Leaf	Sycamore (veins up)	-	-	6
16	Leaf Residue	Leaf residue	4 ml	-	6

Table 4 pendulum test summary

Due to the viscosity of the friction modifiers they were not able to be syringed, instead having to be spread on the railhead using a spatula. Despite this giving little controllability of amount of product applied or film thickness results showed an acceptable level of repeatability.

3.4.1 Results of Laboratory Tests

3.4.1.1 Dry

The average friction coefficient for an uncontaminated rail was 0.67 as shown in Figure 30. This is averaged for all dry tests done including the dry control before each contaminated test. The values ranged from 0.60 to 0.75.

3.4.1.2 Water

The water test dry control value averaged at 0.64. Results with water varied between 0.25 and 0.28 giving a mean value of 0.25, see Figure 30.

3.4.1.3 Oil

SAE multi-grade 10W40 Diesel Oil was used as the contaminant in these tests. This oil is typical of that used by diesel and diesel-electric locomotives which could potentially be leaked onto the track. The dry control reading for these tests was 0.62. The readings for oil varied between 0.13 and 0.16 with a mean value of 0.15 (See Figure 30).

3.4.1.4 Oil Water Mixture

It is plausible that an oil contaminated rail could be subject to rain fall. To simulate this oil and water mixtures were assessed in the following (water:oil) ratios: 50:50, 25:75 and 75:25 with 1 representing 0.01 ml, e.g. 25:75 represents 0.25 ml of water to 0.75 ml oil. It can be seen in Table 5 that the amount of water in the mix has insignificant effect on the friction level. It is also interesting that these results show lower friction than oil alone. Mean results are shown in Table 5:

	Mixture				
	Water	**Oil**	**50:50**	**25:75**	**75:25**
C.O.F	0.25	0.15	0.12	0.11	0.12

Table 5 oil water mixture results

Oil clearly has the overriding influence in the mixture, with results lying toward the oil end of the spread of results for oil and water alone.

3.4.1.5 Leaves

A Sycamore leaf was chosen for the main tests. The control test prior to the leaf contaminated tests gave an average value of 0.74. Values for the leaf varied depending on whether the veins were positioned toward the rail or slider. For tests with veins facing the rail readings were between 0.19 and 0.28 with a mean of 0.23, see Figure 8. For the case with the veins facing upward toward the slider, readings varied from 0.16 to 0.19 with an average of 0.17. However, in the field and small scale testing which more accurately represents the true wheel/rail contact, leaves will actually reduce friction similar to that seen under oil contaminated conditions [Olofsson, 2004]. It was clear from the high-speed footage that the leaf was simply been swept along the rail and in effect what the pendulum is really measuring is the friction from a leaf sliding on steel. However, in the actual wheel/rail contact or twin disc test the wheel rolls over the chemically reacted leaf layer [Cann, 2006] on the rail.

3.4.1.6 Leaf Residue

The leaf tested in section 5.5 was soaked in water for a 24 hour period. This soaking water was then syringed onto the rail head in the same manner as the pure water tests with friction ranging between 0.10 and 0.15 with a mean of 0.13, see Figure 30. This soaking water gave significantly lower friction than pure water showing that the soluble components of leaves have a large effect on lowering friction.

3.4.1.7 Friction Modifiers

Friction modifiers are products which are put on the wheel or rail to alter the friction characteristics of the wheel/rail system. Tests were done on four different types of friction modifier, including three Kelsan® products (Trackside Transit, HiRail and VHPF) and Sandite®. Sandite® is a mixture of water-based gel and sand, and along with VHPF is

designed to restore traction under levels of severe contamination. Trackside Transit and HiRail are designed to be placed on uncontaminated track and bring traction within a controlled range for better wear and energy consumption characteristics. The Kelsan® products were tested both wet and dry. For practicality reasons Sandite® was only tested dry. Results for each friction modifier are shown in Table 6.

	Friction Modifier				
	Dry Control	**T.T.**	**HiRail**	**VHPF**	**Sandite®**
C.O.F Wet	-	0.09	0.09	0.12	-
C.O.F Dry	0.68	0.41	0.49	0.72	0.52

Table 6 tests with friction modifiers

Figure 30 shows the mean friction coefficient obtained for each contamination condition both with the old and new pad. The error bars show the standard deviation shown in each case.

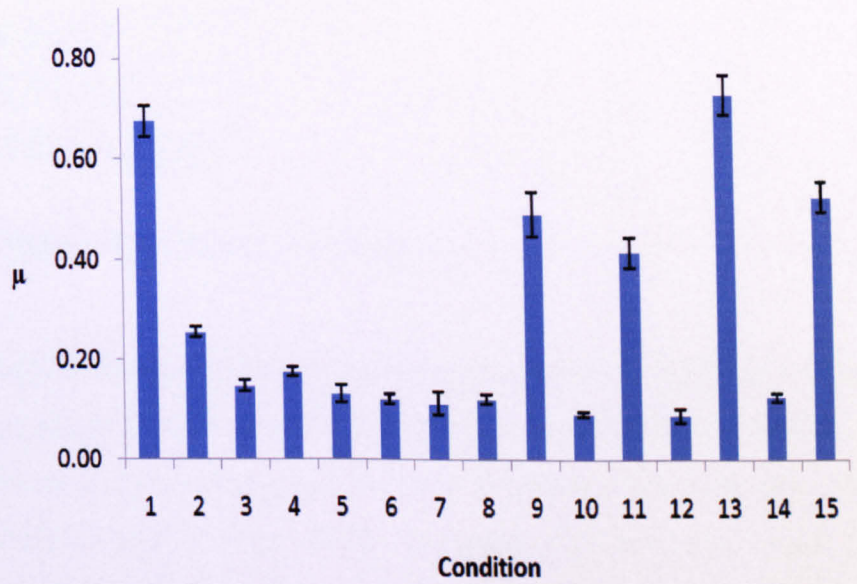

Figure 30 results of laboratory testing for various contamination conditions with old and new pad. Numbers refer to those in Table 7.

Test No.	Condition
1	Dry
2	Water
3	Oil
4	Leaf Veins up
5	Leaf Residue
6	Oil Water (50:50)
7	Oil/Water 25:75
8	Oil/Water (75:25)
9	HiRail (Dry)
10	HiRail (Wet)
11	TT (Dry)
12	TT (Wet)
13	VHPF (Dry)
14	VHPF (Wet)
15	Sandite® (Dry)

Table 7 contamination conditions

3.4.2 Comparison with Other Methods

There are marked differences between the operation of the pendulum (rubber/steel sliding contact) and the actual wheel/rail contact (steel/steel rolling-sliding contact). Despite these differences there is a good correlation between pendulum and twin-disc data taken from [Gallardo-Hernandez, 2006; Lewis, 2009b; Li, 2009]. Figure 31 and Figure 32 show creep curves generated from twin-disc tests.

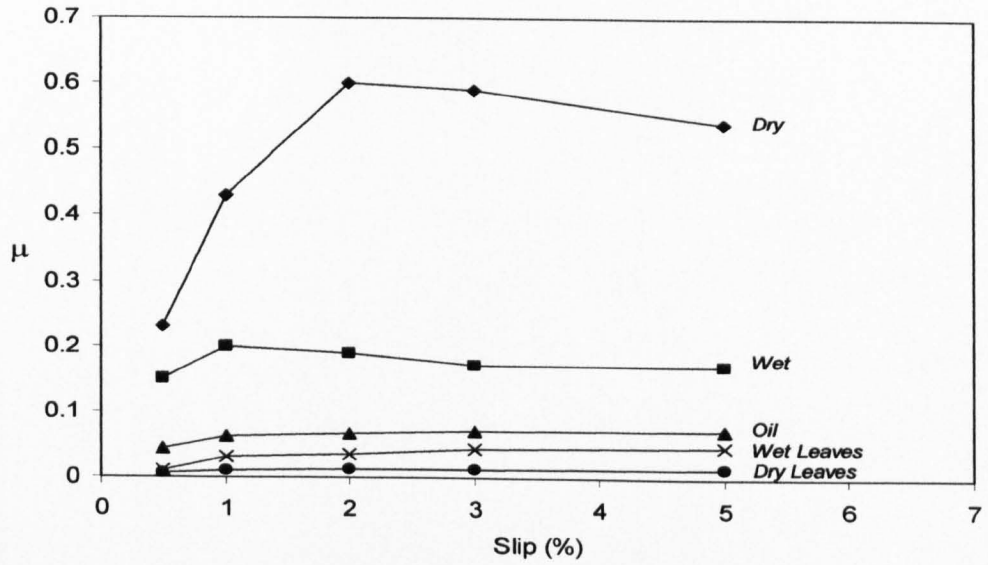

Figure 31 creep curves from twin-disc testing for a range of contaminants [Gallardo-Hernandez, 2006]

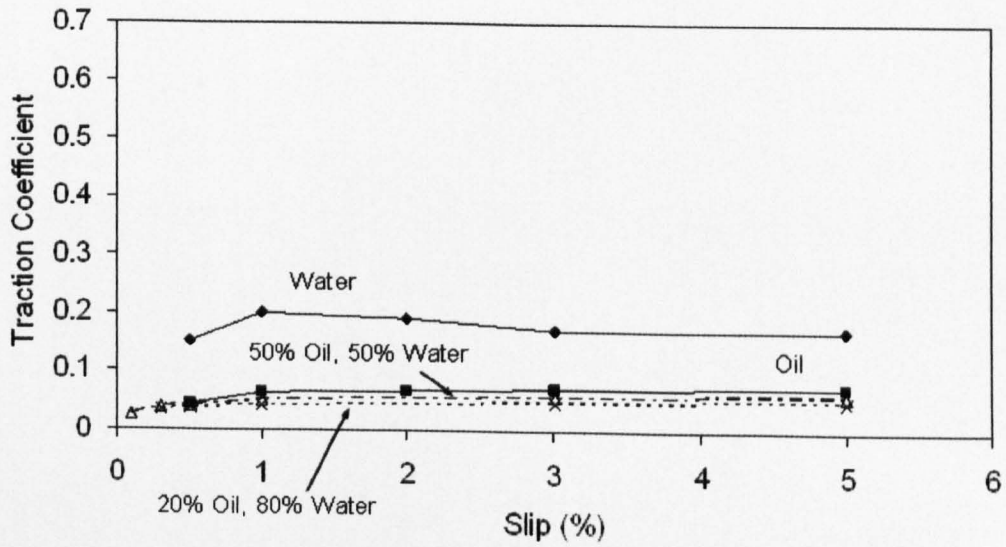

Figure 32 creep curve from twin-disc testing for oil water mixtures [Lewis, 2009b]

When comparing twin-disc data with that from the pendulum it is important to understand what is happening in each test, specifically the contact. In the case of the pendulum there is a pure sliding contact. However, in the case of the twin-disc test the contact is rolling/sliding and, as shown in Figure 33, what happens in the contact depends on the slip/creep (difference in relative surface speeds between the two bodies).

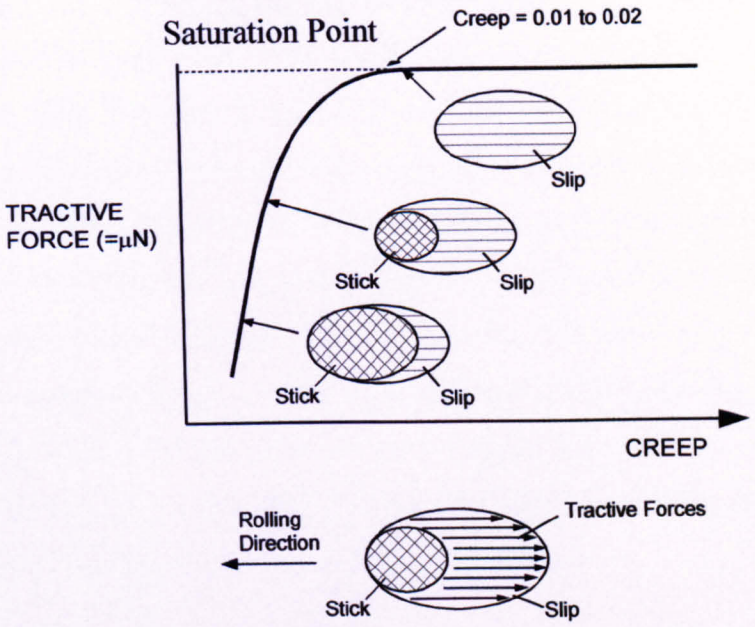

Figure 33 typical creep curve under dry, un-contaminated conditions

Figure 33 shows that the level of slip in a rolling/sliding contact increases as the creep increases reaching saturation point (full slip) between 1 and 2% creep. This point also corresponds with a peak in friction coefficient. This point is comparable to friction levels in the pure sliding that is seen in the pendulum test. Figure 34 compares friction data from the pendulum laboratory tests with saturation point values of twin-disc tests. The numbers refer to those in Table 7 .

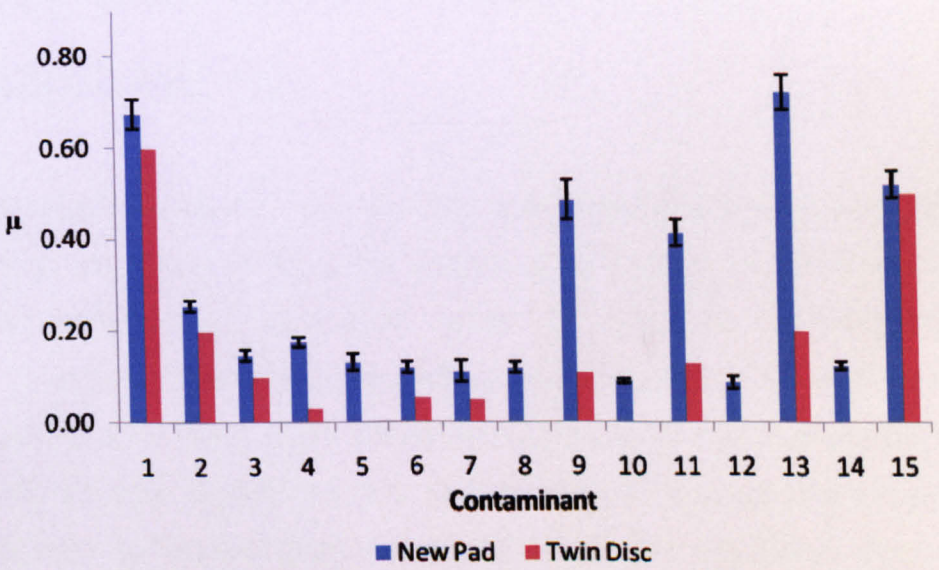

Figure 34 comparison between pendulum and twin disc data from [Gallardo-Hernandez, 2006; Lewis, 2009b; Li, 2009]

Figure 34 shows that four of the tested contaminant cases (Dry, Water, Oil and Sandite®) matched closely to twin-disc. This is in stark contrast to tests with leaves and friction modifiers. However, this difference becomes clear when looking at how the contaminants are entrained/applied in both test methods. The cases of water, oil and no contamination are evenly represented in either test method. However, the cases of leaves and friction modifiers are different. In the twin-disc test these contaminants form a thin film on the discs after being subject to high pressures and temperatures. It is therefore the friction of these films that is measured when using this technique. In the case of the pendulum test this film is not formed as the contaminants cannot be subjected to these unique temperatures and pressures. It is interesting to note in the Dry, Water and Oil cases that there seems to be an almost fixed error between the pendulum and twin-disc data as shown in Table 8.

	New Pad	Twin-Disc	Error
Dry	0.67	0.60	0.07
Water	0.25	0.20	0.05
Oil	0.15	0.10	0.05

Table 8 error between pendulum and twin-disc data

This error is quite large in terms of percentage (up to 50% in the case of oil). However, the actual error is almost fixed between the two test methods (i.e. 0.5 for water and oil) and this could be solved using a compensation factor. Taking this error into account there seems to be good correlation between the pendulum and twin-disc.

3.5 Pendulum Field Tests

With the pendulum laboratory tests showing good correlation against other techniques; the pendulum rig was tested on an actual section of railway on the Stockholm underground. Testing was performed on two separate sections of track. One was being treated with the Keltrack© (Trackside Transit) friction modifier and situated in a tunnel. This coincidentally was the same product tested in the laboratory. The other was an over-ground section which had been wetted from rainfall. The two sections of track were simultaneously tested with a Salient Systems Tribometer [Harrison, 2002] to provide benchmark data. A section of replaced rail from the underground test was also taken to the laboratory and tested with the pendulum. The underground (friction modifier) track was measured with the Tribometer in

100m sections and a total of 700m was tested. The track was on a shallow curve and both the inner and outer rails were measured. It was not practical to test all 700m of track with the pendulum. It was therefore decided to measure the two spots where there was the largest difference in Tribometer reading with the pendulum. The data from the Tribometer indicated that the largest differences in friction reading were seen at the 200 and 700m sections on both the inner and outer rail (outer indicating the rail on the outside of the curve). The average friction readings for the inner and outer rails are summarized in Table 9.

	Section	
Rail	200 m	700 m
Inner	0.71	0.54
Outer	0.48	0.36

Table 9 average Tribometer readings on Stockholm underground (friction modifier)

Tests on the over-ground (wet) section were measured by researchers at KTH university and results are analysed by the author. The measurements were taken at 3 points, 2 on the right rail and 1 on the left. Table 3 shows average friction readings from the Tribometer.

Rail	
Right	0.36
Left	0.4

Table 3 average Tribometer readings on Stockholm over-ground (water)

To provide a level platform a stand was constructed for the pendulum. This also raised the pendulum to the height of the rail. The stand was placed at the area of measurement and then the pendulum placed on top as shown in Figure 35. Once the rig was levelled and the correct strike length set, 6 consecutive swings of the pendulum were carried out to obtain an average friction coefficient for that spot.

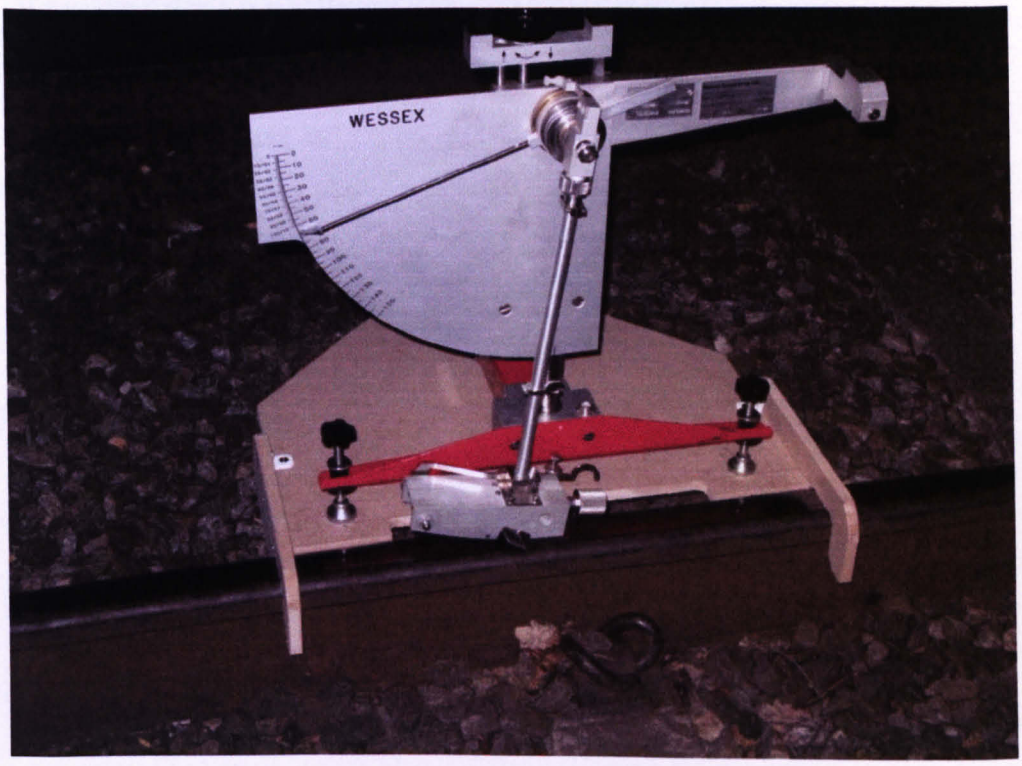

Figure 35 image of pendulum setup on Stockholm underground rail

The pendulum performed well on three out of four rail sections. However, at 200m on the inner line; no reading could be obtained from the rig. At this section the rig would judder when the pendulum slider came into contact with the railhead. Large variations in friction reading were accompanied by this juddering and the data could not be used. This phenomenon has also been witnessed in the laboratory and usually occurs after tests with oil. It was obvious during these tests that the rails were dry. However, when the rig was moved to the same section of the outer rail it functioned normally. It is interesting to note that this is the same section of rail where the Tribometer gave its highest reading (0.71) which is greater than would be expected for a rail dry or treated with Keltrack©.

3.5.1 Comparison between Pendulum and Tribometer on Underground Track

Pendulum readings and Tribometer readings for the three sections of underground track measured were compared (see Figure 36-38). The section of rail tested in the laboratory was also removed from the inner rail close to the 700m section and is also compared with field data in Figure 36.

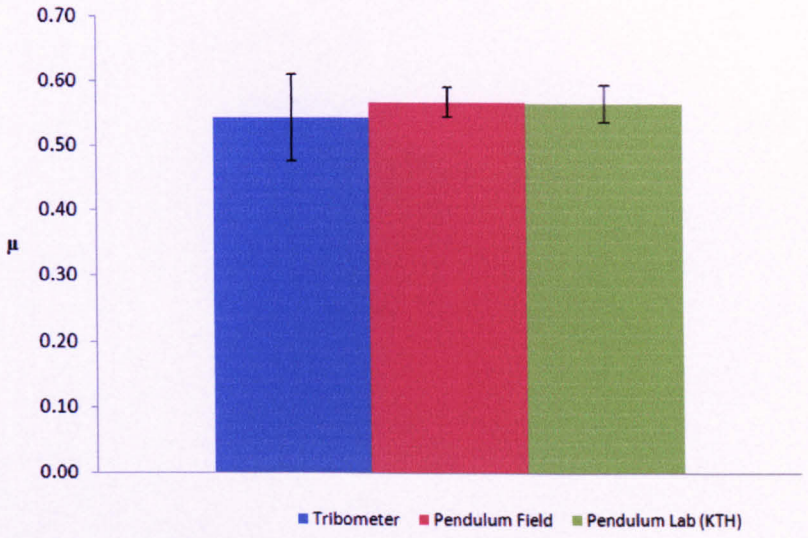

Figure 36 comparison of Tribometer and Pendulum readings at 700m on inner rail

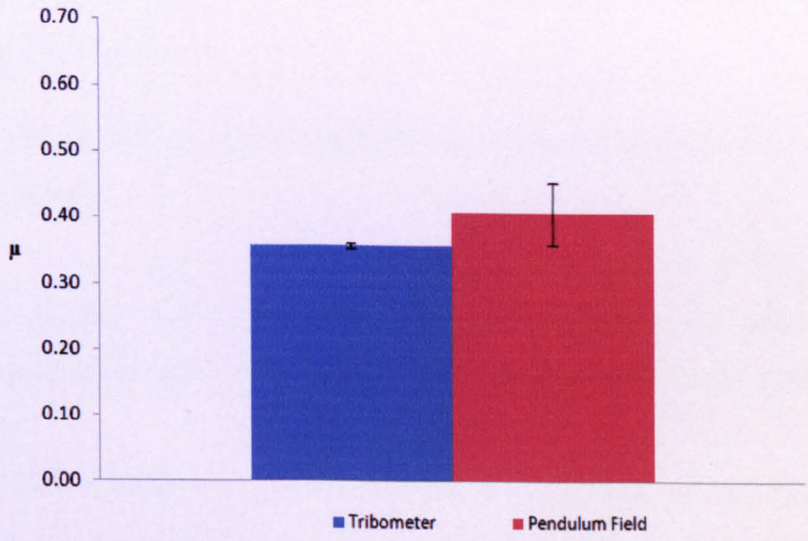

Figure 37 comparison of Tribometer and Pendulum readings at 700m on the outer rail

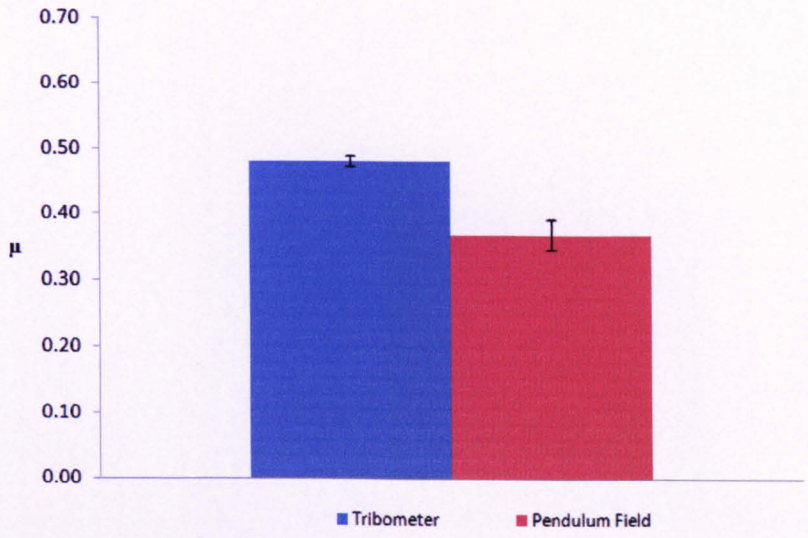

Fig. 38 comparison of Tribometer and Pendulum at 200m on the outer rail

Figure 36-38 show that there is little variation in reading depending on location regardless of the measurement technique.

3.5.2 Comparison of Pendulum Laboratory Results with Field for Underground Track

As the Stockholm track was treated with Keltrack®, results were also compared with (Sheffield) laboratory tests carried out with the same friction modifier (section 5.7, Trackside Transit) shown in

Figure 39. Note the pendulum field column shows the mean of the three tests on the underground.

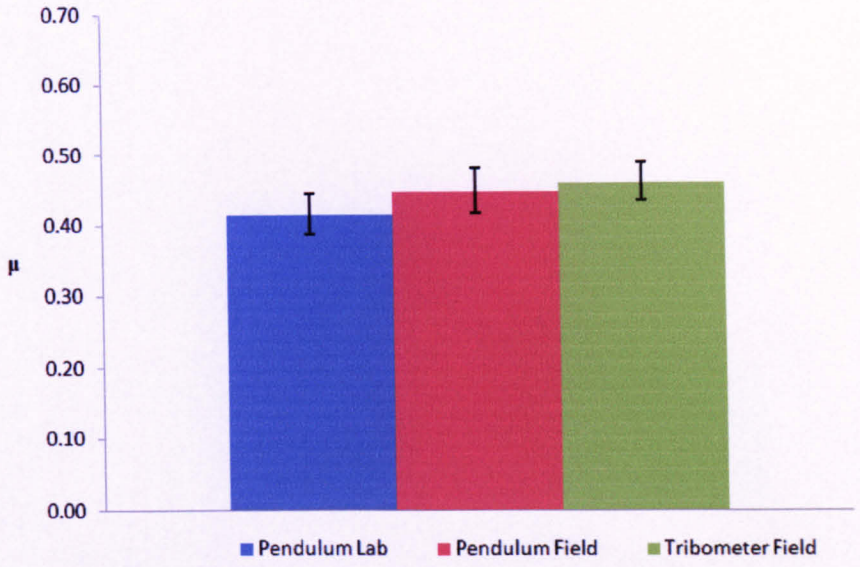

Figure 39 comparison of Keltrack® measurement in laboratory and field with average Tribometer reading

3.5.3 Comparison of Pendulum Field and Laboratory with Tribometer and Twin Disc Data for Over-ground Track

Measurements at the over-ground track were taken by researchers at KTH and results are compared with comparable data from the pendulum in the Sheffield laboratory (section 3.4) and twin-disc data. Results are shown in Figure 40-42.

It is interesting to note in Figure 40-42 how the pendulum laboratory and field results are close to each other for all three cases. The level of correlation is also surprising as the amount of water on the rail in the field was not controlled as had been in the laboratory. Both sets of pendulum data are also closer to twin-disc data than the Tribometer in each case. In the latter two cases the Tribometer friction coefficient is almost 0.1 above the pendulum data. This difference is quite significant and it is interesting that the Tribometer reading does not vary much between the three tests.

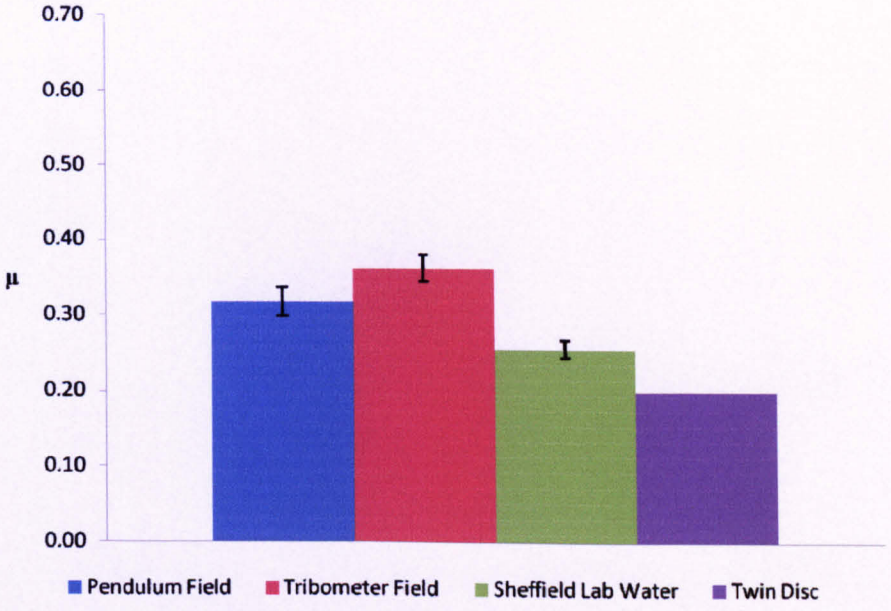

Figure 40 comparison of Tribometer and pendulum on right rail point A

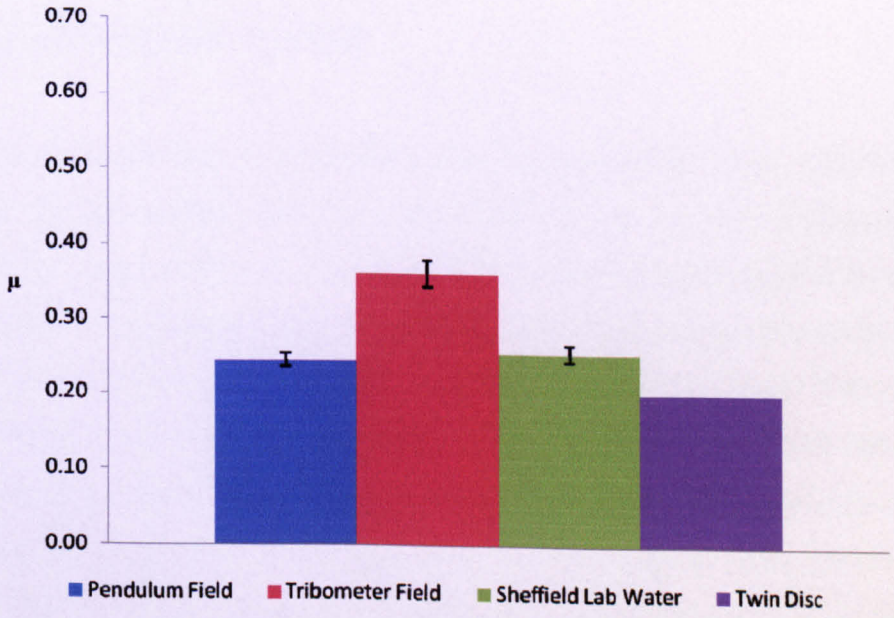

Figure 41 comparison of Tribometer and pendulum on right rail point B

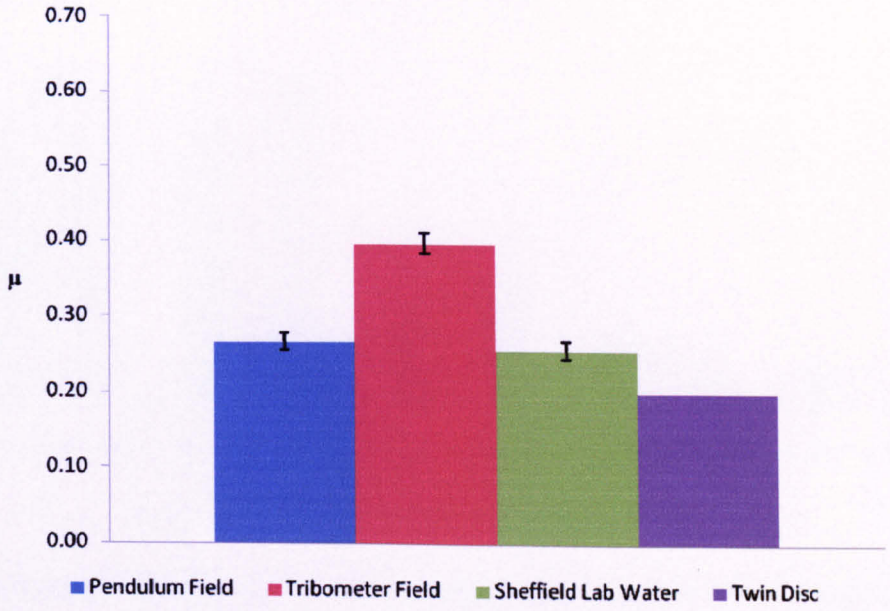

Figure 42 comparison of Tribometer and pendulum on Left rail

3.6 Further Laboratory Testing

Further laboratory based tests were carried out by researchers at KTH, and the results have been analysed by the author. The tests were carried out on two extracted sections of Stockholm metro track. Section A was clean with no black contamination layer. Section B had the black contamination layer on its running band. Black layers are usually formed by crushed leaves as in [Olofsson, 2004; Cann, 2006; Vasić, 2008; Li, 2009]. The track sections were placed in an environmental chamber so that humidity and temperature could be controlled. They were then tested with the pendulum at three different atmospheric conditions. A reference condition of 20°C at 30% RH was used to represent typical summer operating conditions on the Stockholm network. The other two conditions were 5°C at 68% RH and -2°C at 85% RH which are conditions where low adhesion has been reported. Figure 43 shows the results of the tests.

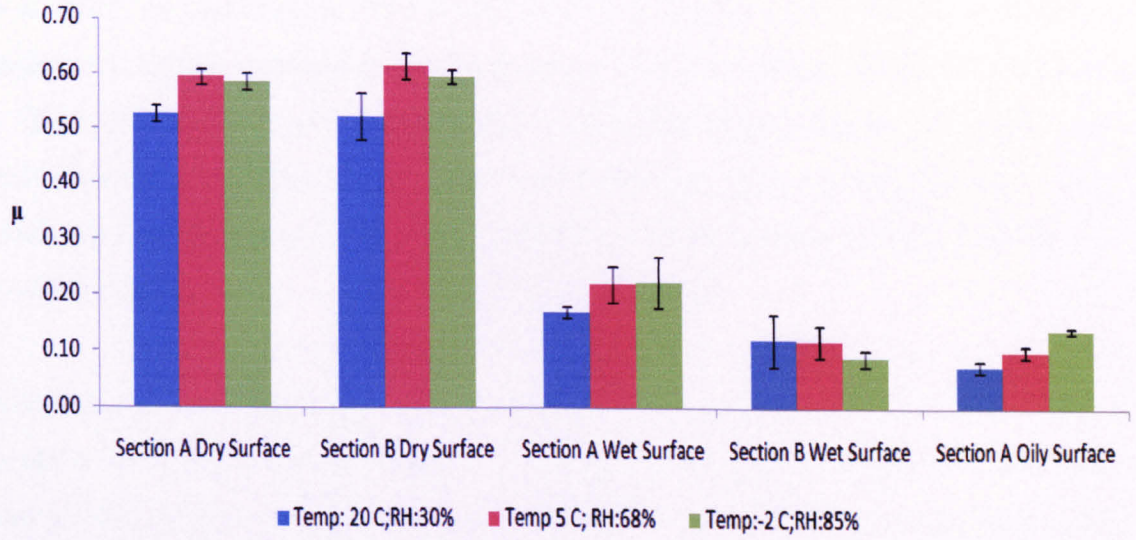

Figure 43 pendulum laboratory data on extracted sections of rail under different contamination and atmospheric conditions.

Leaf layers are only expected to present dangerously low levels of friction when wetted. When dry, leaf layers will lower the friction; however the friction coefficient should stay above 0.1. It is therefore surprising to see that the dry leaf layer yielded results almost identical to an uncontaminated rail as shown in Figure 43. For all surface contamination cases except the wet leaf layer case the friction is lower for the baseline condition than it is for the reported adhesion loss conditions. Under wet conditions, the contamination layer shows a significantly lower friction level than the clean rail. This is what is expected and the friction also reduces further under the conditions of reported adhesion loss. These results are also compared to that of a non-leaf layer rail with an oily surface. This shows that the wet leaf layer yields friction levels in the same region as an oil contaminated track.

3.7 Discussion

The Pendulum rig has been adapted from a road surface friction and floor slipperiness measuring device, to a railhead friction measuring tool. Laboratory tests have been undertaken to prove that the pendulum can reliably measure railhead friction under a variety of contamination conditions. Tests were also carried out with friction modifiers. Initial tests were performed to determine the ideal setup and develop a method for applying contaminants in a consistent manner and results from twin-disc testing [Lewis, 2009b; Li, 2009; Gallardo-Hernandez, 2008] were used as a benchmark. A high-speed camera was used to observe the interaction of the slider and contaminant and was also used to measure the speed of the slider

as it struck the test surface. The pendulum is designed to work with sliders of two different hardness's. It was determined that the harder of the two rubber sliders yielded results closer to that of twin-disc tests. Initially there was quite high variance in results with liquid contaminants. A solution to this was to evenly disperse a fixed volume of contaminant onto a fixed area on the railhead. This gave satisfactory levels of repeatability. This shows that the set-up is critical.

It is, at first, surprising that rubber-on-steel gave the same level of friction/traction as steel-on-steel. However, reference must also be given to the type of contact in both cases. In the case of the pendulum we have a pure sliding contact and a rolling/sliding contact. The traction value that has been used from the testing done by Gallardo-Hernandez et al [2006] to compare with the pendulum is from the saturation point of the creep curve. This is the point where full slip is established in the contact and thus equals the friction coefficient of steel sliding on steel (presuming identical contact parameters: speed, contact pressure etc). It is thus coincidence that the fiction of rubber sliding on steel is in the same region as steel sliding on steel for the contact parameters in both tests. To yield a friction coefficient of 0.6 from steel-on steel contact not only does there need to be a rolling-sliding contact but the creep needs to be sufficient enough to cause saturation in the contact i.e. between 2 and 3% as in Figure 33.

Laboratory results show good correlation for contamination cases which can be easily replicated in the laboratory i.e. dry, water and oil. Even though there is not an exact match between the two sets of data, there seems to be a fixed difference between them. This difference could be adjusted for by using a compensation factor or by adjusting the strike length of the pendulum. It was concluded at the time of testing to stick with the manufactures setting to which the rig was calibrated as this did match the closest to twin disc data. Note that at all other lengths apart from 12.7cm the friction will be false, as the formula used to convert is calibrated to 12.7cm.

Other contaminants tested in the laboratory could not be fully represented as they would be in the field. For example in the field (or the twin-disc test) leaves are rolled over and crushed by the wheel. The leaf becomes subject to extreme pressures and flash temperatures and as a result a chemical reaction occurs between the leaf and the rail [Cann, 2006] and a black low

shear strength layer is formed on the rail head. This leaf layer cannot currently be produced on a section of rail in the laboratory. This is the same for other contaminants tested which did not match up to twin disc data (oil/water mixtures, friction modifiers and leaves). Hence in these test conditions the contaminant/friction modifier was not represented as it is in the field.

The trailing edge of the rubber slider will wear leading to the formation of a chamfer, see Figure 28. The slider strikes the test surface at an angle of approximately 45° and hence any chamfer will increase the area of contact between the pad and rail. It is given that friction is independent of surface area. However, tests carried out with a worn pad yielded significantly higher friction results than a new one under a dry condition. It may be the case here, however, that that the worn surface area has a difference texture or the older rubber has chemically deteriorated. Changes in humidity cannot be ruled out. Figure 27 shows that friction coefficients can reach 0.76 at low humidity. No wear was observed with the new pad throughout testing. Also the wear rate of the pad will vary depending on contamination making it very difficult to calculate a wear rate and suggest a pad life. It is therefore suggested that pad chamfer always be checked before testing and the pad replaced when the chamfer reaches 2mm as specified by the manufacturer.

It is clear in the results that there is variation in the readings given by the rig. Changes in temperature and humidity levels were suspected as the causes for these variations. Figure 27 shows that friction readings can be affected by modest changes in relative humidity. However, changes in temperature could not be investigated as it did not vary enough during testing to have noticeable effect on the readings. Changes in humidity and temperature as well as pad wear are variables that cannot be controlled by the user easily. It is therefore difficult to isolate the weightings of each factor on the pendulum reading. It is therefore suggested that further investigation is needed to understand this with the use of atmospheric chambers etc.

Tests were carried out with both types of the slider that the rig is designed to work with. The sliders are of two different hardness' measured using the IRHD system [HSE, 2004]. Test results indicated that the harder, Four-S, slider yielded results closer to those seen in twin-disc testing. It is therefore recommended that the Four-S slider be used for testing on rail related applications.

The pendulum is a cost effective and convenient alternative for measuring railhead friction in the field. Most conventional methods are time and resource consuming, offering little in the way of controllability when compared to their laboratory based equivalents. There are two main methods of field testing, the first using actual locomotives. These tests require a huge amount of planning and organisation time and railway vehicles offer little control. A recent alternative to this is the hand-pushed Tribometer which can only be used in the field. As such track access is still required. Although the Tribometer is not an exact replica of the wheel/rail contact it does offer a more accurate method for the measurement of railhead friction. Laboratory techniques include pin-on-disc and twin-disc testing both of which offer greater levels of controllability although, like the Tribometer are not true representations of the real wheel/rail contact. Again the pendulum itself is far from representing the actual wheel/rail contact; however, it has been shown in this investigation that it yields results close to those seen from twin-disc testing which is itself an accepted method for researching the wheel/rail contact. The pendulum is also a quick test method, and as it can be used in the field it offers a greater cost and time advantage over other field test methods.

The pendulum was taken to a stretch of track on the Stockholm underground for field trials. The track section was on a large radius curve and approximately 700m in length. The curve was being treated with Keltrack® friction modifier as was tested in the laboratory at Sheffield. The track was also being measured with the Salient Systems Tribometer so that there was a baseline to compare to. Four points were tested with the pendulum (two on either rail). Results matched well with the Tribometer for three of corresponding points tested. At 200m on the inner rail the pendulum failed to produce any repeatable data and would judder during each swing. This phenomenon was also witnessed in the laboratory usually after testing with oil. However, when the rig was moved to the same section on the opposite rail it functioned normally.

The best overall correlation with the pendulum and the Tribometer data was at 700m on the inner rail. At this point the Tribometer gave an average reading of 0.54 and pendulum 0.57. A section of rail from the proximity of this point was removed and tested with the pendulum in the laboratory with an average friction coefficient of 0.57. This difference of 0.03 was very small considering the difference in method of operation of the two different measurement devices. At the same section on the outer rail the Tribometer gave a lower value of 0.36 and

the pendulum 0.41 representing a difference of 0.05 still relatively small. At the final section tested, 200m on the outer rail the average result from the Tribometer was 0.48 with 0.37 from the pendulum; an error of 1.1. What is interesting here is that there is a large variation in readings depending on the position measured on the rail. Even so the pendulum results are in line with those of the Tribometer.

These results from the field were then compared with results from the testing at the Sheffield laboratory with the Keltrack® product. An average result for the laboratory testing was compared with a mean of both the pendulum and the Tribometer from the field tests. The correlation between these three averaged values is very good. The pendulum in the laboratory at Sheffield gave 0.41, pendulum field 0.45 and Tribometer field 0.46. It should be noted, however, that the friction modifier used in the lab at Sheffield had not been rolled over such as those films tested in the field.

A second field trial of the pendulum was performed by researchers at KTH on an over-ground section of the Stockholm metro network. The rail was wetted having being subject to rainfall. The rail was measured at three separate locations, 2 on the right rail and 1 in the left rail. The tests were again performed along with the Tribometer. In all three tests the Tribometer gave the highest reading with an average value of 0.38. The average reading for the pendulum, however, was 0.28. The reason for this significant difference is not clear, and may be due to the larger area covered by the Tribometer i.e. 3m as compared to 127mm for the pendulum. The pendulum readings from the field were compared to results from testing with water in the Sheffield laboratory (see section 3.4) and wet twin-disc testing data. In all three field tests the pendulum compared well with data from the laboratory and twin-disc testing.

A further series of laboratory tests were performed by researchers at KTH. These tests were carried out on two sections of extracted track from the Stockholm metro network. One of the rail sections was observed to have a black contamination layer, rail B. The other had a clean running band, rail A. The rails were measured in the KTH environmental chamber both dry and wet and at three different environmental conditions: a baseline and two conditions where adhesion loss has been reported. Under dry conditions both rail A and rail B showed the same levels of friction. In the wet condition, however, rail B showed much reduced levels of

friction compared to rail A. This was also the only case where the friction reduced when subject to the reported low adhesion atmospheric conditions. Tests were also performed on rail A under oily conditions and Figure 43 shows that the wetted leaf layer shows results very similar to this. Gallardo-Hernandez & Lewis, [2008] showed that a leaf contaminated contact gave similar traction levels to an oil contaminated one. However, there is an order of magnitude difference between the leaf contaminated friction levels from the pendulum and those seen in [Gallardo-Hernandez, 2008; Vasić, 2008; Cann, 2009] where a rolling/sliding contact was tested. Friction coefficients yielded from these rolling/sliding tests is in the region of 0.01-0.03, whereas the friction coefficients obtained with the pendulum ranged from 0.089-0.12. This difference can only be explained by the different mechanisms occurring between each test type. Firstly the pendulum is pure sliding test as opposed to the rolling sliding seen in twin-disc testing. Secondly the pendulum has a rubber slider.

It can be concluded that the pendulum shows potential as an alternative tool for the measurement of railhead friction. Within the testing contained in this chapter the pendulum has proven two of the benchmarks originally put forward. The first being a suitable alternative for friction measurement in the field, achieved due to its good level of correlation with the Tribometer. Secondly that it could be used successfully both in the laboratory and field, which again is shown by its correlation between laboratory and field data for the same contamination condition.

This is very close correlation for two different measurement tools; however, more field testing is needed with both of the devices under various contamination cases.

3.7.1 Calculation of HDL/EHL Film

A 2D form of Reynolds equation, adapted by Halling (see equation 2) [Halling, 1975] was used to study any hydrodynamic lubrication effects occurring between the slider and the rail. In this form Reynolds equation can be used to model lubricated contacts where there is a distinct difference in hardness between the two interface materials, i.e. rubber/steel. In this situation the soft slider material is able to deform, developing the conditions necessary for EHL to occur. At the loads and speeds the pendulum operates at, may not be possible to generate this film with a steel-on-steel contact.

$$h = 1.551\left(\frac{W}{B}\right)^{-0.2} E'^{-0.4}(R\eta U)^{0.6} \quad (4)$$

Where: B is the slider/pad width (m), W the total load on pad (N), E' is the reduced modulus, R is the pad contact surface radius (m), η is the absolute (dynamic) viscosity (Nsm^{-2}) and U is the relative contact surface velocity (ms^{-1})

Film thickness calculations were performed for the rig using the harder Four-S pad for the water, oil and wet friction modifier cases. Footage high-speed camera was used to calculate pad sliding speed. Calculated film heights were compared with the surface roughness (R_a) of the rail, and it was assumed that if the film height was smaller than the R_a of the rail then there would be no HDL film in the real case. The roughness (R_a) of the rail was measured to be approximately 1 μm. Film heights calculated for the water and oil cases are an order of magnitude smaller than the R_a of the rail being 0.03 and 0.02 μm respectively. Hence, it is assumed that there is no lubrication film in these cases. However, in the case of the friction modifiers, the greater viscosity resulted in average film thicknesses of 39.08 μm for Trackside Transit. VHPF, which is much more viscous, although it had a similar sliding speed, gave a film thickness of 360.47 μm.

It was thought that the softer rubber of the TRL pad would yield a greater film thickness as it could deform more easily than the Four-s. Data on sliding speed and other parameters were assumed to be the same as in the Four-s case and only the reduced modulus was changed due to the softer rubber. This was the case for the friction modifiers however results showed that there was no film in the case of water and oil. The film thicknesses calculated for the Trackside Transit was 108 μm and for VHPF 994 μm. All film thicknesses are shown in Table 4.

Film Thicknesses, μm		
	Four-S	**TRL**
Water	0.0319	0.0879
Oil	0.0209	0.0457
T.T.	39.08	108.00
VHPF	360.47	994.00

Table 4 calculated film thicknesses for pendulum with Four-s and TRL slider

It seems that the pendulum does not operate at enough speed or load to promote a HDL lubrication regime in the case of contaminants with relatively low viscosity. As it was calculated that there was no film for either water or oil it must be assumed that there is a boundary lubrication mechanism occurring in these cases as friction is lower than in the dry case. The case where a film is calculated is when there is a wet friction modifier. However, these friction modifiers are designed to work when fully dried and are only initially wet as they are spread on the railhead by a passing locomotive. Once the FM has dried the film thickness will be much smaller. It can be concluded thus, that there is no HDL seen when using the pendulum for any of the above tests where the contamination case has been accurately represented in the laboratory as it is in the field.

Chapter 4: Development of a Standard Test Method to Measure Performance of Traction Gels

4.1 Introduction

This chapter discusses the development of a standard test to assess the performance of traction gels and friction modifiers. The Sheffield University ROlling Sliding (SUROS) test rig was employed for this experiment and a traction enhancing gel was used. More information on the development of the rig can be found in [Fletcher, 2000b]. Traction enhancers are types of friction modifiers which are adapted to restore traction in situations of low adhesion such as leaf contamination. Traction enhancers usually consist of solid particles, usually sand, suspended in a carrying gel. Four different traction enhancers were supplied for this study, each with a different particle size, nominally 212, 415, 600 and 800 μm. Their performance was compared with that of Sandite® which is a similar product and is currently used on the UK rail network to combat low adhesion. Sandite® contains a much wider distribution of particles ranging from 300 to over 2000 μm and has been shown to perform well under leaf contamination by Arias-Cuevas et al, [2010b]. These traction gels consist of sand particles suspended in water based gel. The traction gel is designed to combat the low adhesion contamination layer commonly found on the rail network in autumn. The aim of the tests was to assess the effects of different sized sand particles on the performance of the traction gel. Previous testing using the SUROS machine has been performed to investigate the use of railway sanding and friction modifiers on factors including: friction [Li, 2009; Arias-Cuevas, 2010; Arias-Cuevas, 2010b], wear [Grieve, 2001; Lewis, 2005], RCF [Lewis, 2005] and isolation [Lewis, 2009a]. The SUROS machine offers an ideal compromise between scalability/representation of the actual wheel/rail contact verses controllability and measurement precision. Hence, the SUROS is a suitable test rig for this investigation.

4.2 Test Equipment

Testing was performed using the Sheffield University ROlling Sliding (SUROS) machine (schematic shown in Figure 44). This test rig consists of a Colchester Mascot lathe with an A.C. motor on the tailstock.

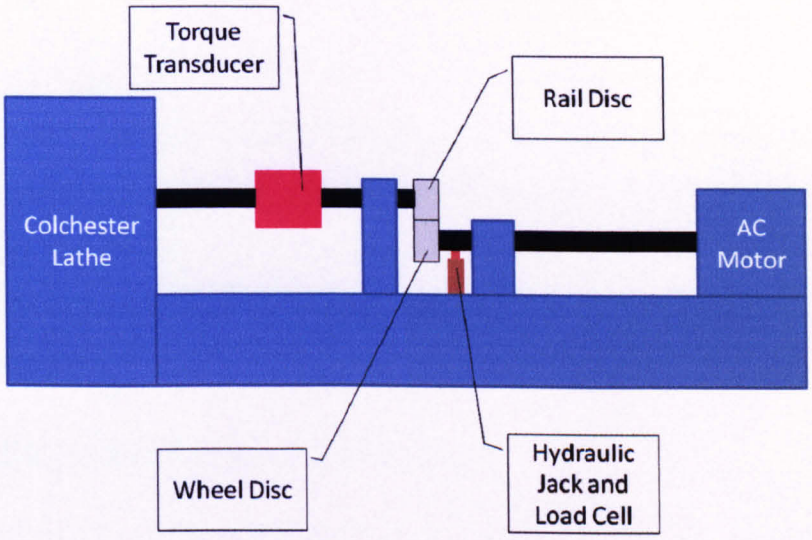

Figure 44 Schematic of SUROS machine

This arrangement allowed two 47 mm diameter discs to be loaded against each other and be independently driven. The discs are cut from sections of wheel and rail (R8T and UIC60 900A respectively) with the rail disc attached to the lathe and wheel to the A.C. motor. Details of the disc specimens are shown in Figure 45. The discs are independently driven allowing a certain amount of creep (difference between surface speeds) between the discs. A hydraulic jack forces the discs together to achieve a required contact pressure. The torque transducer on the lathe shaft allows tangential contact force to be measured and hence a calculation of traction coefficient can be made. For these tests the lathe was run at 400 RPM with 3% creep in the contact and 1500 MPa contact pressure. A creep of 3% (wheel driving) was chosen as it is to the right of the saturation point on the creep curve; representing conditions where a traction enhancer may be required.

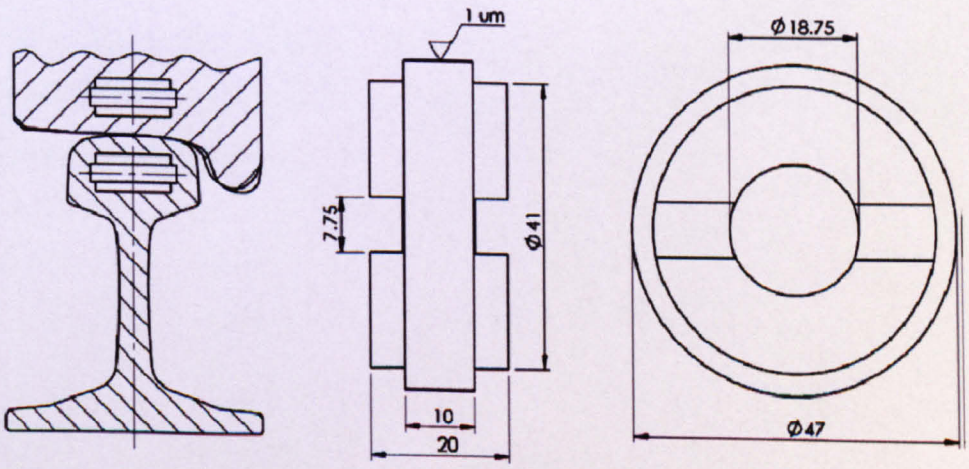

Figure 45 cutting positions and dimensions of SUROS specimens (dimensions in mm)

4.3 Trials

Initial trials were performed to develop a technique for building a consistent contamination layer on the discs and a method of controllably applying the traction gel to the disc interface. In order to assess the performance of the traction enhancers a low adhesion environment needed to be created on the disc surface. Contamination layers in the field are generated mainly from leaf layers.

4.3.1 Developing Contamination/Leaf Layer

Vasić et al, [2008] experimented with techniques to form leaf layers using the SUROS rig. The best results were found by covering the running band of the rail discs with thin strips of leaf and then compressing with a jubilee clip. The discs were then left for up to 4 days. After this initial coating process the discs were run in the machine under conditions of pure rolling with continual strips of leaf fed into the contact. It was shown in that low traction levels (< 0.1) under leaf contaminated conditions only occurred when the leaf was wet. Under testing of these layers it was clear that the leaf film would be removed quickly unless moist conditions were maintained using a continuous mist spray or dripping water onto the discs. Although leaf layers were generated in [Vasić, 2008] it is clear that these would be unsuitable for the tests in this chapter due to the need for a constantly moistened environment. The artificial creation of moisture could skew the results as the traction enhancers may potentially be subject to varying amounts of water. What was needed for the tests in this chapter was a durable dry leaf layer. For these tests a supply of fresh sycamore leaves was sourced. Sycamore leaves are commonly found line side and have been used in [Li, 2009] and [Arias-Cuevas, 2010a]. To apply to the disc interface these leaves were turned into a mulch using a blender and mixed with water at 50% by weight. This mixture (leaf Mulch) was then injected into the contact as in Figure 46.

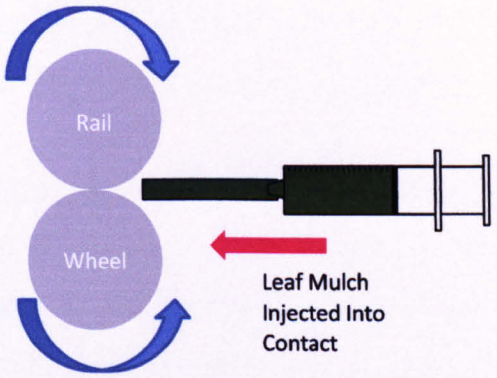

Figure 46 illustration of leaf mulch added to contact

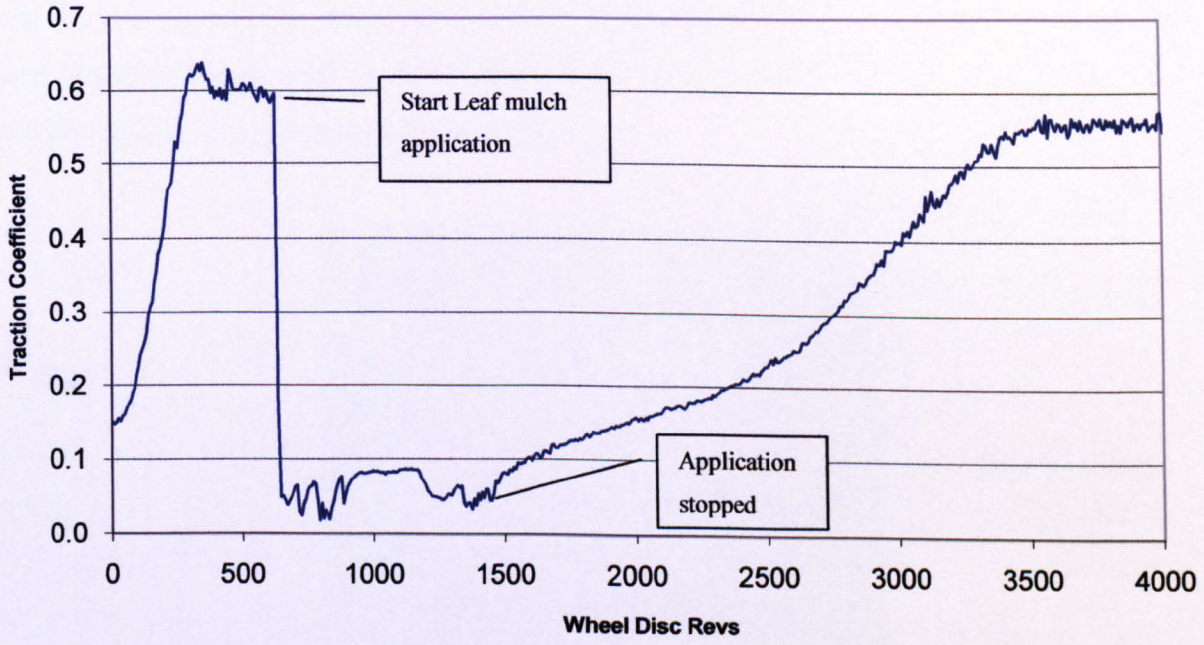

Figure 47 friction vs. wheel disc revolutions for leaf mulch application

Figure 47 shows the friction curve for the application of the leaf mulch. The test was run at 1500 MPa and 3% slip. The Dry friction was allowed to reach saturation (0.62) and then the leaf mulch was applied. The point at which the leaves were applied can be clearly seen as a sharp drop (almost instant) in the traction coefficient. The COF observed during leaf application was 0.04. The large fluctuations were due to the syringe blocking and hence an uncontrolled flow rate of mulch into the contact resulted. Mulch was applied for approx 1.5 minutes. The application of mulch was then stopped at 1500 revolutions and the discs run until dry values of friction were attained. It is clear that a contamination layer has been formed because of the slow rate of friction increase after the leaf application compared to the initial saturation gradient. However, no black layer was seen on the discs.

This technique proved inconsistent as the syringe would frequently block meaning it was difficult to provide a constant flow of leaf mulch to the contact.

A solution was found by painting the leaf mulch onto the rail disc and then running the rig at half load and 0% creep to generate a layer. The viscosity of the mulch was thickened to a consistency resembling a paste by adding Carboxymethylcellulose CMC to the leaf mulch. Cellulose is also a major component of leaf layers, as found in Cann [2006], however the amount added to the leaf mulch was thought to be insignificant to effect the results being less than 1% of the overall mixture. This allowed the mulch to adhere to the disc and resist centrifugal forces as the discs were rotated. Trials showed that 3 layers of contamination layer needed to be applied via this method to provide a consistent layer. The prepared discs were then allowed to dry before being tested.

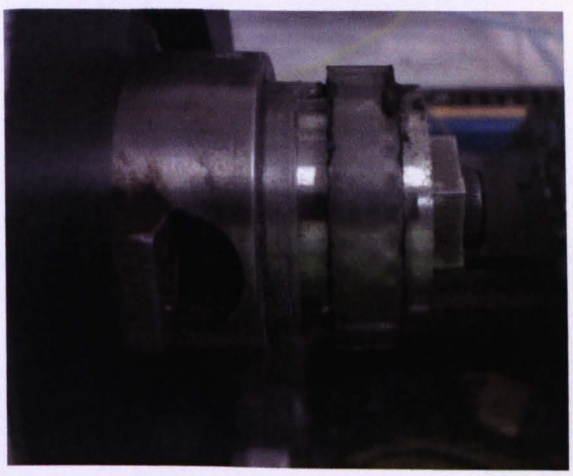

Figure 48 contamination layer on rail disc after 3 applications of leaf mulch

Figure 48 shows the dark contamination layer developed on the rail disc. In Figure 49 the traction curve for this dry leaf layer is compared to the curve for a dry, uncontaminated set of discs. Here a leaf layer was built up on the discs by the method described above. The contaminated disc was then run at 1500 MPa, 400 RPM and 3% creep to wear the dry leaf layer off. The hard wearing nature of the contamination layer is clear to see due to the longer time required to return to dry levels of friction. Even though this dry layer showed friction levels within the safe operating zone i.e. > 0.1, it is ideal for these tests due to its durability. The ability of each traction gel to remove this leaf layer and restore friction back to dry levels will be an indication of its performance. This method of generating a leaf layer was chosen for the main tests.

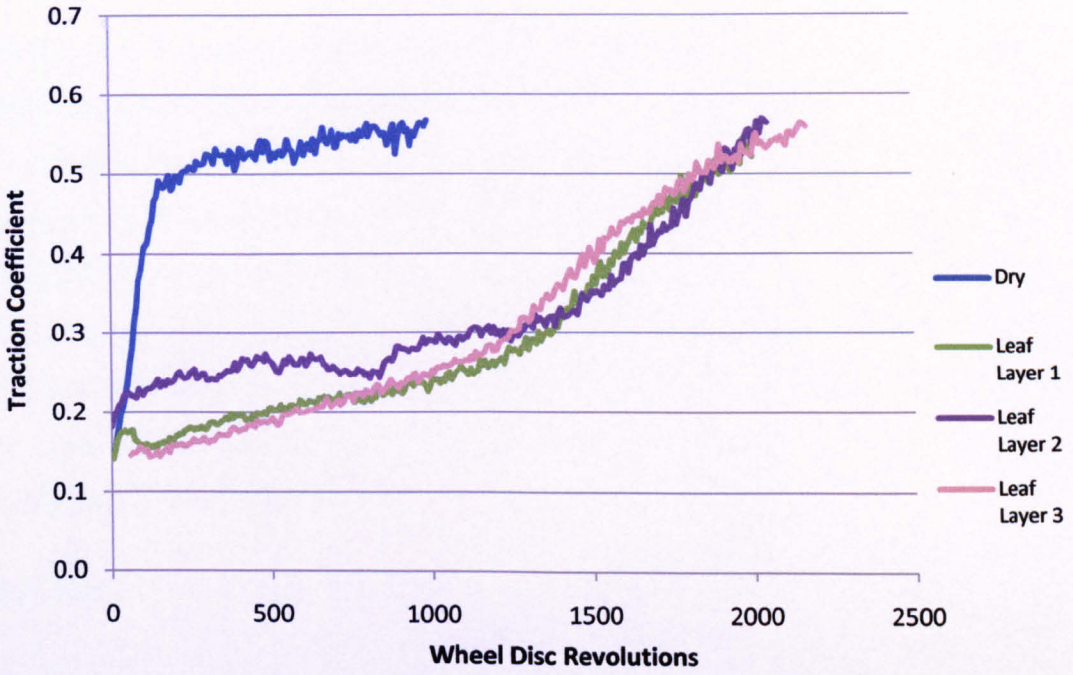

Figure 49 chart showing traction curve for discs with leaf layer compared to dry discs

Traction was recorded during the leaf build up stage when the leaves are wet. Traction coefficients are shown in Figure 50 for three different examples of leaf layer generation. The traction levels are extremely low during this stage and complementary to what has been observed/hypothesised by other authors [Vasić, 2008; Fulford, 2004] i.e. that leaf layers only present dangerously low (< 0.1) levels of friction when wet.

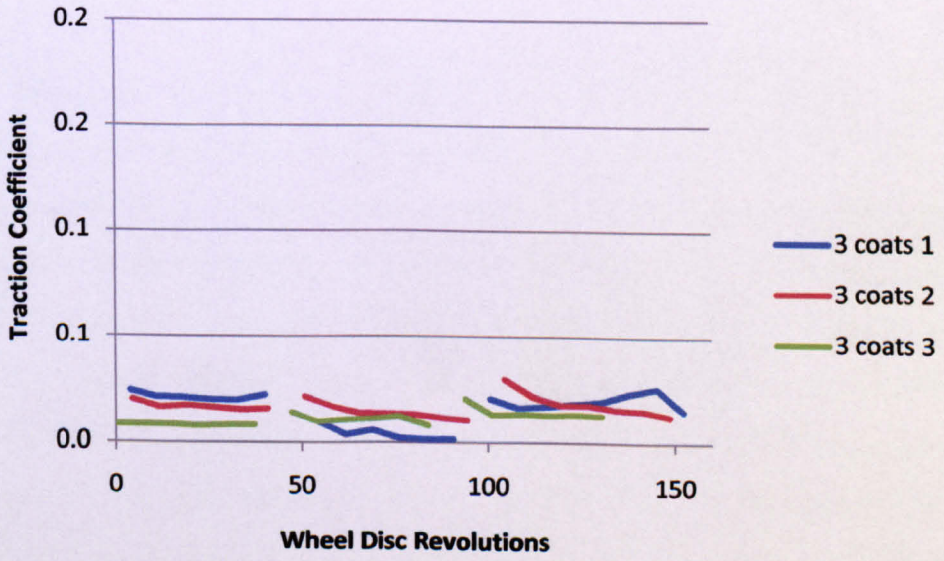

Figure 50 traction curves recorded during generation of leaf layer

4.3.2 Applying Traction Gel to Interface

In the field, traction gels are delivered to the rail head by peristaltic pump for both trackside and Multi Purpose Vehicle (MPV) application solutions. Thus it was decided to use the same method to deliver the gels to the disc interface. This did prove problematic however, as the traction gels would rapidly wear the pumping mechanism and regularly cause blockages. It was also difficult to manage the delivery tubes to the interface, as not all traction gel would enter the interface. It was decided to inject the traction gels on to the pre-contaminated disc surface prior to the start of the test as had been done with the leaf paste. In this way a fixed quantity could be delivered to the contact zone. This provided consistent results and was the method chosen for the final tests.

4.4 Results

Tests were run in two formats. The first looked at the effect of particle size with a fixed sand to gel ratio of 45% by weight. Gels were prepared at a fixed solid loading to gel ratio and a fixed volume of gel was applied to the tests discs. As the particles get larger therefore there will be less of them suspended in the gel. The second test series used the same gel composition (sand to gel ratio of 45% by weight) yet the volume of product applied to the discs was varied to give a fixed number of particles in each test run with varying particle size. Thus the volume of gel applied to the discs was increased as the particle size was increased.

4.4.1 Fixed Volume of Gel

Results for these tests are shown in Figure 51 which shows the traction curves for the different particle sizes including Sandite® as well as for dry disc and discs with a leaf layer only. It can be seen how the addition of the traction gel in all cases significantly improves the rate of increase in friction from the leaf only test. This gradient is close to that seen under dry cases. Both 212 and 415 μm particles bring the friction back above 0.5 (i.e. dry traction) within the time tested. Sandite® also shows similar performance to the smaller particles. However, 600 and 800 μm particles only bring the friction to 0.4 in the same amount of time 0.5 was eventually reached, but nearly 600 cycles later than the two smaller particles. This can be explained by the fact that larger particles are crushed in the contact [Grieve, 2001]. This crushing in itself will in effect lubricate the contact. Also larger particles do greater

surface damage to the discs. It was witnessed during subsequent testing how discs with damaged surfaces exhibit lower friction compared to those without.

There is also a very clear trend with the traction gels where the friction drops to around 0.06 just after the start of the test then begins to rise. This is the lubricating effect of the gel. Friction then increases as the gel evaporates from the contact. What is interesting to note here is that the lubrication of the gel is much more influential than the adherence of the sand particles i.e. the sand only starts to raise the friction once the gel has gone from the contact.

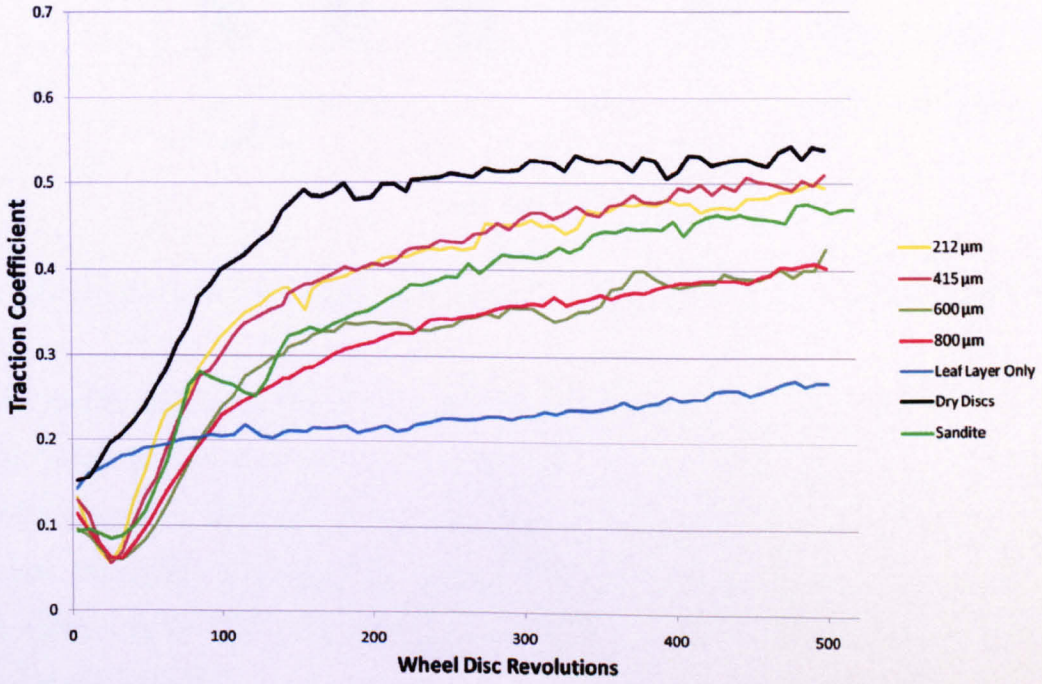

Figure 51 traction curves for first series of tests (fixed volume of gel)

To assess the performance of these traction gels the initial gradient of the traction curves was measured. This is a measure of how each gel aids in restoring traction back to dry levels.

These are summarised in
Figure 52. The gradient is taken from the point after the friction drops and starts to rise at a constant rate. This is the point where it is considered that majority of the gel has evaporated from the contact and the sand particles are starting to take effect. There is a significant change (decrease) in gradient as the friction starts to increase it is at this point that it is thought that the sand is consumed and it is only the sliding in the contact that is working to increase traction. This is the point to which the gradient is measured using a trend line.

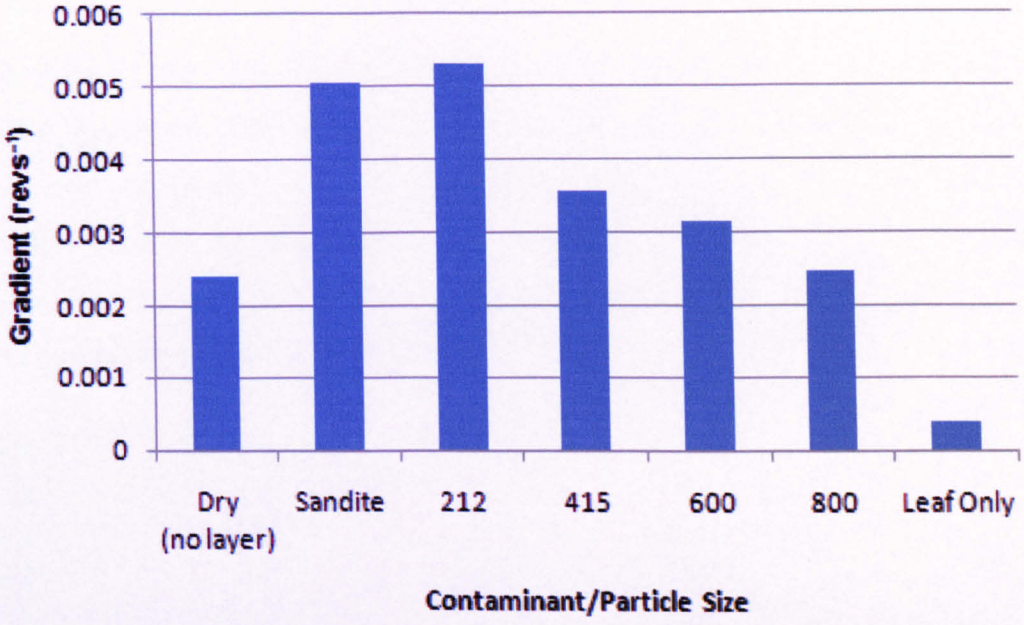

Figure 52 chart showing rate traction increase for different particle sizes for a fixed volume of gel

Figure 52 clearly illustrates an inverse relationship between particle size and initial rate of leaf layer removal. Columns for a dry contact and a leaf layer only have been added for comparison purposes. Sandite® gives almost the same removal rate as the smallest particle traction gel. However, there is quite a large difference between 212 μm and 415 μm. The gradient values from 415 – 800 μm seem to have smaller step changes between them compared to the 212 μm.

From these results it would suggest that 212 μm is the optimum particle size due to its superior contamination removal rate plus the fact that it caused the least amount of damage to the discs. However, with these fixed gel volume tests there will be a vastly different amount of particles in the contact between the two extremes. Therefore this testing did not necessarily highlight the contributions of particle size specifically, more a combination of particle size and volume of solid material entrained into the contact. It was therefore decided to run a second series of tests which used the same number of sand particles in each test for a given particle size.

4.4.2 Same Number of Particles

A second series of tests was run which used the same number of particles on the discs for each particle size tested. This was to isolate the effects of particle size alone. The number of particles to test was derived from the smallest accurately applicable volume of traction gel that could be applied to the discs. This volume was 0.1 ml which equated to 4901 particles of the 212 µm size. The volume of gel needed to obtain 4901 particles for the other sizes tested could then be calculated and are summarised in Table 5.

Particle Size (µm)	No of Particles	Volume (ml)
212	4901	0.100
600	4901	2.196
800	4901	5.336

Table 5 volume of gel needed to obtain 4901 particles

Results of testing with the same number of particles are shown in Figure 53.

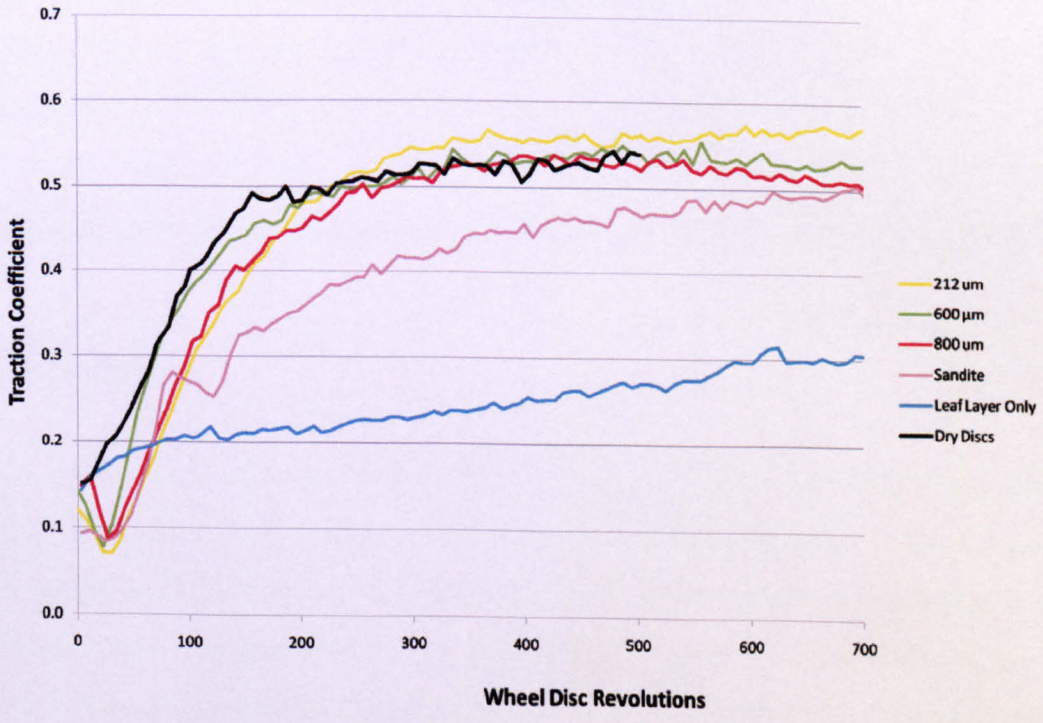

Figure 53 traction curves for fixed number of particles

Figure 53 shows traction curves for tests performed with the same number of particles compared to that of a dry (uncontaminated disc) and a disc with leaf layer only. Notice how this time it is the 600 µm grain size which gives the highest rate of friction increase. (212 µm

gave the highest rate in the fixed ratio tests). This is illustrated in Figure 54. Surprisingly 212 and 800 μm gave almost identical results in terms of leaf layer removal. The only difference being that 212 μm grains reached an end of test traction coefficient of 0.58 where as 800 μm grains peaked at 0.53, but at test end fell to 0.5. It is presumed that this falling in traction coefficient is an effect of surface degradation due to surface fatigue initiated by the larger particles.

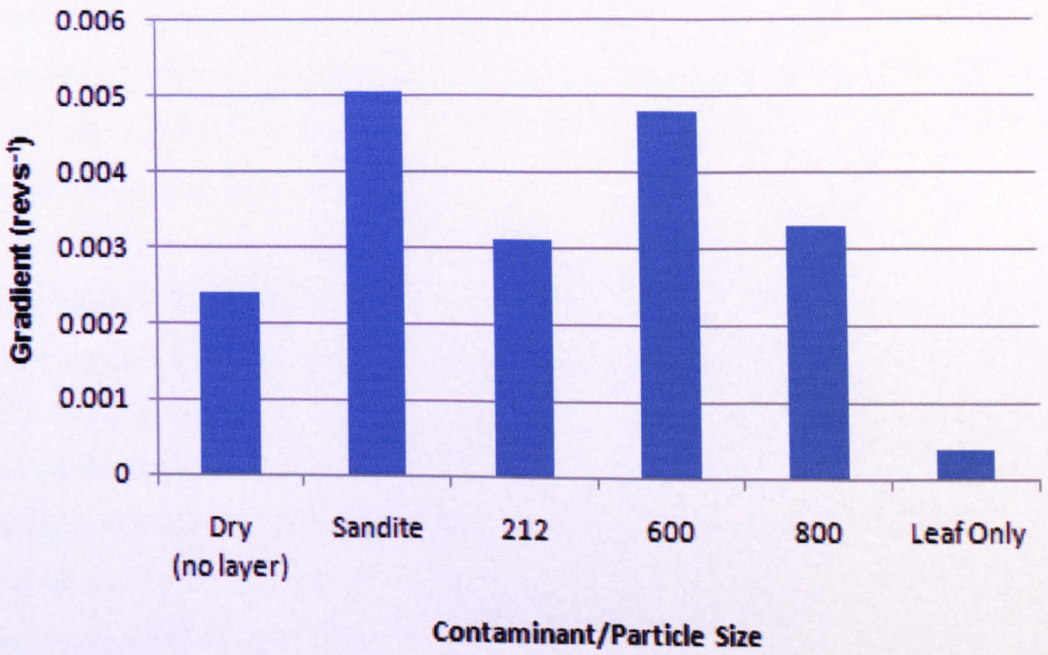

Figure 54 chart showing rate of friction increase for different sized particles for a fixed number of particles

4.5 Discussion

Tests have been carried out to assess the effects of particle size on the performance of traction enhancers. These traction enhancers consist of sand particles suspended within a water based gel. The purpose of the gel is to function as a carrier matrix maintaining a uniform distribution of sand when applied to the rail head. As shown in these tests the gel quickly evaporates as it is entrained into the wheel/rail contact leaving the sand. The gel itself acts as a lubricant on the rail head and thus it is vital that it is quickly removed from the overall mixture.

Initial trials were run to develop a technique for generating a leaf layer on the discs and also delivering the traction enhancers to the contact. The solution which provided the most

consistent results was to paint both the leaf and traction enhancer on to the discs before running the tests. For this a leaf mulch was created by blending the leaves with water and Carboxymethylcellulose (CMC) added to make a viscous paste.

The performance of each traction enhancer was measured in terms of the rate at which it increased the traction from leaf contaminated back to dry levels. This was compared to a baseline of the rate of traction increase by a mechanism of pure slip in the contact i.e. without traction enhancer. This required the generation of a leaf layer on the discs which was done by painting a leaf mulch onto the disc surface and then running the machine at half load. This gave a very thin black layer on the discs which kept traction levels low until worn off. Figure 49 shows the difference in traction curves for a dry and leaf coated pair of discs.

In the first series of tests traction enhancers with different sized sand grains were tested with a fixed mass added to the contact (hence, differing number of particles for different particle sizes). Traction enhancers are prepared with a fixed solid loading to gel ratio by mass. Hence in these tests the number of particles would vary with particle size. The results from this first series of tests showed that the smaller (212 μm) sand grains performed better in terms of removing the leaf layer. Minimal surface damage to the discs was also observed during these tests. The worst performing particle size in these tests was the largest tested (800 μm). This showed the least amount of friction increase and the most surface degradation.

The results from the first set of tests seem to be due to the solid loading rate of the traction enhancers, this is 45% by weight. Thus as particle size increases there will be less sand grains in the traction enhancer. This explains what is seen in
Figure 52 where it is clear that the performance of traction enhancers decreases with increasing particle size.

The second series of tests focused on using a fixed number of particles on the discs for each particle size. This would give a clearer indication of the performance of each different traction enhancer. The number of particles was calculated to be 4901, which equates to the smallest volume of the 212 μm traction gel that could be accurately applied to the contact. The calculations used a particle density of sand of 2.65 g/cm^3. Table 5 shows the volumes of liquid needed to yield this number of particles.

Results of series 2 showed a slight contrast to that of series 1. This time it was the 600 μm particles which gave the highest rate of traction increase as compared to 212 μm from series 1. Comparison of the gradients from each test series is shown in Figure 55.

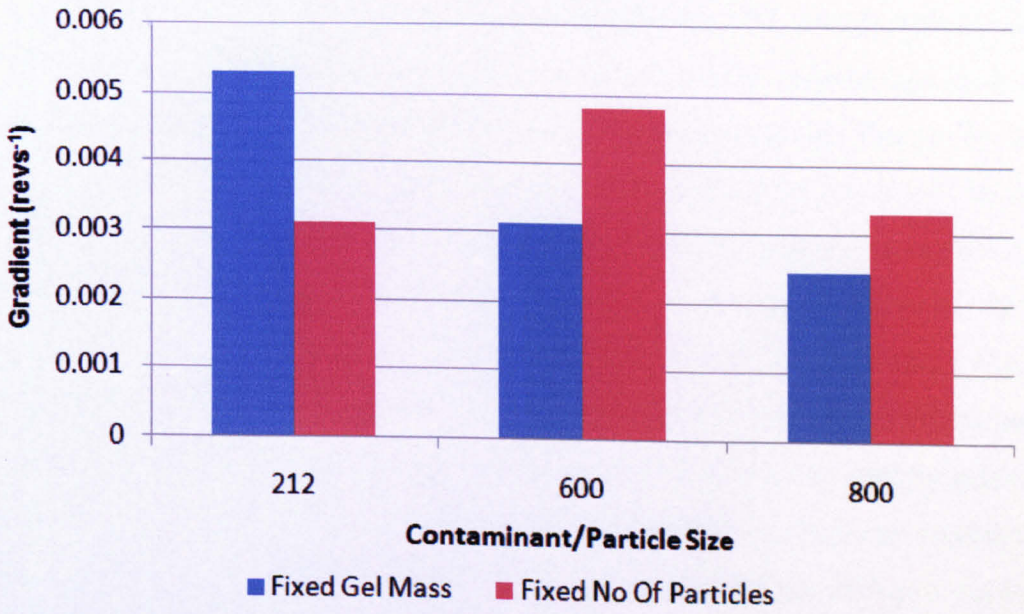

Figure 55 comparison of rate of increase of traction for series 1 and series 2 tests

It is also interesting to note how 212 and 800 μm particles give nearly the same performance in terms of friction increase rate. However, once again the 800 μm particles showing high damage of the disc surface. This was not only observed visually but also confirmed in the friction readings as the 800 μm test peaked at 0.53, compared to 0.58 for 212 μm, and then dropped to 0.5. What is also interesting is that 600 μm shows almost the same performance for the fixed gel mass tests as 212 μm and 800 μm showed in the fixed number of particles tests. It was also intended in these tests to perform a wear test in conjunction with friction by measuring the mass of the discs before and after testing. However, it quickly became clear during testing that leaf and traction gel residue would build up on the side of the discs (off the main wear band). The effect of this increased the mass of the discs masking any mass loss due to wear. However, wear was observed on the disc surfaces and was witnessed to increase with particle size. Results from testing with the 800 μm particles showed rapid fatigue of the disc surfaces, something not seen below a particle size of 600 μm.

Results from these tests showed that 800 μm particles performed worst in both of the tests. Figure 55 shows that these particles gave the lowest fiction increase rates seen in either of the tests and the highest wear rates.

Overall 212, 415, and 600 μm sized particles have performed quite well in comparison, with 212 μm giving the greatest friction increase rate while showing the lowest surface damage in the first series of tests. However, in the second series of tests the highest leaf layer removal rate was shown by the 600 μm particles. This is no surprise as in the first series of tests a fixed mass of traction gel is added to the contact. This means that there will be a greater number of smaller particles entering the contact compared to the larger ones (as the gels have a fixed solid loading rate of 45%). In the case of the smaller particles more work will be done in the contact due to more particles. In the second series of tests where there was a fixed number of particles added to the contact it was the 600 μm/larger particles which performed the best in terms of increasing the traction. However, this result may be slightly misleading as there was 53 times as much gel put into the contact for the 600 μm particles compared to the gel containing the 212 μm particles, meaning the gel containing the 600 μm particles may just have clung to the discs longer before it wore off.

As such, a definite conclusion of which is the best suited particle size for the job cannot be reached and more tests will be needed that will look at other issues such as track circuit shunting and nominal wear rates.

The work from this chapter has led to the creation of a standard technique for the test of traction enhancers and other friction modifiers which is outlined below:

- Fresh pre-soaked leaves are blended with an equivalent weight of water. Carboxymethylecellulose is then added to the mixture to give a leaf paste.
- A leaf layer is generated on the test discs by painting on a layer of leaf paste. The discs are then rotated at 400 RPM with 0% slip (pure rolling) for 40 cycles. This sequence is repeated a further two times to develop a black contamination layer on the surface of the discs. The layer is then allowed to dry.
- A nominal volume of traction enhancer/friction modifier is then applied to the disc surfaces by syringe prior to the test.

- For traction enhancers which have different sized particles at a fixed solid mass loading rate two series of tests will need to be run. In the first series the same volume of each gel will be applied to the discs regardless of particle size. This simulates how the gels may be applied in the field. To independently assess the contribution of each particle size a second series of tests will need to be run. In this second series the volume of each traction enhancer will be varied to give roughly the same number of particles independent of particle size.
- The performance of each type of traction enhancer can then be assessed in terms of the rate at which traction levels will be restored to those of dry conditions by measuring the initial gradient of the traction curve.

This test method will be used in the next series of tests to assess the isolation and wear inducing properties of the traction enhancers.

Chapter 5: Friction, Isolation and Wear Assessment of Traction Enhancers using Standard Test Method

5.1 Introduction

The focus of this work was to look at the effects of traction enhancers using the standard test technique developed in chapter 4. As well as measuring traction this study also focused on track circuit isolation and wheel/rail damage/wear. Traction gels consist of sand suspended in a carrying gel. Previous work has shown how sand in the contact can have adverse effects on track circuit isolation [Lewis, 2003a; Lewis, 2006c] and wheel/rail wear [Lewis, 2006b; Dwyer-Joyce, 2003]. This study was carried out using the SUROS twin-disc machine [Fletcher, 2000b] which is described in Chapter 4. The same conditions were used to perform these tests: 1500 MPa contact pressure and 3% creep.

An electrical circuit was constructed to replicate the internal resistances of a TI21 track circuit. The TI21 track circuit is used widely on the UK rail network [Lewis, 2006c] and operates in the audio frequency range (approximately 100 Hz to 10 kHz). Track circuits are a vital part in railway signalling systems worldwide. They are used to detect the presence of a train on a section of track, thus adjusting nearby signalling and controlling traffic accordingly. Sections of track are usually electrically isolated from one another by means of an insulated joint as shown in Figure 56. When no train is present the current flows freely from the transmitter to the detector indicating a free section of track. Surrounding signals will hence show a green light. However, when a train is present in a section of track the track circuit will be shorted and thus no current will be seen at the detector. In this situation surrounding signals are automatically turned to a red light to avoid train collision. It can also be seen how this system is fail safe. If for any reason there is a loss of power signals would automatically be turned to red.

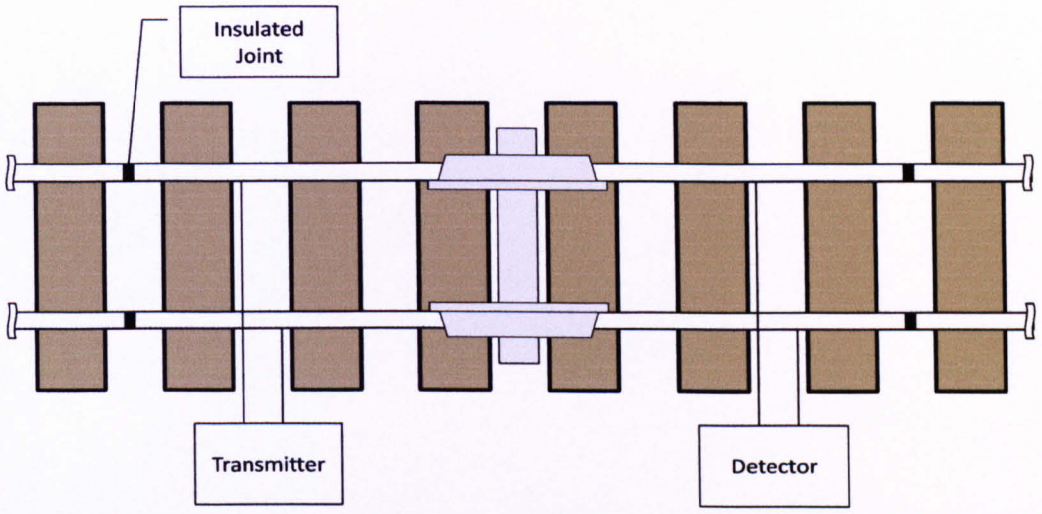

Figure 56 schematic of occupied isolated rail section and track circuit [adapted from Lewis, 2006c]

5.2 Test Equipment

An electrical set-up representing the TI21 circuit used in the UK was used in conjunction with the SUROS machine. The circuit represented the transmitter and detector of a TI21 track circuit with two 10 Ω resistors: R1 the transmitter and R2 the detector. The circuit has the test discs in parallel with R2 as shown in Figure 57. This circuit has been used in Lewis et al, [2003a] and Lewis & Massing [2006c].

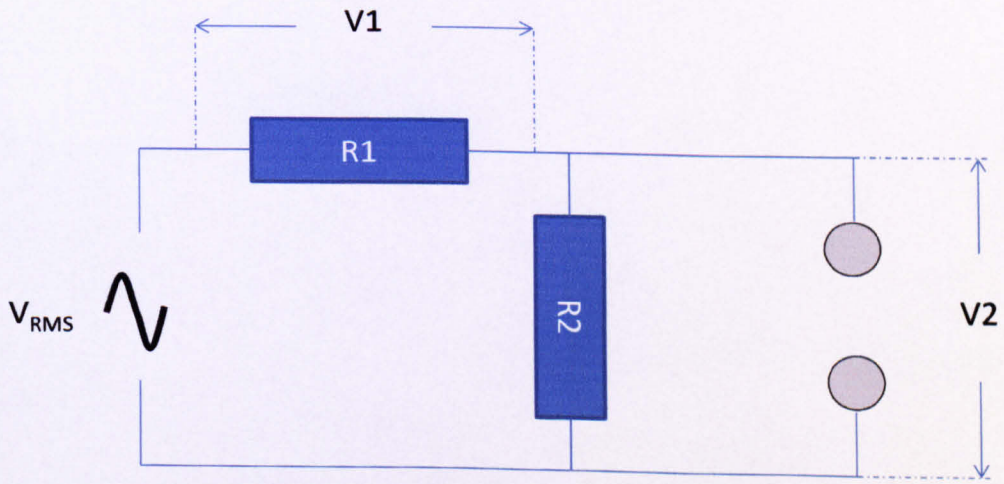

Figure 57 electrical diagram of circuit used in this testing

When the test discs are brought into contact more current will be drawn through them due to the lower resistance of the contact (between 0.5 – 0.6 ohms) compared to R2 (10Ω). The current flowing through the disc contact can then be calculated by measuring the voltage across them. Using Ohm's and Kirchhoff's laws the impedance of the disc contact can then be calculated as shown in Figure 58.

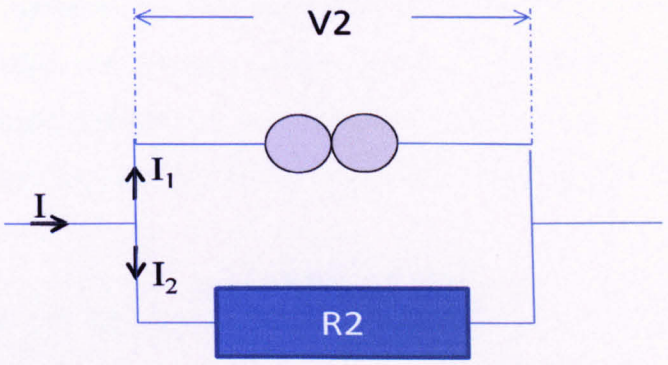

Figure 58 electrical diagram to explain calculation of impedance

The current flowing through R2 (I_2) can be calculated using Ohm's law and is given by:

$$I_2 = V_2 \div R_2 \quad (5)$$

Kirchhoff's law then states that the current flowing into a junction is equal to the sum of the current flowing out of it. Hence:

$$I = I_1 + I_2 = \frac{V_1}{R_1} \quad (6)$$

Therefore:

$$I_1 = \frac{V_1}{R_1} - \frac{V_2}{R_2} \quad (7)$$

and hence, as current through the discs is known as well as the voltage across them the impedance can now be calculated.

$$Z_{DISCS} = V_2/\left((V_1/R_1) - (V_2/R_2)\right) \quad (8)$$

Note here that the magnitude of impedance, $|Z|$ is being calculated only. True impedance, however, is a complex number and therefore has magnitude and direction/phase difference, Φ. In this case it is very difficult to measure the phase angle or directional component. This is due to the difference in current signals and limited data sampling rate of the equipment.

Impedance is the term given to the total opposition of current flow in an A.C. circuit not just by resistance, *R*, but also reactance, *X*, which is present in the form of inductance, *L* and capacitance, *C*. Impedance, resistance and reactance are all measured in Ohms. Therefore, what is measured at the discs can be labelled as an impedance because all three components are present:

- Resistance – due to the opposition of current flow in the form of the discs and circuit wires.
- Inductance – which occurs whenever current flows through a metallic body.
- Capacitance – present whenever an electrolyte/semi-conductor such as traction gel, sand or leaf layer becomes entrained between the contact.

Inductive or capacitive reactance is dependent on frequency and thus impedance is also frequency dependent. All experiments in this work were performed with a circuit frequency of 2 kHz which is within the audio range and is also used in [Lewis, 2003a] and [Lewis, 2006c].

It must also be noted here that any impedance measured in these tests will differ greatly from what would be seen in the field. Therefore it is more important to concentrate on the differences in impedances measured rather than their absolute values.

5.3 Test Methodology

The method of preparing the discs with the leaf layer was the same as defined in chapter 4. To fully assess the effect of different sizes of particles within each gel two types of test were run:

1) Fixed volume where the traction gel was applied to the discs at a rate of 1ml per test, and

2) Fixed particle tests where the volume applied to the discs was controlled as to give a consistent number of particles independent of particle size.

These two test methods were defined in chapter 4. A new leaf paste, which had a different ratio of leaf: water: thickener was used for these tests giving a leaf layer that appeared more

like that seen in the field (see Figure 59). Sycamore leaves were also used for these tests as in the previous testing. However, in these tests dead leaves which were dry stored prior to the tests were used. It was found in [Lewis, 2006c] that dead leaves showed significantly more impedance than fresh ones. Thus dead leaves were thought to be more appropriate for this test. The amount of leaf paste applied to the discs could not be controlled: however, the mass readings taken before and after the leaf layer generation are relatively consistent. The average amount of leaf generated on the rail discs was 12 and 11 mg for the fixed volume and fixed particle cases respectively.

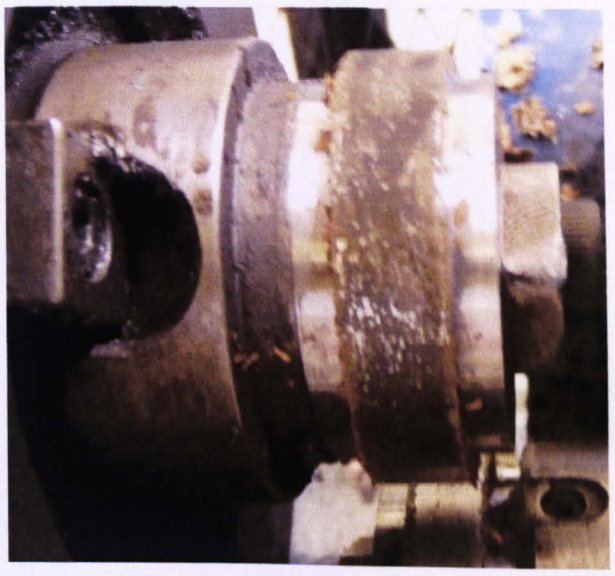

Figure 59 image of new formulated leaf layer on disc after application

The main differences between these tests, and tests in the previous chapter, was that impedance changes and wear rates of the discs were being measured. Wear was measured by weighing the discs before and after the test. As wear was being measured the number of cycles that each test was run for was kept constant at approximately 1000 wheel disc revolutions apart from the leaf only tests which needed to be run for longer so that dry traction levels could be reached. Table 6 and 7 show the tests carried out. Each test was repeated once and in some cases repeated a third time in the case of any discrepancies occurring.

	Test	Name	Slip (%)	Contact Pressure (MPa)	Conditions
Control	1	Dry Disks	3	1500	Run until Dry Friction is reached
	2	Dry Disks	3	1500	Run until Dry Friction is reached
	3	Leaf Build up	0	900	40 Cycles
	4	Leaf Build up	0	900	40 Cycles
	5	Leaf Build up	0	900	40 Cycles Free Rotate for 5 min
	6	Leaf Layer only	3	1500	Run until Dry Friction is reached
Fixed Mass Tests	7	Leaf Build up	0	900	40 Cycles
	8	Leaf Build up	0	900	40 Cycles
	9	Leaf Build up	0	900	40 Cycles Free Rotate for 5 min
	10	212 µm particle size	3	1500	Run until Dry Friction is reached
	11	Leaf Build up	0	900	40 Cycles
	12	Leaf Build up	0	900	40 Cycles
	13	Leaf Build up	0	900	40 Cycles Free Rotate for 5 min
	14	415 µm particle size	3	1500	Run until Dry Friction is reached
	15	Leaf Build up	0	900	40 Cycles
	16	Leaf Build up	0	900	40 Cycles
	17	Leaf Build up	0	900	40 Cycles Free Rotate for 5 min
	18	600 µm particle size	3	1500	Run until Dry Friction is reached
	19	Leaf Build up	0	900	40 Cycles
	20	Leaf Build up	0	900	40 Cycles
	21	Leaf Build up	0	900	40 Cycles Free Rotate for 5 min
	22	800 µm particle size	3	1500	Run until Dry Friction is reached
Control	23	Leaf Build up	0	900	40 Cycles
	24	Leaf Build up	0	900	40 Cycles
	25	Leaf Build up	0	900	40 Cycles Free Rotate for 5 min
	26	Leaf Layer only	3	1500	Run until Dry Friction is reached
Fixed Mass Tests	27	Leaf Build up	0	900	40 Cycles
	28	Leaf Build up	0	900	40 Cycles
	29	Leaf Build up	0	900	40 Cycles Free Rotate for 5 min
	30	212 µm particle size	3	1500	Run until Dry Friction is reached
	31	Leaf Build up	0	900	40 Cycles
	32	Leaf Build up	0	900	40 Cycles
	33	Leaf Build up	0	900	40 Cycles Free Rotate for 5 min
	34	415 µm particle size	3	1500	Run until Dry Friction is reached
	35	Leaf Build up	0	900	40 Cycles
	36	Leaf Build up	0	900	40 Cycles
	37	Leaf Build up	0	900	40 Cycles Free Rotate for 5 min
	38	600 µm particle size	3	1500	Run until Dry Friction is reached
	39	Leaf Build up	0	900	40 Cycles
	40	Leaf Build up	0	900	40 Cycles
	41	Leaf Build up	0	900	40 Cycles Free Rotate for 5 min
	42	800 µm particle size	3	1500	Run until Dry Friction is reached

Table 6 fixed volume and reference test conditions

	Test	Name	Slip (%)	Contact Pressure (MPa)	Conditions
Fixed No. of Particles	43	Leaf Build up	0	900	40 Cycles
	44	Leaf Build up	0	900	40 Cycles
	45	Leaf Build up	0	900	40 Cycles Free Rotate for 5 min
	46	212 µm particle size	3	1500	Run until Dry Friction is reached
	47	Leaf Build up	0	900	40 Cycles
	48	Leaf Build up	0	900	40 Cycles
	49	Leaf Build up	0	900	40 Cycles Free Rotate for 5 min
	50	415 µm particle size	3	1500	Run until Dry Friction is reached
	51	Leaf Build up	0	900	40 Cycles
	52	Leaf Build up	0	900	40 Cycles
	53	Leaf Build up	0	900	40 Cycles Free Rotate for 5 min
	54	600 µm particle size	3	1500	Run until Dry Friction is reached
	55	Leaf Build up	0	900	40 Cycles
	56	Leaf Build up	0	900	40 Cycles
	57	Leaf Build up	0	900	40 Cycles Free Rotate for 5 min
	58	800 µm particle size	3	1500	Run until Dry Friction is reached
Fixed No. of Particles	59	Leaf Build up	0	900	40 Cycles
	60	Leaf Build up	0	900	40 Cycles
	61	Leaf Build up	0	900	40 Cycles Free Rotate for 5 min
	62	212 µm particle size	3	1500	Run until Dry Friction is reached
	63	Leaf Build up	0	900	40 Cycles
	64	Leaf Build up	0	900	40 Cycles
	65	Leaf Build up	0	900	40 Cycles Free Rotate for 5 min
	66	415 µm particle size	3	1500	Run until Dry Friction is reached
	67	Leaf Build up	0	900	40 Cycles
	68	Leaf Build up	0	900	40 Cycles
	69	Leaf Build up	0	900	40 Cycles Free Rotate for 5 min
	70	600 µm particle size	3	1500	Run until Dry Friction is reached
	71	Leaf Build up	0	900	40 Cycles
	72	Leaf Build up	0	900	40 Cycles
	73	Leaf Build up	0	900	40 Cycles Free Rotate for 5 min
	74	800 µm particle size	3	1500	Run until Dry Friction is reached

Table 7 fixed particle test conditions

5.3.1 Leaf Layer Analysis

A leaf layer was prepared using the method outlined above. The rail disc with leaf layer was then observed using a scanning electron microscope and chemical analysis was done using Energy-Dispersive X-ray Spectroscopy, EDS. EDS works on the principal that each element has its own unique structure i.e. protons electrons and neutrons. When these elements are stimulated by a high energy source, such as x-rays as in the case of EDS, an X-ray of certain energy will be given off from the atom. The energy of the X-ray is unique to each atom and is measured by a spectrometer where identification of each element can be made. Figure 60 shows a series of SEM images at various magnifications. The leaf layer can clearly be seen as a dark layer on the surface of the steel disc. Plough lines show the direction of rolling of the disc and are shown on both the steel and dark surface. The leaf layer also appears to be brittle as can be seen in Figures 60 b) and c) with cracks formed through it.

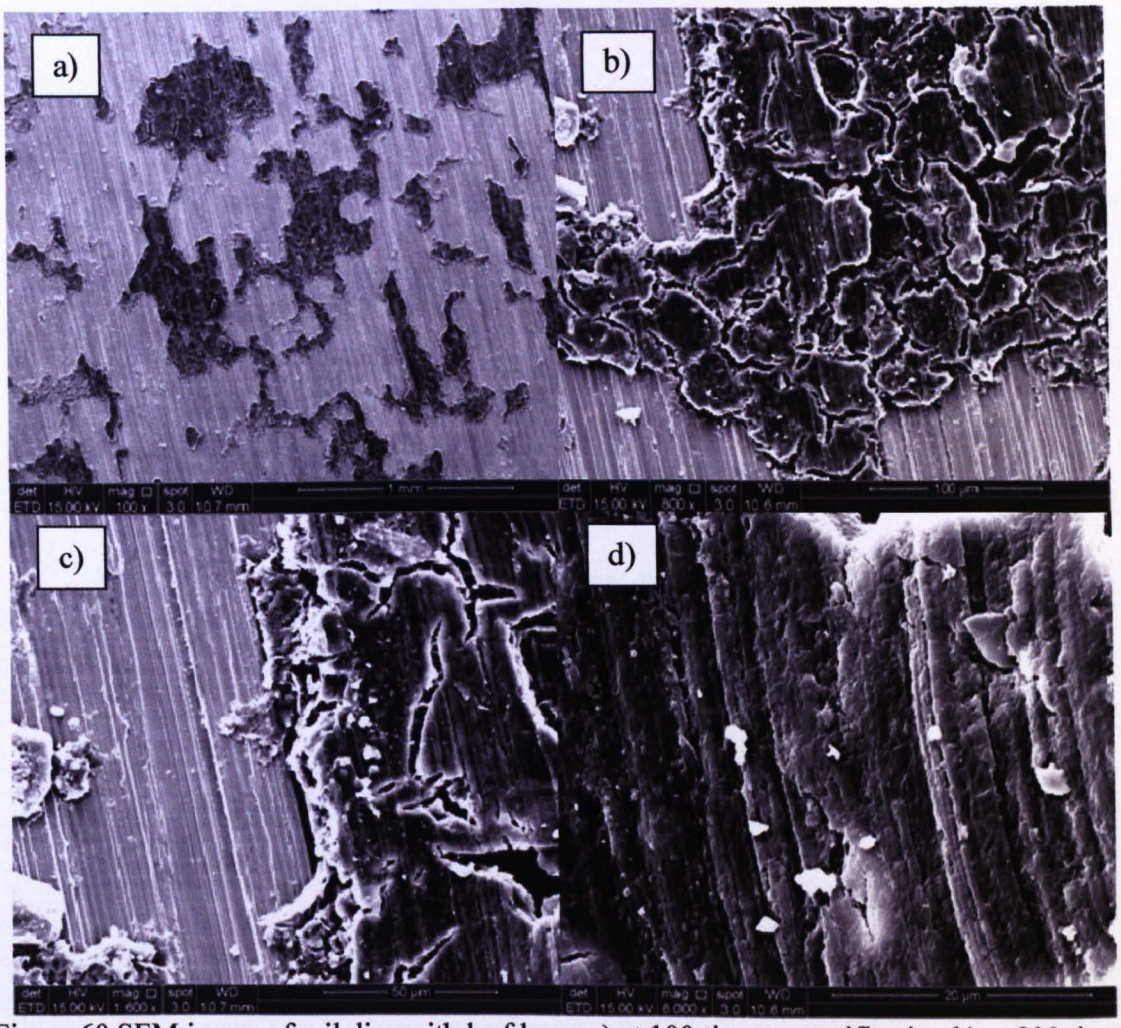

Figure 60 SEM image of rail disc with leaf layer a) at 100 times magnification b) at 800 times magnification c) 1600 times magnification d) 6000 times magnification

Figures 61 and 63 show the results of the EDS for both the metal matrix (a) and the leaf layer (b). Figure 61 shows results from x-rays detected from the smoother surface (lighter surface in figure 60) and shows a peak in Iron, Fe, being detected. Figure 62 on the other hand shows the energy spectrum from the leaf layer and shows a spike in Carbon which is larger than the Iron peak for the same area. There is also a spike in Oxygen and Calcium in figure 62 which was not seen for the matrix. This confirms that there is an organic layer on the disc surface. Previous testing by Li et al [2009] and Cann [2006] showed three main chemicals found in laboratory generated leaf layers. These are Lignin, chemical formula $C_9H_{10}O_2$, Pectin, $C_6H_{10}O_7$, cellulose, $C_6H_{10}O_5$, Water, H_2O and Iron, Fe. All of these complex organic molecules are found in plant cell walls. Figure 62 shows that there is a large spike in Carbon detected from the EDS accompanied with a significant spike in oxygen detected. EDS cannot detect elements with an atomic number less than 4 as their reflected energy is too low. This explains why there is no spike for Hydrogen as would be expected in organic compounds. However, the strong peaks in Carbon and Oxygen strongly suggest that the layer on the disc

surface is constructed of organic constituents and although EDS cannot reveal individual compounds it is likely that this layer is constructed from the chemicals mentioned above.

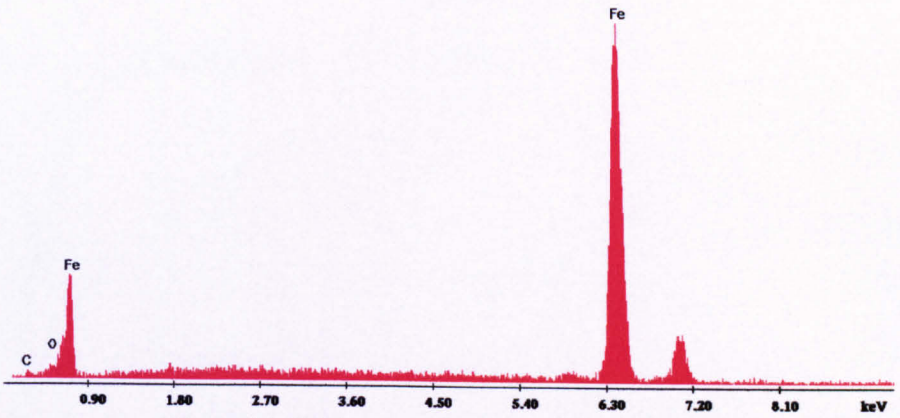

Figure 61 EDS output for exposed steel matrix

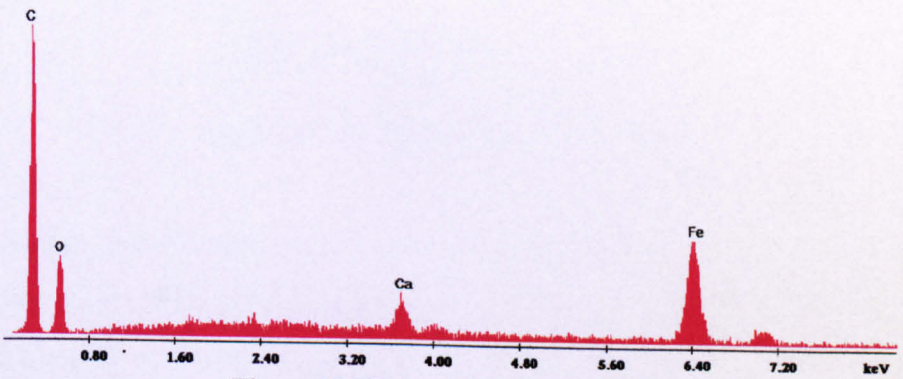

Figure 62 EDS output for leaf layer

5.4 Results

5.4.1 Fixed Volume

5.4.1.1 Traction

A summary of the traction results from the fixed volume testing is shown in Figure 63. The first thing that is noticeable from Figure 63 is that the 600 μm gel seems to perform in line with the 212 and 415 μm gels. This obviously differs from testing in the previous chapter as the 215 and 415 μm gels both outperformed the 600 and 800. It can also be seen that it is taking longer for the traction to reach its peak friction compared to the previous work, i.e. in

the case if the 212 µm gel traction coefficient of 0.5 was reached within 500 cycles. In these tests it now takes over 600 cycles to reach this traction level.

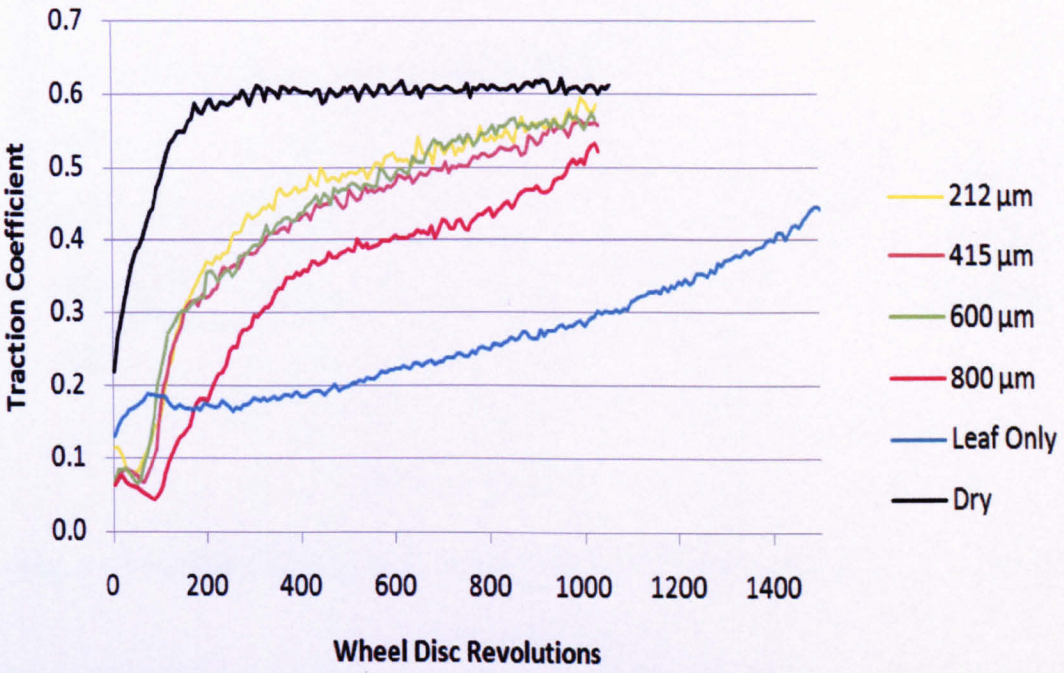

Figure 63 fixed volume traction curves

A new batch of the traction enhancers was used for the testing outlined in this chapter and it was noticed that these gels had a lower viscosity than those previously tested. The rate of increase in traction, as measured by the initial gradients of each of the cases above, are shown in Figure 65. In comparing these results with the corresponding ones from the previous chapter, it can be seen that they are approximately half their value. These differences can only be put down to two things, as all other test parameters remained the same: either the change in viscosity of the gel or the new formulation of leaf layer. In reality both of these factors will play a role. It was noted when preparing the test samples that the 800 µm traction enhancer was very difficult to draw into the syringe with a uniform distribution of sand particles. It seemed as if the particles could not be suspended properly in the lower viscosity gel. This meant that even though a fixed volume of the product was placed on the discs it is possible that the number of particles in the product could have varied widely. Figure 64 shows the lack of repeatability in the case of 800 µm particles as compared to 200 µm as a result of this inconsistency.

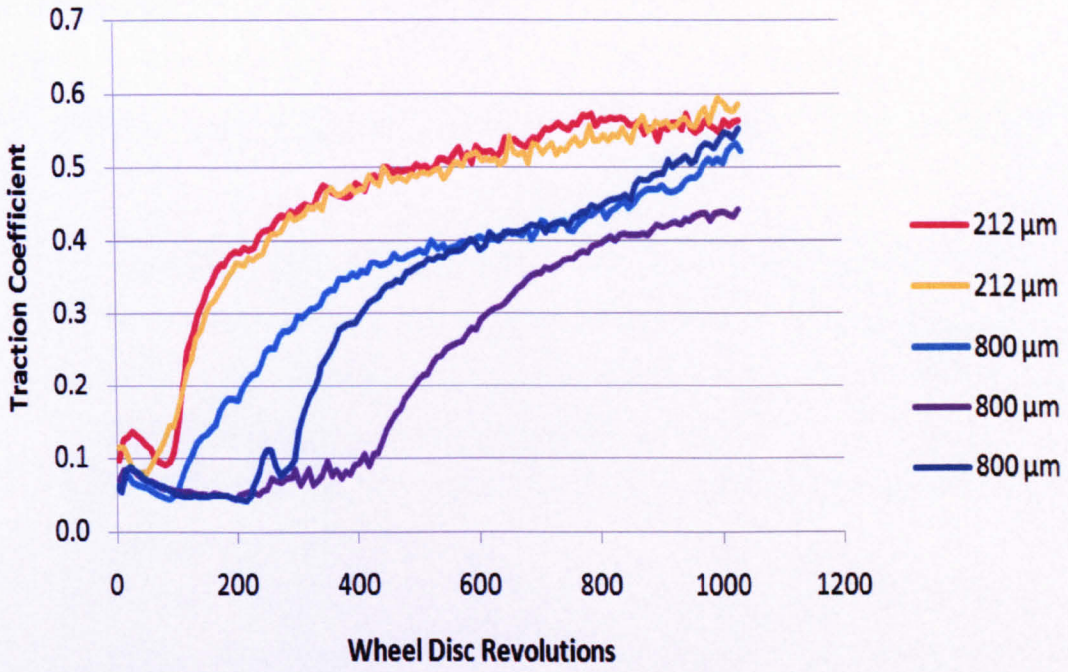

Figure 64 chart showing repeat traction curves for 212 and 800 µm traction enhancers

The strong repeatability shown by the 212 µm products are typical of that seen for both the 415 and 600 µm variants. For this reason the 800 µm gel was not used for the fixed particle testing (section 5.4.2) as control of the mass of particles was critical.

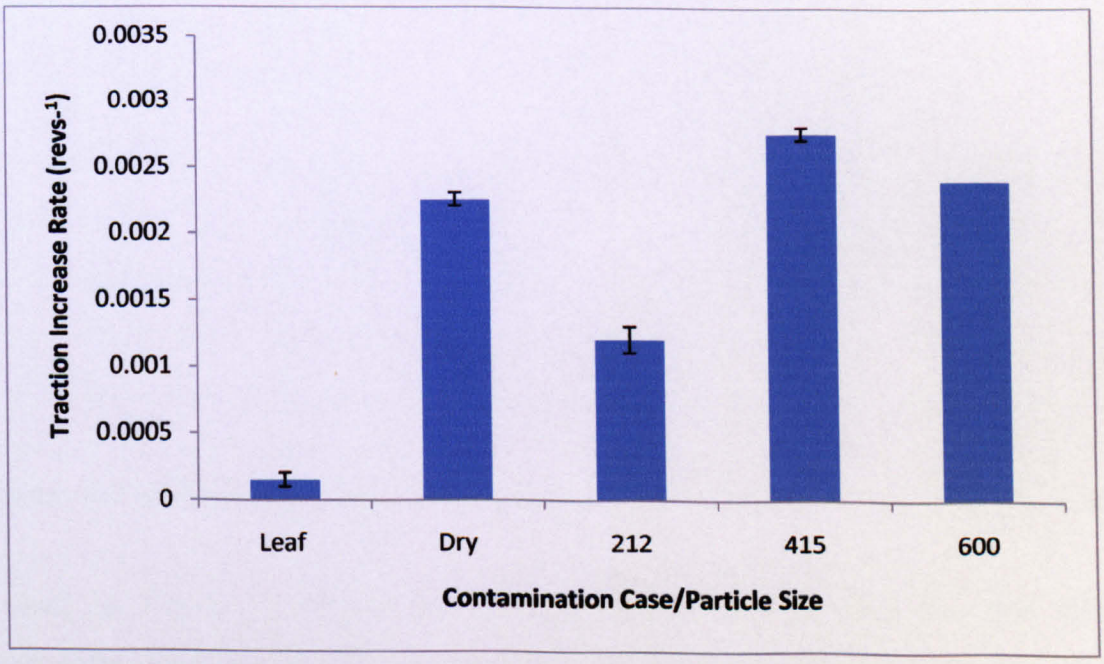

Figure 65 chart showing rate traction increase for different particle sizes for a fixed volume tests

5.4.1.2 Impedance

Figure 66 shows a typical impedance trace for a test. The trace can be summarised in 4 stages:

1. This is just before the start of a test when the test discs are separated.
2. As the discs are brought together the resistance will drop. In doing so it will become an impedance due to the sand and gel between the discs acting as an electrolyte hence producing a capacitance effect
3. As full contact is achieved there will be a measurable impedance due to the leaf layer or traction enhancer
4. As test progresses the impedance level will drop back to that of a dry/uncontaminated contact as the leaf and traction enhancer residue are slowly removed from the contact

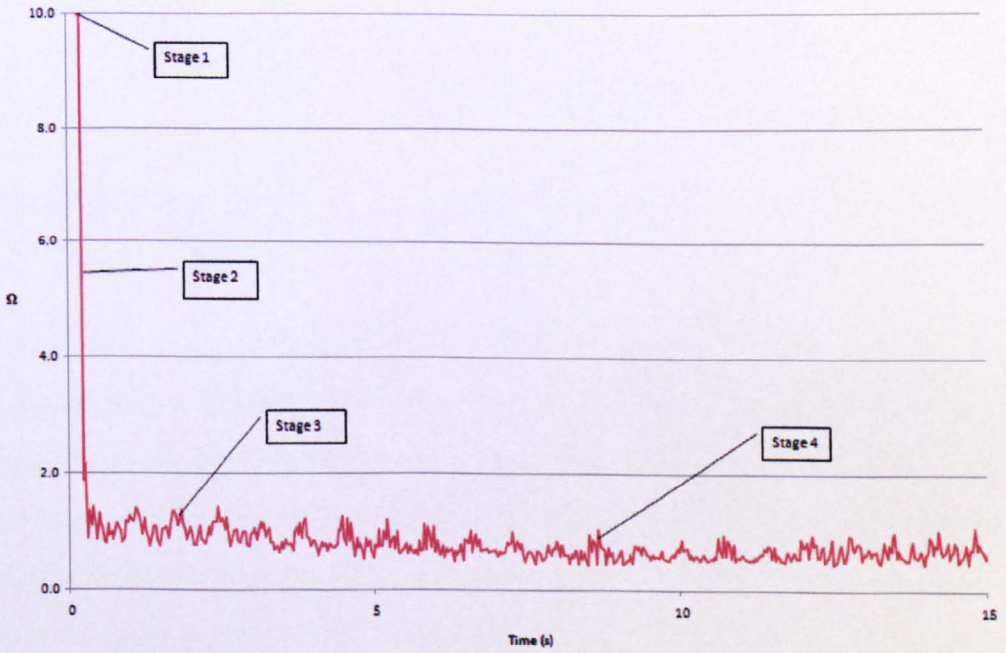

Figure 66 chart showing typical impedance trace for a test with traction enhancer (600 μm is shown)

The chart in Figure 67 shows the average impedance calculated for each different contamination condition/particle size tested (note error bars indicate standard deviation between original and repeat test i.e. tests 11 and 31 according to table 1). The impedance was averaged over the first 5 seconds and then 5 - 10 seconds of each test. (Note that for the static

case the discs were hand loaded for periods of 5 seconds only hence no 5-10 second data for this column, no reduction in current was witnessed during this period). It was proposed (from the calculation of the gradients in section 4.1.1) that the traction enhancers remained effective for roughly 20 seconds of the test. Hence, taking the impedance within the first 10 second window of each test would ensure that the impedance due to the traction enhancer was captured.

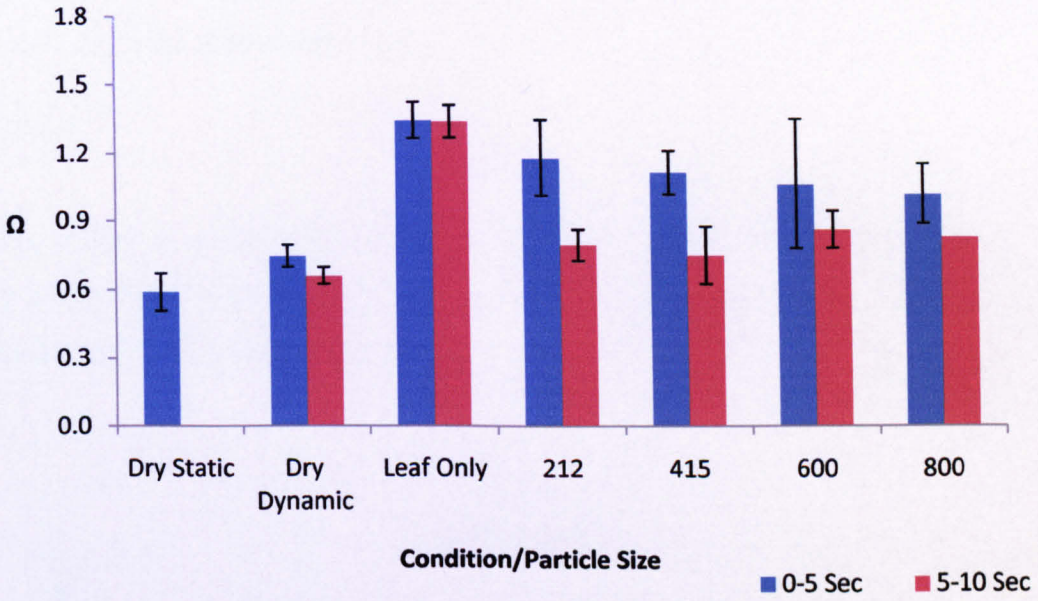

Figure 67 chart showing average impedance calculated for each contamination condition over 5 and 15 seconds

It can be observed in Figure 66 that the impedance between 0 and 5 seconds is relatively steady. Between 5 and 10 seconds, however, the impedance starts to drop towards the dry level. Figure 67 shows that the highest impedance was shown for the leaf only condition and unlike all other cases there is little difference between the 5 and 10 second readings. In the case of the traction enhancers however, average impedances drop back towards the dry level during this 5-10 second period. This would suggest that the traction enhancer has gone from the contact; however, the traction gradients suggest the product is still working up to at least 20 seconds after the test has started. Perhaps at this 5 second mark any excess product has been removed from the contact and any product remaining is not enough to cause a significant rise in impedance. It is interesting also to note that the time taken for the leaf layer test to reach dry levels of impedance was approximately 170-200 seconds. This again shows how durable the leaf layer is. The impedance for the dry/uncontaminated condition was

measured with the discs both stationary and rotating. It can be seen that impedance seems to be higher for the dynamic case. This could be due to the vibrations in the electrical connections (slip rings) as the machine is running. What is surprising is that the range of impedances seen under the traction enhancers for the 0-5 second period is quite narrow with particle size seeming to have little effect on impedance levels. It appears that there is a weak negative correlation between particle size and impedance; however; this is overshadowed by the relatively large standard deviation seen in the 600 μm case. There is also a drop in dry impedance after 5 seconds showing the dynamic nature of the contact may also have a lesser part to play in this impedance reduction.

5.4.1.3 Wear

Wear rates of the discs were calculated by mass loss and expressed per disc revolution. Figure 68 shows the wear rates of the rail discs only. This is because in most cases the mass of the wheel actually increased after each test.

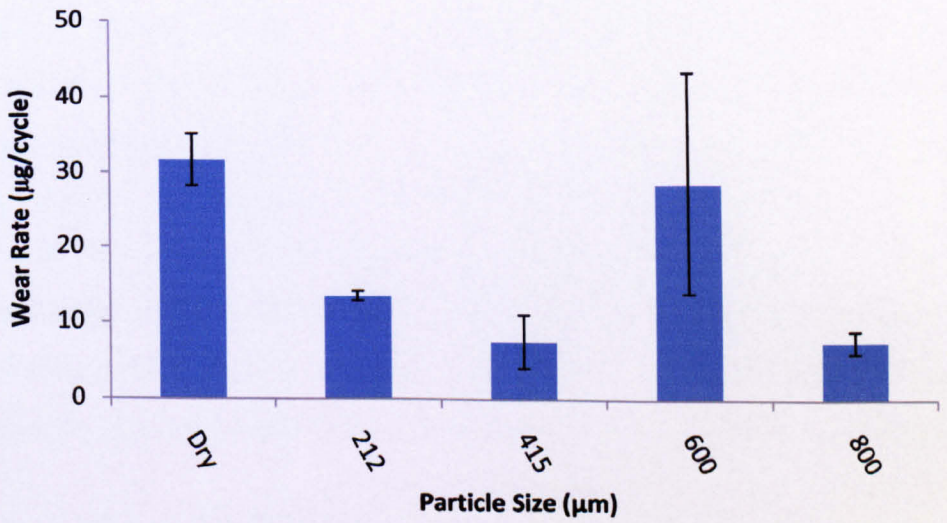

Figure 68 rail disc wear rates for fixed volume tests

What is surprising here is that the maximum mean wear rate is seen under dry conditions. It was shown in [Lewis, 2006b] that adding sand to a twin-disc contact will increase the rail wear by a factor of approximately 7.5. However, in [Lewis, 2005] a wear rate of 21 μg/cycle was shown for a dry contact at 1% slip. This seems to confirm the dry wear rate seen here (31 μg/cycle) as the values are within good agreement. Lewis & Dwyer-Joyce, [2006b] show much higher wear rates in the range of 3000 to 6000 μg/cycle. However, this work was done

under very different conditions at extreme slip rates of 20% for durations of 3000 cycles, compared to the 3% slip and 1000 cycles used in these tests. Particle sizes used in that work also ranged from 1-2 mm. It needs to be noted that in this work there was also the presence of a leaf layer in the contact. In the work reported in this chapter there is also the difference that the sand particles are suspended in a gel. The leaf layer (and possibly the gel) in these tests seems to have been protecting the discs from excessive wear. This can be seen in Figure 68 as the wear rates are significantly lower (apart from the 600 μm case) for the leaf layer with traction enhancer cases than for the dry case (i.e. no leaf layer no traction enhancer). A very different wear mechanism seemed to be occurring in [Lewis, 2006b] due to the extreme testing conditions. It was proposed that a rapid fatigue process was occurring initiated by the large sand particles indenting the wheel material.

It seems that in these experiments the very different and less severe wear process of three body abrasion has actually occurred. This is a process whereby the harder of the two materials (in this case the rail) wears faster than the softer (wheel). This happens because the solid particles (sand) embed into the softer material (wheel) and thus abrade the harder material (rail). Evidence for this has been shown in the fact that the mass of the wheel actually increased in all tests. Photos taken after the tests as in Figure 69 show that the wheel has developed a shiny black surface with evidence of crushed sand embedded in the surface. The rail disc, on the other hand, has developed a polished surface and the leaf layer has been completely removed. It is also interesting to see what appears to be the "black leaf layer" having been transferred from the rail disc to the wheel disc. However, this new black layer is much shiner than the leaf layer and traction results (traction coefficient of 0.5 plus) confirm that this is may be an altered layer from the leaf layer that was generated on the rail disc.

Figure 70 shows a diagram of the proposed wear mechanism and entrainment of sand grains into the contact. Figure 70 (a) shows the discs just after the test has started. The sand grains are held onto the disc surfaces by the gel. The particles, however, are prevented from entering the contact because the gel acts as a lubricant lowering the friction as seen in Figure 63. The hydrodynamic film which separates the discs causes a pressure at the disc interface which prevents the suspended particles from entering the contact. In Figure 70 (b) excess gel evaporates from the discs allowing the sand grains to enter the contact and increase traction as in Figure 63. As the particles enter the contact they will be crushed and some of these

crushed fragments become embedded in the wheel disc as in Figure 70 (c). The particles embedded in the wheel disc will now abrade the rail disc with its surface leaf layer. At some point the leaf layer seems to be transferring to the wheel disc perhaps as it is being scraped from the rail disc by the wheel's embedded particles. Thus a new leaf and sand layer is created on the wheel. Figure 70 (d) shows the 600 μm Hertzian contact width between the two loaded discs. This shows that an embedded particle could potentially scratch an equal length into the rail disc. This would be the case if the rail disc was stationary and the wheel rotating. However, a creep rate of 3% was used in these tests and any scratch caused by an embedded particle is likely to be a fraction of the contact width in the region of 15-20 μm.

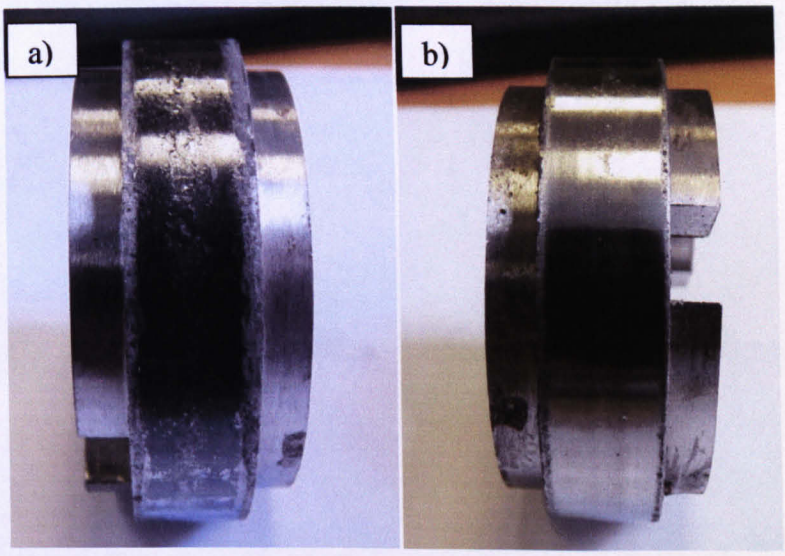

Figure 69 (a) image of post test wheel disc with evidence of crushed sand grains on blackened surface (b) rail disc with shiny polished surface

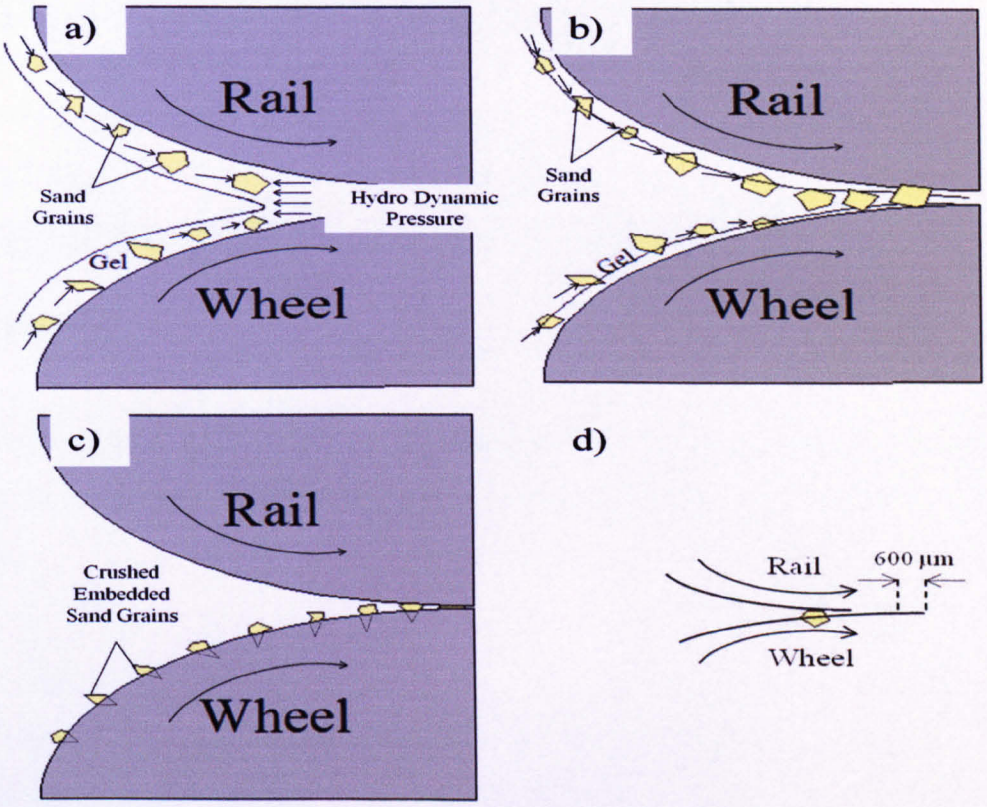

Figure 70 illustrations of proposed wear mechanism and particle entrainment

5.4.2 Fixed Number of Particles

As in the previous chapter tests were also done with a fixed number of particles to assess the performance and damage directly attributable to particle size. This was done by weighing a known volume of the traction enhancer. It was known that the gels are loaded at a rate of 45% sand by weight. Thus 45% of this weighed volume was then divided by the approximate mass of each particle (dependent on particle size) hence giving an indicated number of particles. By assuming that each sand grain is spherical in shape the mass of each particle was calculated first calculating its volume (e.g. $^4/_3 . \pi . \left(\frac{212}{2}\right)^3$) then multiplying by a typical density of a sand grain (2.65 g/cc). The number of particles for each test was based on the smallest amount of the 600 µm gel which could be controllably applied to the discs in this case 1ml. This amounted to approximately 5200 sand grains. In the previous chapter this value was 4901. This difference was put down to the lower viscosity of the gel used in this work. Table 8 shows the volumes of each gel used to achieve this number of particles. Note figures are given to the nearest hundred due to assumptions made in calculations.

Particle Size (µm)	No. of Particles	Volume ml	Particles Per ml
212	5,200	0.1	51,700
425	5,200	0.752	6,900
600	5,200	2.190	2,400

Table 8 volume of each gel required to achieve a similar number of particles

5.4.2.1 Traction

Figure 71 shows a summary of the traction results for testing with a fixed number of particles. Note that in these tests the 800 µm gel was not used because it could not be syringed uniformly.

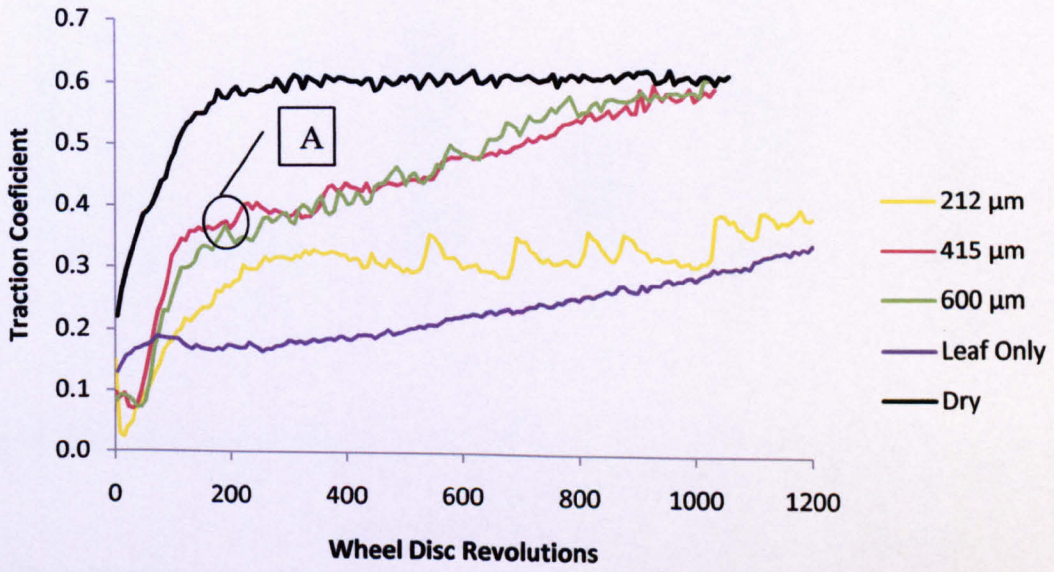

Figure 71 fixed number of particles traction curves ("A" is point where initial gradient changes)

There are some vast differences in these tests compared to the equivalent tests in the previous chapter. Most notably is the traction curve for the 212 µm gel which performs more in line with a leaf layer in this test compared to in the previous chapter where it performed in line with the dry case. The 415 and 600 µm gels also seem to underperform, with the linear part of the gradient ending early at approximately 100 revolutions highlighted in Figure 71 as point A. It is hypothesised at this point the traction enhancer has completely gone from the contact and thus it is only the micro-slip in the contact which is removing the leaf layer, restoring the friction to dry levels. Evidence may be seen in the gradient of the curve after point A is equivalent to the leaf only case. This may also be the case for the 212 µm gel

where only 0.1 ml of gel was put onto the discs corresponding to an even shorter period in which the gel was active.

Initial gradients for the fixed number of particle test are shown in Figure 72. Again the gradients in these tests are almost half of what is seen in the previous chapter. However, the pattern where the mid range size particle shows the greatest rate of traction increase as seen in the previous chapter seems to be repeated in Figure 72, albeit with the 800 μm column now replaced with the 415 μm gel.

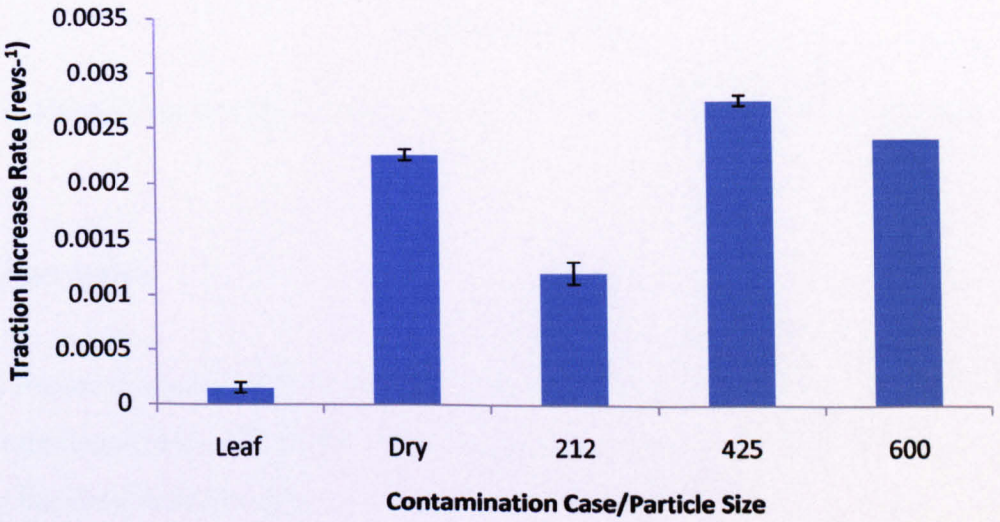

Figure 72 chart showing rate traction increase for different particle sizes for a fixed no. of particle tests

5.4.2.2 Impedance

Figure 73 shows the average impedances from the tests with fixed number of particles. It is interesting to note in Figure 73 that highest impedance is now seen for the 212 μm traction enhancer at 1.55 Ω. It is also the only traction enhancer to give higher impedance than the leaf layer. The Inverse relationship between impedance and particle size, as identified in Figure 68, is confirmed in Figure 73. This relationship does seem counter intuitive seemingly as there are a similar amount of particles on the discs. However, this does not mean that there is the same number of particles in the contact. Evidence in the 5-10 second columns seems to support the hypothesis proposed in section 4.2.1, in that the traction gel seems to be all but gone from the contact around the 100 cycle mark (20 seconds). This is because in the 5-10 second period the impedance drops within close proximity of the dry dynamic impedance.

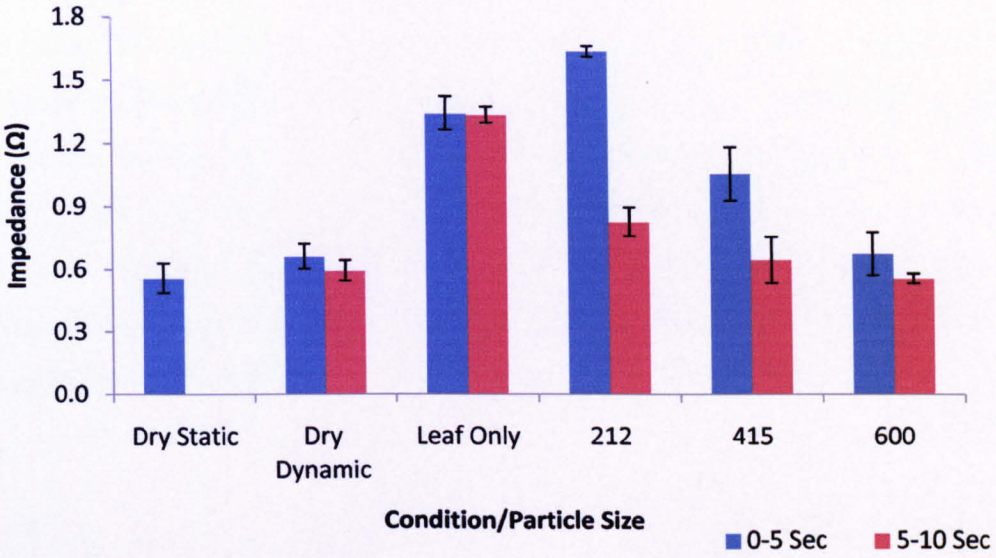

Figure 73 chart showing average impedance calculated for each contamination condition over 5 and 15 seconds

5.4.2.3 Wear Rates

Figure 74 shows the mean wear rates seen in the fixed particle tests and compares them with the wear rates seen under the fixed volume tests. It can be seen that the wear rates are much higher for the fixed particle tests.

Table 8 shows the number of sand grains used for both the fixed volume and fixed particle tests. The biggest difference was with the 212 µg gel were the 1 ml used in the fixed volume tests would have contained approximately 51,700 particles, ten times more than was used for these fixed particle tests. For the 415 µm gel the difference was less pronounced with 6900 grains used in the fixed volume tests. Only in the case of the 600 µm gel were less particles used in the fixed volume tests with 2400. However, these differences in number of particles between fixed volume and fixed particle tests do not seem to correlate. The large wear rate for the 600 µm gel is in the range seen for the leaf layer only which was performed on used discs. It was reported above how the wear rate of the used discs suddenly jumped from levels below 20 to over 150 µg/cycle. Therefore this wear rate cannot be relied upon. It is most likely that this is a false reading caused by a shift in the wear regime from mild to severe due to the age and test distance of the discs. According to the standard deviation of the fixed particle 212 and 415 columns the average wear rates are deemed to be within range of their fixed volume counterparts. Focusing on these two columns it can be said that there is an

increase in the wear rate for a decreasing amount of particles used. Just like with the impedance results this would also seem counter intuitive. It was observed during testing that some gel would be flung off of the disc surfaces during the test's calibration period (this is the period before the start of the test and involves the discs rotating out of contact). The amount of fling off could not be measured, however, it may have been the case that less of the product was flung off from the 212 and 415 fixed particle cases as less volume was applied to the discs compared to the fixed volume case. This was especially the case for the 212 µg as only 0.1 ml was put on to the discs and no fling off was observed.

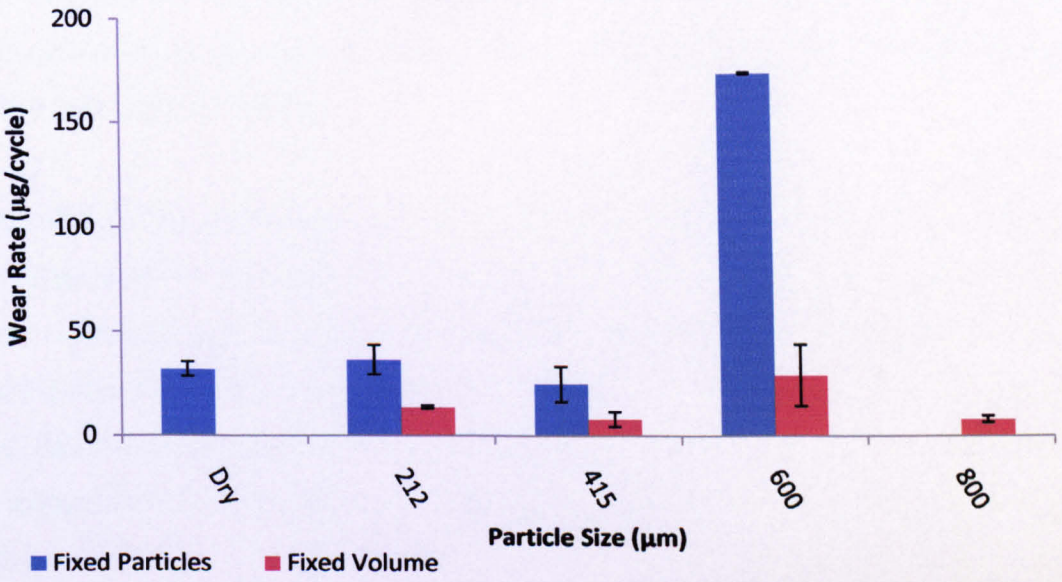

Figure 74 combination of rail disc wear rates for fixed volume and fixed number of particle tests

5.5 Discussion

In this chapter a technique has been developed to measure wear and electrical impedance due to contaminants/friction modifiers/ traction enhancing products becoming entrained within the wheel/rail contact. This was done using the University of Sheffield Rolling Sliding test rig (SUROS). This work was complementary to the work done in the previous chapter where a technique for measuring the performance of traction enhancers by traction measurement was developed. There was an unintentional difference in viscosity of the traction enhancers used in this study than in the previous chapter. A new leaf formula was also used in these tests giving a leaf layer which appeared similar to one which is seen in the field. This new layer also increased the impedance of the contact to over 1.2 ohms whereas no significant

impedance change was seen with the previous formula. It has been seen in [Lewis, 2006c] that dead leaves can cause significant isolation. It was therefore decided that this new leaf layer would be more appropriate for this study as it involved isolation testing. Hence, the isolation of the leaf layer and product together would be measured which would be more likely the case in the field. The combination of the new leaf layer and lower viscosity gels affected the traction measurements and marked differences in performance can be seen between the two chapters. However, the focus of this chapter has been the development of a technique to measure impedance posed by these products. It should be noted that any impedance measurement seen in these tests cannot be translated directly to the actual wheel/rail contact due to the relative difference in the size of the contact patch in either case. It is therefore more important to focus on relative changes in impedance levels versus particle size rather than absolute values.

As with testing in the previous chapter tests were both performed using a fixed volume of gel (i.e. different number of particles for each particle size) and a fixed number of particles (different amount of gel for each particle size). It was important to see the contribution of isolated particle sizes; however, the gels were all loaded with a fixed ratio of sand (i.e. 45% by mass) and this is how they would be delivered in the field. Therefore it was also important to test using a fixed volume of gel meaning a fixed mass of sand regardless of particle size in each test.

One of the main studies of this chapter was the effect of contamination/friction modifiers/traction enhancers upon impedance levels. This is a major issue for rail network operators around the world who employ electrical track circuits to manage their signalling systems. It is difficult to define exactly what impedance level would prevent the shunting of an occupied section of track because any impedance below the resistance of the detector (in this test the detector was simulated by a 10 ohm resistor) would still allow a proportion of the current to be shunted by the occupying vehicle's axles i.e. the current will follow the path of least resistance). The only case where shunting of the occupied track would fail to happen is if the impedance in the contact exceeded the resistance of the detector. In this case a very small/insignificant current would be shunted through the vehicles axles. Most of the current would reach the detector, hence showing a clear signal when in fact the track was occupied. It will also depend on the limiting level of current at which the detector will show the track as

occupied or free. If we assume that shunting can only be prevented when the impedance in the contact is greater than or equal to the resistance of the detector, then none of the products or even leaf layer would have prevented the track to be shunted because the highest impedance measured was 1.6 Ω almost one tenth of the resistance of the simulated detector (10 Ω). It is also the case that the SUROS machine represents a worst case scenario of one axle occupying the track section. This could potentially be the case where a train may have stopped within two sections of track. However, locomotives have multiple axles representing multiple contact patches per section of track. In order for a contaminant/friction modifier/ traction enhancer to present a significant signalling threat it would have to cause enough impedance at each of those contact points as to prevent shunting. The chances of such an event would be debatable.

It must also be noted here that the level of impedance seen in these tests will not necessarily match what would be seen in the field. Due to the relatively larger contact patch in the actual wheel/rail contact, impedances would be expected to be much lower. It is known that the impedance across an actual uncontaminated railway axle is in terms of milliohms whereas the lowest impedance measured in this test, for the dry static condition, was 0.55 Ω, an order of magnitude higher. There are a number of possible reasons for this including the relative size of contact patch described above. The distance between the discs and the point of measurement, i.e. the simulated track circuit, will also play a part. The further away the point of measurement from the discs the longer the wires from the discs to the circuit and hence their resistance. However, there is a limit to how close the circuit can be placed to the machine due to the rotating shafts and safety guards.

When initially designing the apparatus for impedance measurement, the circuit was connected to the discs through the bearings of the machine. This was fine for static measurements; however, when the discs were rotating, measured impedance levels were seen to be within the range of 2.0-2.5 Ω for a dry/uncontaminated contact. This significant increase was due to the oil film which built up between the bearings as the shafts rotated. This problem was solved by moving the connections to the shafts themselves using copper slip rings. As can be seen from the results this has brought the dry impedance levels down to the region of 0.5 – 0.65 Ω, a significant reduction. There was a weak negative correlation

seen between particle size and impedance. However, this was outweighed by the standard deviation seen in some tests.

Wear rates were measured by weighing the discs before and after each test as done in [Lewis, 2006b]. A mass loss was measured for the rail discs and this was then divided by the number of cycles which the test had run for to give a wear rate in terms of μg/cycle. Interestingly a mass increase occurred for the wheel discs as shown in Figure 75.

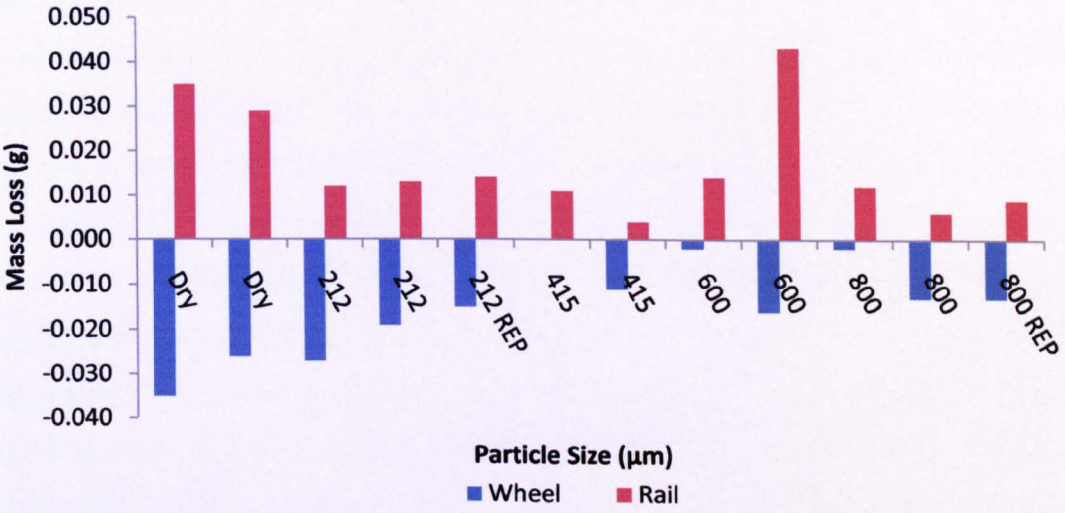

Figure 75 mass loss for discs used in fixed volume tests

There is evidence that some extent of third body abrasion has occurred here. Figure 69 shows a typical wheel disc post test with a darkened running band which seems to have crushed sand particles embedded in its surface. However, it is also clear from the dry case that there is a high degree of mass transfer happening as in this case there is no third body present yet still there the mass of the wheel increases after both tests. In the dry case the mass lost from the rail disc is almost identical to the mass gained by the wheel. However, when cases with the traction enhancers are examined the mass gained by the wheel seems to outweigh the mass lost by the rail. This suggests that both wear processes may be occurring. It should also be noted that the wear rates calculated may not solely be a consequence of the traction enhancers alone. Each test was run for approximately 1000 cycles (±30) and the traction charts indicate that the gels may not have been active for the whole of this period especially in the case of fixed particles see Figure 63 and 64. For these aforementioned tests, especially, a proportion of the wear may be due to a dry/metal-on-metal contact. It could be that the third body

abrasion is occurring while the product is in the contact and once it has gone the mass transfer mechanism takes over.

The standard deviation from the mean of the wear tests was also quite large showing that there was a lack of repeatability in the data. This was especially the case for the 600 μm gels in both fixed volume and fixed particle tests. At the moment of writing this cannot be explained as this seems to be isolated to one particle size in the middle of the range tested. From experience gained in other chapters it seems wear for tests of relatively short duration; is difficult to measure by volume, profiling or surface roughness evolution. It does seem that mass measured before and after the tests is a much more reliable way to measure wear in this case. However, in these tests the test specimens do come out of the test with a dried layer of sand and leaf which has been squeezed out of the contact and has built up on the shoulders of the discs. Although the majority of this layer was removed prior to weighing, there were some small more stubborn layers which could not be removed without abrading the disc. As the changes in mass before and after were in the region of tens of milligrams these layers could have provided a small error in readings. One way to counteract this may be to run longer tests consequently leading to higher mass loss so that these small layers represent less significant errors. The challenge would be finding a way of supplying the gels to the contact over a period of time. In the previous chapter a peristaltic pump was used, however, the abrasive nature of these traction enhancers proved problematic.

Figures 76 and 77 show microscope images of post test disc surfaces. Figure 76 shows the surface of the wheel disc post test. It can be clearly seen that there is a "black" third body layer on the surface which is presumed to be transferred leaf layer from the rail disc. Figure 77 shows the surface of the rail disc post test. It can be seen that the surface is brighter and hence smoother than the wheel in Figure 76. There is also no evidence of the original leaf layer left. This is in agreement with what is seen in Figure 70 (b) where we see a relatively smooth/polished surface.

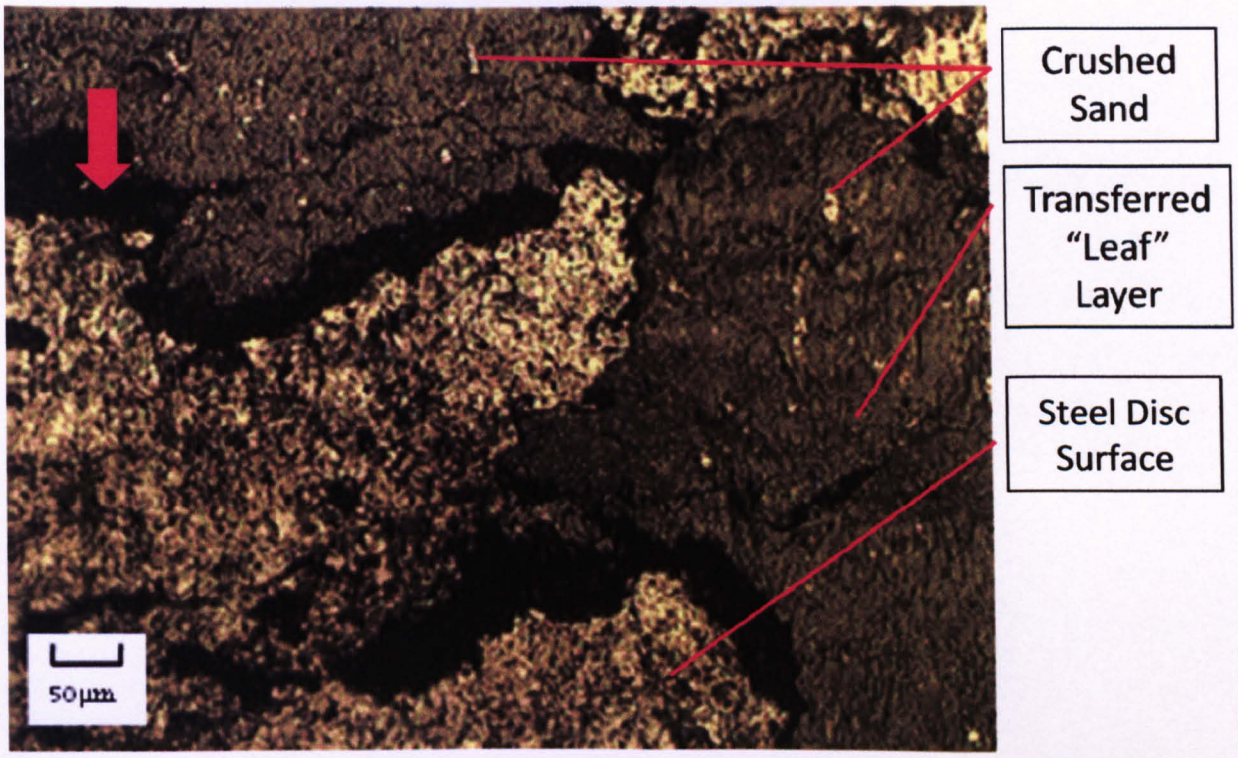

Figure 76 image of wheel disc under microscope (arrow indicates direction of travel)

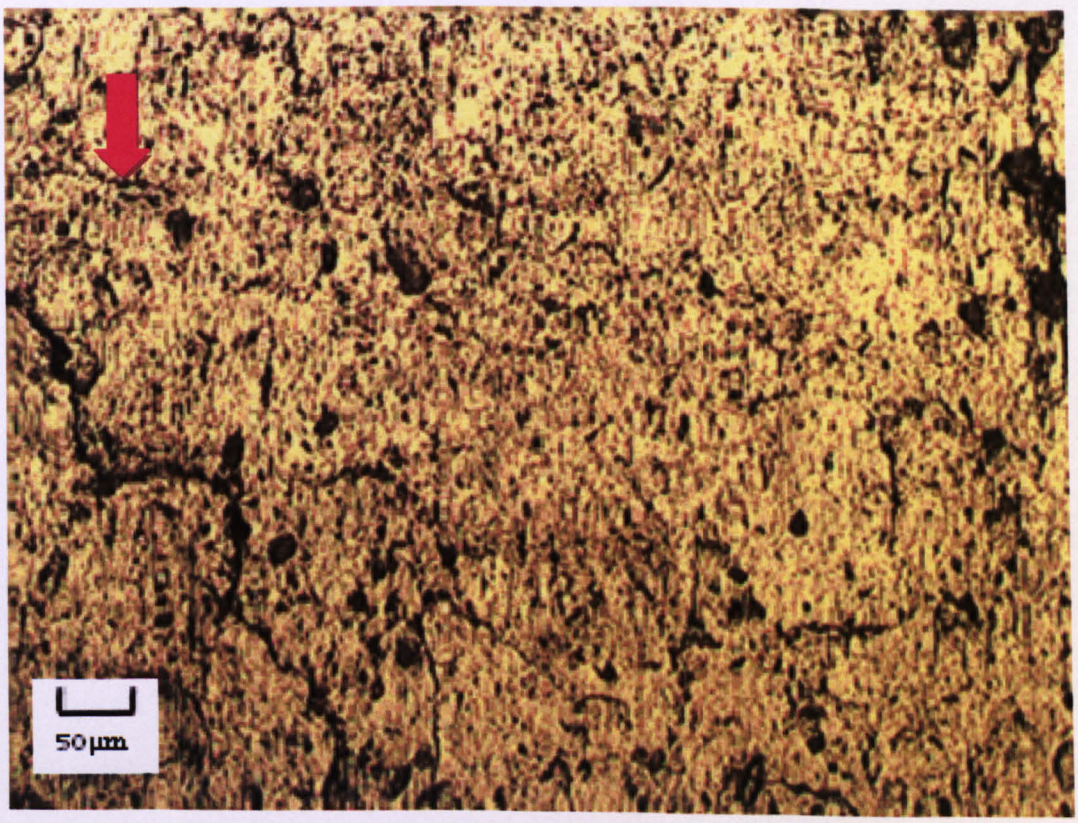

Figure 77 image of rail disc under microscope (arrow indicates direction of travel)

It is not clear whether this transfer of third body layer from rail to wheel would occur in the field. However, as shown in these tests, it may actually be beneficial if it does. The leaf layer

on the rail seems to act as a sacrificial layer which is worn away first by the sand and although metal is lost from the rail the wear rate is lower than that of a dry contact (i.e. no leaf layer or traction enhancer) as shown in Figure 68. The presence of the leaf layer and gel in the contact seem to reduce wear rates many times over what would be expected for sand alone. As the leaf layer transfers to the wheel it seems to go through a change in friction from approximately 0.2 when the leaf layer is on the rail to 0.5 when the layer is transferred to the rail. However, it is not clear whether this wheel layer would still give safe levels of traction when wet.

Chapter 6: Investigation of Influences of Atmospheric Conditions on Performance of Friction Modifiers

6.1 Introduction

The use of friction modifiers (FM's) is becoming more accepted by rail operators around the world. This means that there is an increasing number of different atmospheric conditions under which these friction modifiers are expected to perform. A friction modifier must function the same in the low temperatures of Canada as it does in the high humidity of Spain. It is also the case that FM's are now being used on underground networks offering uniquely different conditions. Railhead contamination levels will also vary from climate to climate, thus it is important to develop an understanding of how all these factors affect the performance of friction modifiers. The friction modifier tested in this investigation was, Keltrack®, which is a top of rail friction modifier developed by the Kelsan Technologies Corporation. Keltrack® is a water based product which is designed to re-engineer the "third body" on the surface of the railhead [Lu, 2005]. Third body is a term used to refer to the interfacial layer between the wheel and rail, which is usually detached from, and of different make-up to, the wheel and rail steels. This layer is mainly made up of oxidised wear debris in the form of Fe_2O_3 (Red Oxide) and under certain circumstances Fe_3O_4 (Black Oxide) but in smaller quantities. Keltrack®, in its liquid form, will be mixed with the third body as it is rolled over by multiple wheel sets of a passing locomotive. When the friction modifier dries, a new third body is created with different frictional properties from the original. The stated friction for a Keltrack® treated rail is in the range of 0.3-0.35 as compared to 0.5-0.6 for non treated rail. This lower operating friction is sufficient to reduce wear levels but not impede braking [Lu, 2005; Fletcher, 2000a]. Other stated benefits include a reduction in rolling noise level [Eadie, 2003], reduced corrugation [Eadie, 2003b], reduced lateral forces [Suda, 2005] and improved fuel consumption [Tomeoka, 2002].

The aim of the work described was to test the performance of the Keltrack® friction modifier under various environmental and contamination conditions. The tests were completed using a pin-on-disc (POD) device contained within an atmospheric chamber. This allowed for the control of relative humidity (RH) and temperature while performing each test. One particular focus of the work was the study of the FM performance at typical underground tunnel

conditions (70 % RH and 10°C). Glow Discharge Optical Emission Spectroscopy (GDOES) analysis was also employed to investigate any chemical changes in the surface of the discs post test.

6.2 Experimental Set-up

6.2.1 Pin-on-Disc Rig

The friction modifier was tested using a pin-on-disc test machine at various humidity and temperature combinations. The friction modifier was mixed with iron oxide prior to the test at different concentrations to simulate different debris situations. Tests were conducted with a pin-on-disc (POD) machine which had an environmental chamber attached, see Figure 78. This allowed the control of humidity and temperature during each test. This rig has previously been used by Olofsson [2004] to study the effect of humidity on leaf layers and Sundh [2009] relating wear transitions to temperature.

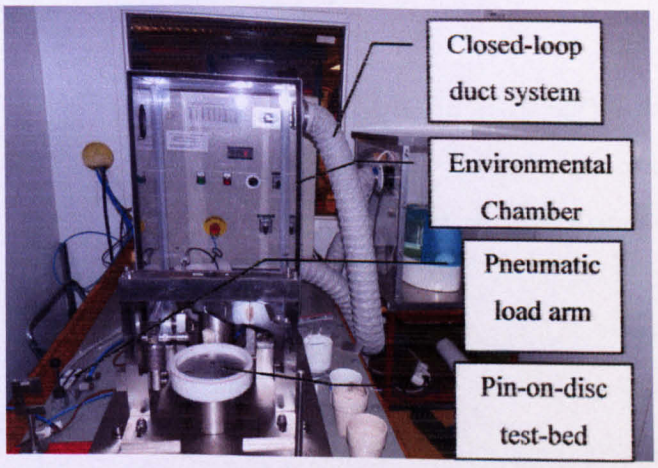

Figure 78 pin-on-disc rig with environmental chamber

The rig was set up to simulate the micro-slip region of the wheel/rail contact. A static pin with 5mm radius was loaded against a rotating disc of 90mm diameter. Load is applied to the pin by hanging a dead weight from a cantilever. Humidity is controlled via a closed loop ducting system, using a water boiler to inject the air around the rig with water vapour. The test area is enclosed in an air tight surround (environmental chamber in Figure 78) hence only the relatively small volume of air directly surrounding the test area is treated. A humidity sensor on the inside of the enclosed space provides feedback to the system, switching the water boiler on and off when required. The rig is situated within its own air conditioned room

allowing air temperatures within the range of -40 to 30°C. The test can be monitored and controlled remotely with pneumatic controls.

6.2.2 Test parameters

The maximum Hertzian contact pressure between the pin and disc was calculated to be 900MPa at a sliding speed of 0.01 m/s. Friction modifier was mixed with iron oxide prior to each test in specific ratios according to Table 10 and 11. The FM/oxide mixture was then painted onto the pin. This technique offered little control in the amount of FM added to the pin; however, results were repeatable. It was also thought to be the best way to replicate how the wheel (pin) transfers the friction modifier to the rail (disc). The sliding speed, at which all tests were conducted, corresponds to the speed in the micro-slip region between the actual wheel and rail [Olofsson, 2007]. The speed was also low enough to ensure that any centripetal forces the friction modifier may have been subject to were negligible.

6.2.3 Test Sequence

6.2.3.1 Reference Tests

Reference data needed to be gathered in order to provide a series of bench marks that all other data could be compared to. Two test conditions were chosen for this with 100% friction modifier and 100% Haematite applied to the surface of the test discs. 100% FM would represent a case where there was very little/no iron oxide layer on the railhead before the FM was applied. 100% oxide would represent a case of a dry rail which was not treated with FM. Iron oxide was attached to the disc surface by diluting it with acetone and then painting it to the disc surface. Once the acetone had evaporated, a thin layer of oxide was coated on the disc. However, this oxide layer was not bonded very strongly to the disc due to its smooth surface. Figure 79 shows a post test surface where the pin has worn through the oxide layer.

Figure 79 image showing wear scars on 100% oxide disc specimen

Test	Condition	Concentration %	Temp °C	RH %
1	Dry	100	10	40
2	Pure FM	0	10	40
3	Dry	100	10	40
4	Pure FM	0	10	40
5	Dry	100	10	70
6	Pure FM	0	10	70
7	Dry	100	10	70
8	Pure FM	0	10	70
9	Dry	100	10	90
10	Pure FM	0	10	90
11	Dry	100	10	90
12	Pure FM	0	10	90

Table 9 test matrix for reference tests

6.2.3.2 Temperature, Humidity and Oxide Investigation

To ensure that the maximum amount of variables and repeat tests were achievable with a limited number of specimens, the tests were separated into two series. Series 1 fixed temperature at 10°C and an oxide concentration at 35%, with humidity and iron oxide type varied, as in Table 10. The test parameters representing tunnel conditions (10°C and 70% RH) are in series 1 (See Table 10, tests 1.3 and 1.4). Series 2 (Table 11) used a fixed humidity of 40% with variable temperature and oxide concentration. Red oxide, Fe_2O_3, is the

major component of railhead rust and hence tests in Series 2 were fixed with Fe_2O_3. The duration of the tests was chosen to be 30 minutes, which was thought long enough to observe the test through to steady state (by friction).

Test No.	Temp (°C)	Humidity (%)	Iron Oxide	Mass Conc. (%)
1.1	10	90	Red	35
1.2	10	90	Black	35
1.3	10	70	Red	35
1.4	10	70	Black	35
1.5	10	40	Red	35
1.6	10	40	Black	35
1.7	10	90	Red	35
1.8	10	90	Black	35
1.9	10	70	Red	35
1.10	10	70	Black	35
1.11	10	40	Red	35
1.12	10	40	Black	35

Table 10 test parameters for Series 1

Test No.	Temp (°C)	Humidity (%)	Iron Oxide	Mass Conc. (%)
2.1	10	40	Red	25
2.2	20	40	Red	25
2.3	10	40	Red	45
2.4	20	40	Red	45
2.5	10	40	Red	25
2.6	20	40	Red	25
2.7	10	40	Red	45
2.8	20	40	Red	45

Table 11 test parameters for Series 2

Samples for the GDOES analysis were prepared separately from the main friction tests. Tests to prepare samples for this analysis were much shorter than the tests in Table 10 and 11, as

there only needed to be contact between the pin and disc for four whole revolutions. All the GDOES samples were prepared according to Table 19.

Test No.	Temp (°C)	Humidity (%)	Iron Oxide	Mass Conc. (%)
G.1	10	40	Pure	35
G.2	10	40	Red	35
G.3	10	40	Black	35
G.4	10	70	Pure	35
G.5	10	70	Red	35
G.6	10	70	Black	35

Table 19 parameters for GDOES sample preparation

Lu et al [2005] sampled levels of railhead oxidation on various North American mainlines and compared this with specified friction modifier application rates. Results of this study showed that once a friction modifier layer had been applied to the rail head, the resulting, "adapted, third body" would consist of 90% oxide. This level of concentration was intended to be replicated in these experiments. However, when this was mixed in the lab it produced a very viscous "clay like" compound which was unrecognisable from a friction modifier/oxide mix as seen in the field and could not be tested. It is perhaps the case that this "adapted, third body" with 90% oxide could be created successfully under the high pressure/high temperature conditions of the actual wheel/rail contact.

6.2.4 Test Procedure

A fresh mixture of FM and iron oxide was prepared prior to each test to prevent the mixture from drying out before the test start. Oxide to FM ratios were determined by weight according to the test mandate; see tables 10, 11 & 19. The FM/oxide mix was applied directly to the pin. This replicated how the FM is applied in the field i.e. from wheel to rail. The test was also set-up to simulate the micro-slip conditions in the area of contact between wheel and rail.

Figure 80 shows what happens to the mixture during the tests. Once in contact with the disc, excess mixture builds up around the edges of the wear track. Tests were run for 30 minutes

each to allow the FM mixture to dry and begin to wear out of the contact. As well as recording the friction coefficient, surface chemical compositions were measured using Glow Discharge-Optical Emission Spectroscopy (GDOES) analysis. GDOES is an erosive technique which detects chemical traces layer by layer through the depth of the material.

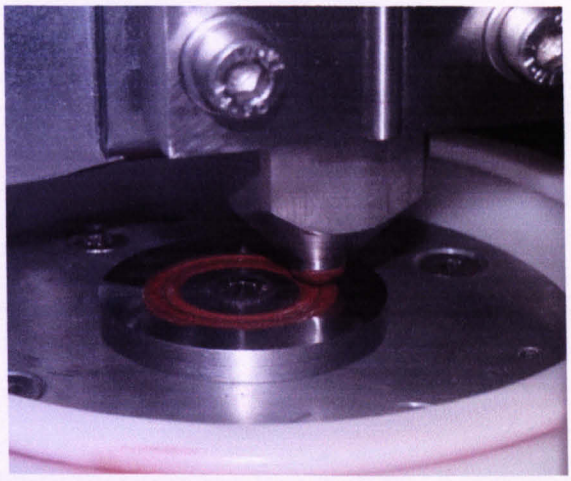

Figure 80 friction modifier mixed with red oxide painted on pin

6.3 Results

Friction data from each test was gathered and is shown in Figure 81 - 87. Test numbers refer to those in Tables 10, 11 and 19.

6.3.1 Reference Tests

Friction plots are shown in Figure 81 – 83. Results for pure friction modifier do not change and remain steady at a friction coefficient of approximately 0.2. These results seem largely unaffected by changes in humidity. Results for the 100% oxide conversely do seem to be effected by humidity changes. At the lower humidity (40%) the friction seems to rise continually throughout the test, only settling during the last couple of metres of the test at a friction coefficient of approximately 0.7. At 70% RH the friction settles relatively quickly at approximately 0.55. Again at 90% RH the friction seems to stabilise relatively soon at approximately 0.5.

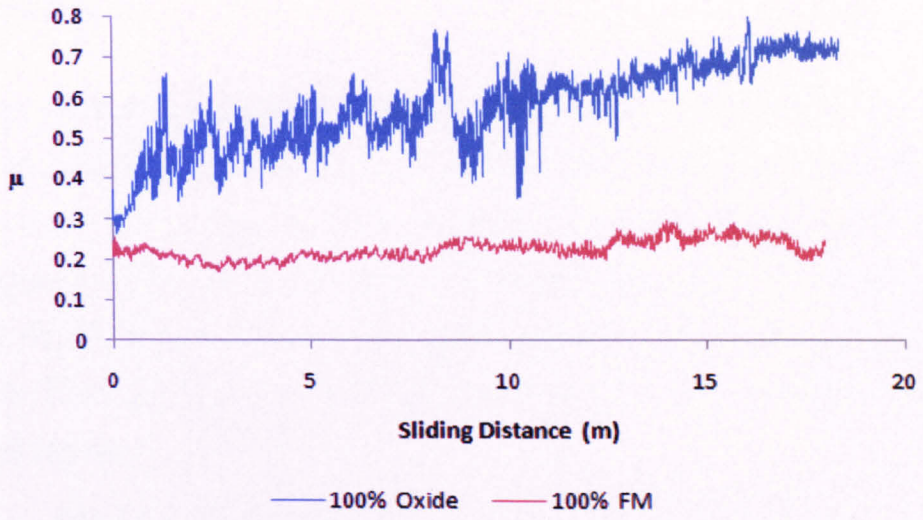

Figure 81 friction plots for test R1 and R2 at varying oxide concentration, 40% RH and 10°C

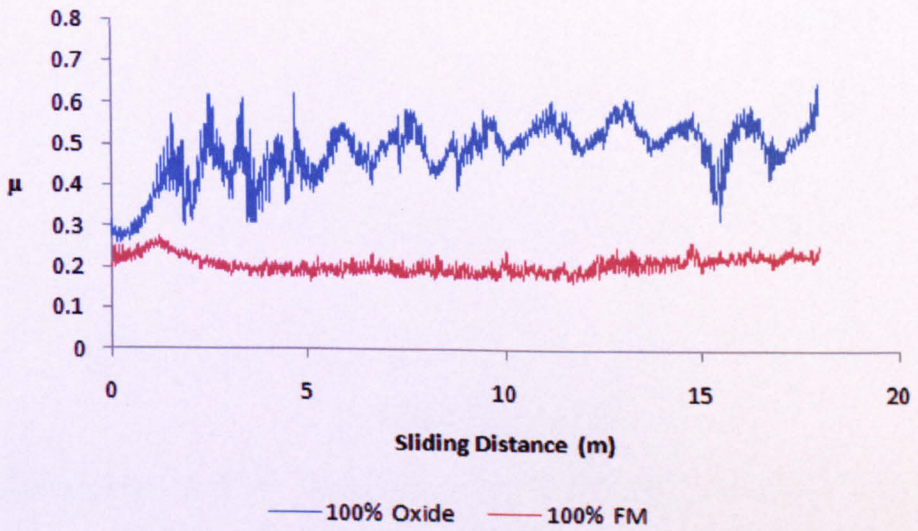

Figure 82 friction plots for test R3 and R4 at varying oxide concentration, 70% RH and 10°C

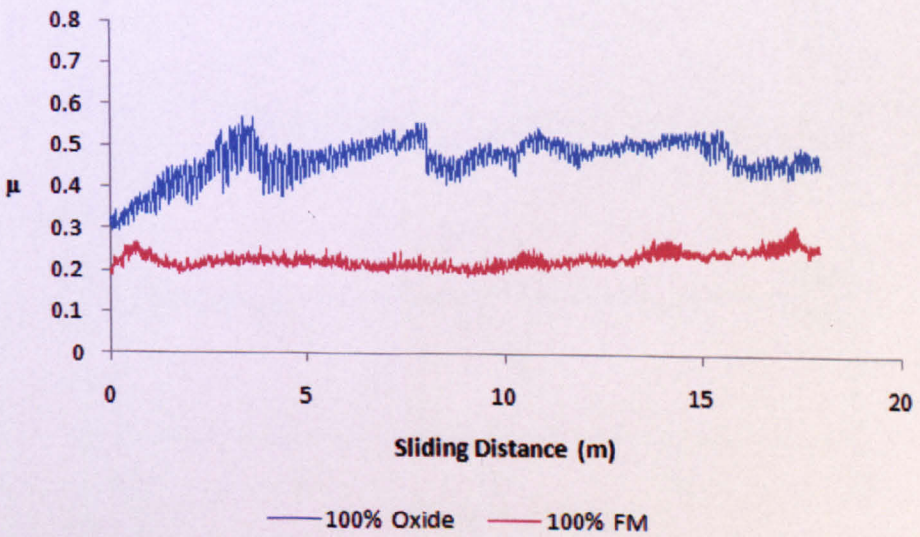

Figure 83 friction plots for test R5 and R6 at varying oxide concentration, 90% RH and 10°C

6.3.2 Test Series 1

Figures 84 and 85 show results from test series 1. These show a comparison between red and black oxide at a fixed temperature of 10°C. In both charts you can see how friction rises at the lower humidity but remains steady at the higher humidity's. Figure 85 also shows that friction is generally higher for black oxide with the 40% humidity line rising at a faster rate also. Data in Figures 84 and 85 is subject to a 100 period moving average to counteract noise from the tests. There is a clear transition between 40 and 70% RH at which the film will stay wetted or will dry out.

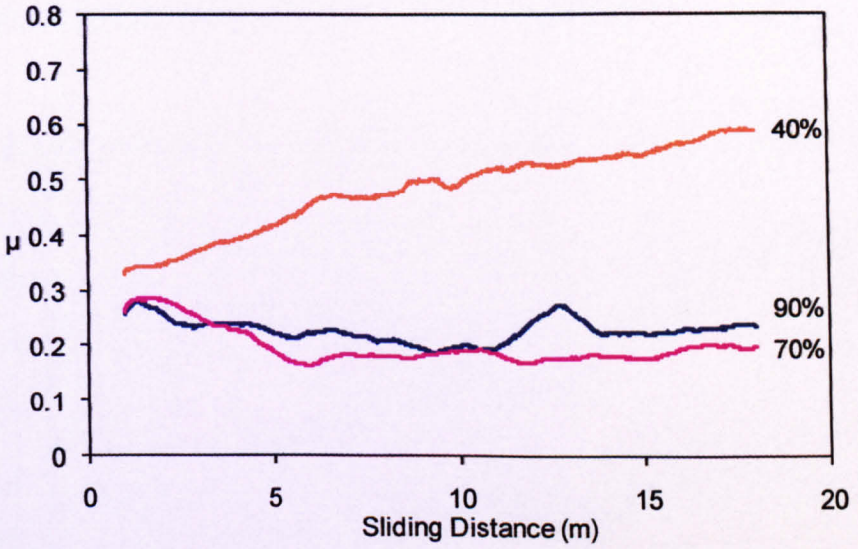

Figure 84 friction plots for tests 1.1, 1.3 and 1.5 with red oxide (concentration 35%), at varying humidity and 10°C

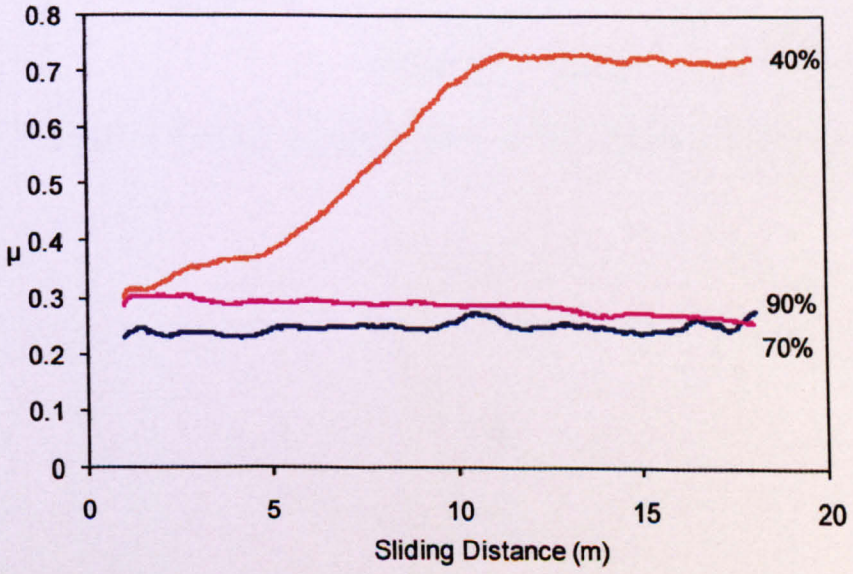

Figure 85 friction plots for tests 1.2, 1.4 and 1.6 with black oxide (concentration 35%) at varying humidity and 10°C

6.3.3 Test Series 2

Figures 86 and 87 show results for Series 2 tests. Figure 86 shows the results of tests fixed at 40% RH and 25% oxide concentration with varying temperature. There is a clear trend that shows friction rising for the lower temperature yet staying steady at the higher temperature. Figure 87 shows tests performed at 40% RH and 45% concentration with varying temperature. These tests seem to show that there is no dependence of the friction to rise with temperature as the friction curves remain steady in all cases. Results from series 2 show a clear relationship that temperature is less of an influence for higher oxide concentrations. These results however, do not take into account the effects of humidity.

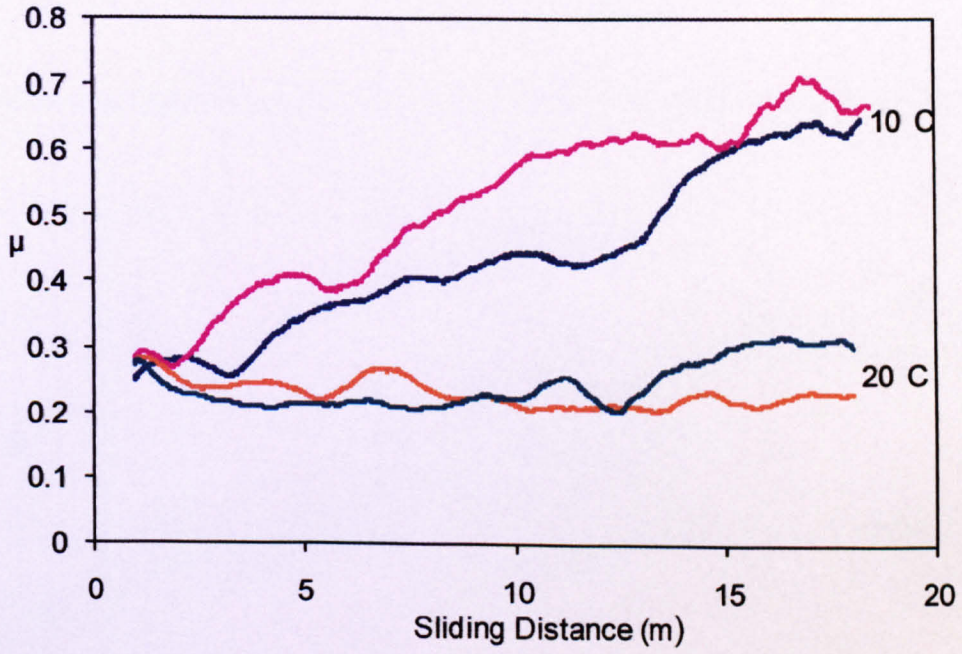

Figure 86 friction plots for tests 2.1, 2.2 2.5 and 2.6 at a concentration of 25% and RH of 40%

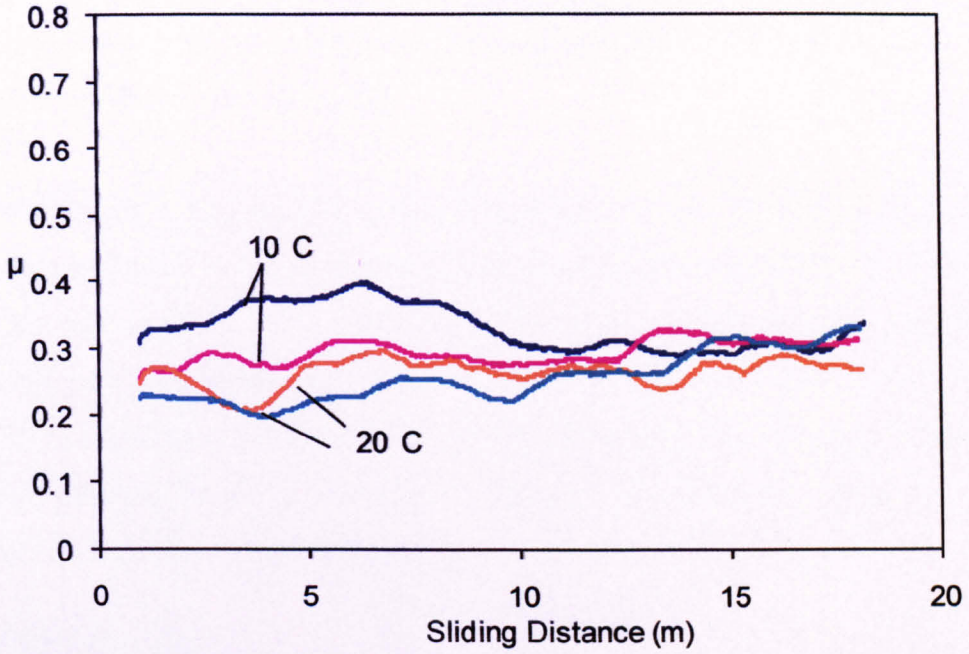

Figure 87 friction plots for tests 2.3, 2.4, 2.7 and 2.8 at a concentration of 45% and RH of 40%

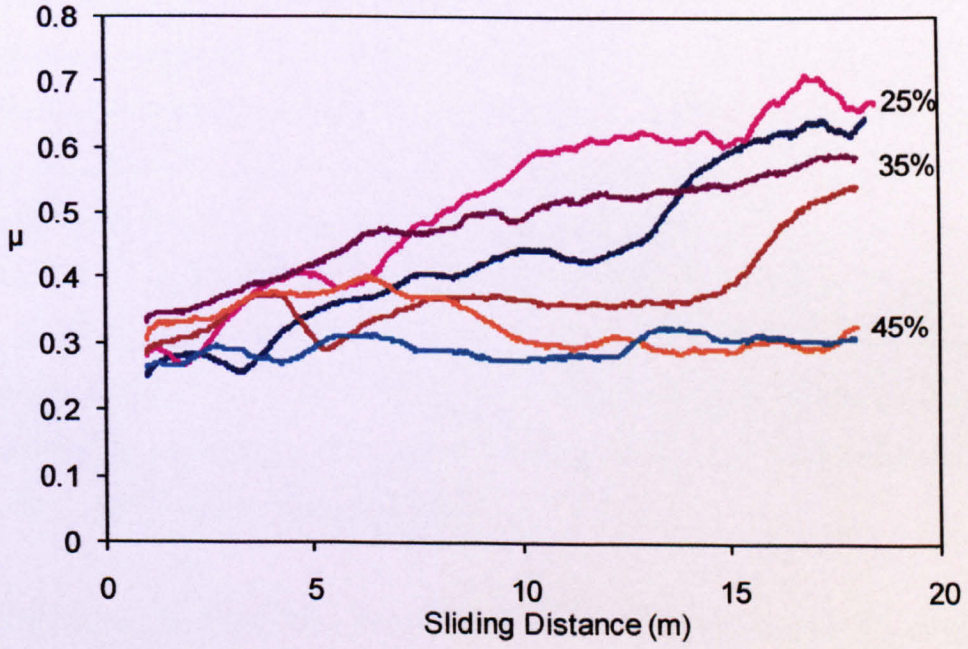

Figure 88 friction plots for tests 2.1, 2.3, 2.5, 2.7, 1.5 and 1.11at a RH of 40% and temperature of 10°C

Figure 88 incorporates data tested under the same conditions from both Series 1 and 2 at three different oxide concentrations. All of the tests in this chart use red oxide and were performed at 10°C.

This chart highlights the inverse relationship between the rate of friction increase and concentration of oxide in the mixture. At a concentration of 45% there is no increase in friction levels for the duration of the test.

It should also be noted here that the retentivity (defined as how long the FM can effectively provide friction control) of these samples could be affected by its viscosity. It was observed that samples with a lower oxide concentration are less viscous and hence could be more easily pushed away from the pin/disc contact zone, thus resulting in a lower retentivity. In contrast, those with higher solid content could hold themselves within the contact zone and modify the pin/disc surface, providing a greater retentivity and helping to maintain a relatively low friction level for a longer time.

6.3.4 GDOES Results

The Glow Discharge Optical Emission Spectroscopy, GDOES, was used to analyse the surface of test discs in a post test condition. Six cases were analysed and are shown in Table 12. The technique for preparing a GDOES sample is the same as running a normal pin-on-disc test; however, the pin only needs to be in contact with the disc for four whole revolutions in order for the near surface to be modified. The load and speed were kept the same for the GDOES tests. Only the discs were analysed as the technique can only work on flat surfaces. GDOES has a focal patch of 4 mm diameter as in Figure 89. To improve the quality of the surface to be scanned, a 4 mm wide test zone was created by running 10 individual tests tightly within the 4 mm section each completing 4 complete revolutions as in Figure 89. This was repeated for all six samples. Tests lasted between 24 and 35 seconds each as the contact radius was changed to fill the 4 mm focal area.

GDOES analysis works as follows. First the sample is placed in Argon, Ar, to give an inert atmosphere. Next a voltage is applied between a cathode the disc surface, which acts as a sacrificial anode. This causes the Argon to become ionised which in turn causes a sputtering of the disc surface. Atoms in the disc surface are thus excited releasing energy in the form of a photon [Hoffmann, 1993]. The type and amount of each element in the surface is identified by the wavelength and frequency of this emitted light. This test methodology has been previously used to evaluate environmentally adapted lubricants by Bergseth et al [Bergseth,

2008], biological layers on rail [Olofsson, 2007] and roller bearing lubricants by Olofsson and Dizdar [Olofsson, 1997].

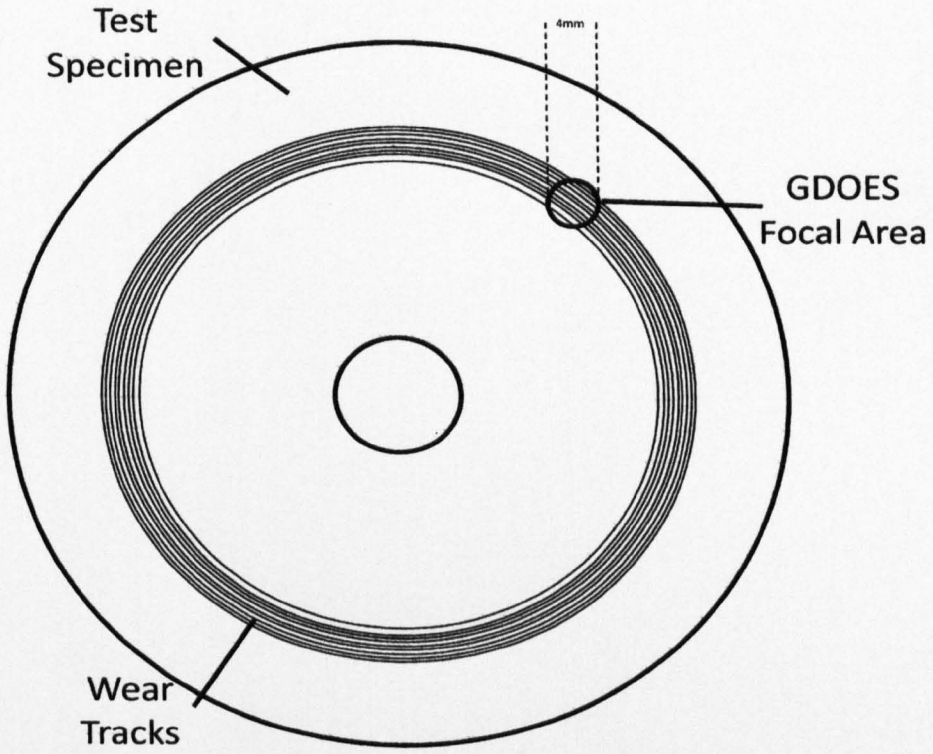

Figure 89 illustration of preparation of GDOES sample

Condition/ Case	Iron Oxide		Temp. °C	RH %
	Type	Conc. %		
Pure FM	-	0	10	40
Pure FM	-	0	10	70
Red FM	Fe_2O_3	35	10	40
Red FM	Fe_2O_3	35	10	70
Black FM	Fe_3O_4	35	10	40
Black FM	Fe_3O_4	35	10	70

Table 12 conditions for GDOES Tests

Results of the GDOES analysis are shown in Figures 90-95 below.

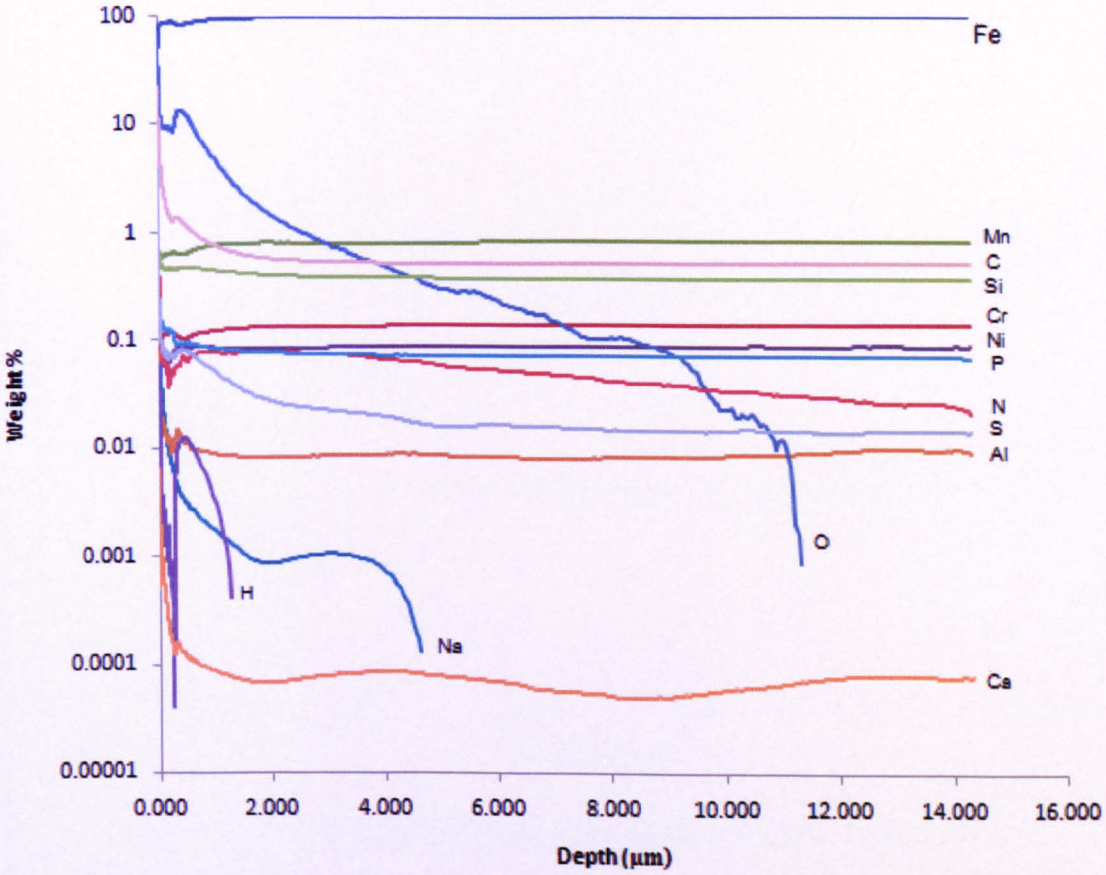

Figure 90 GDOES results for pure-FM test performed at 40% RH and 10°C

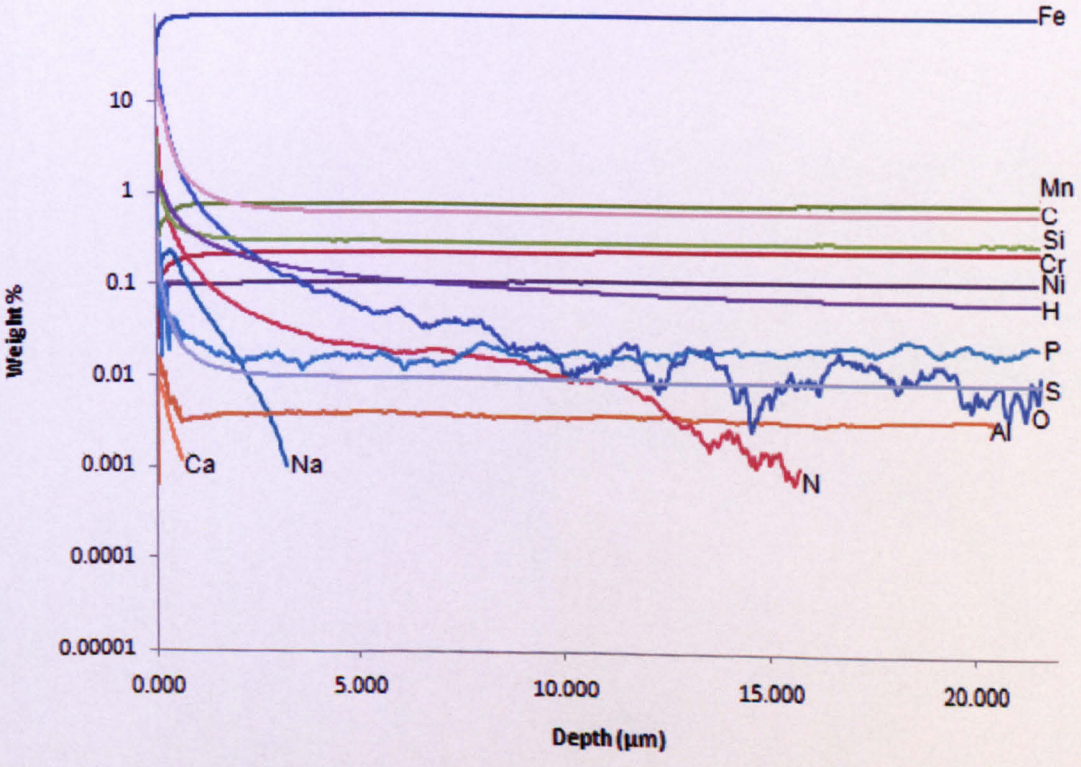

Figure 91 GDOES results for pure-FM test performed at 70% RH and 10°C

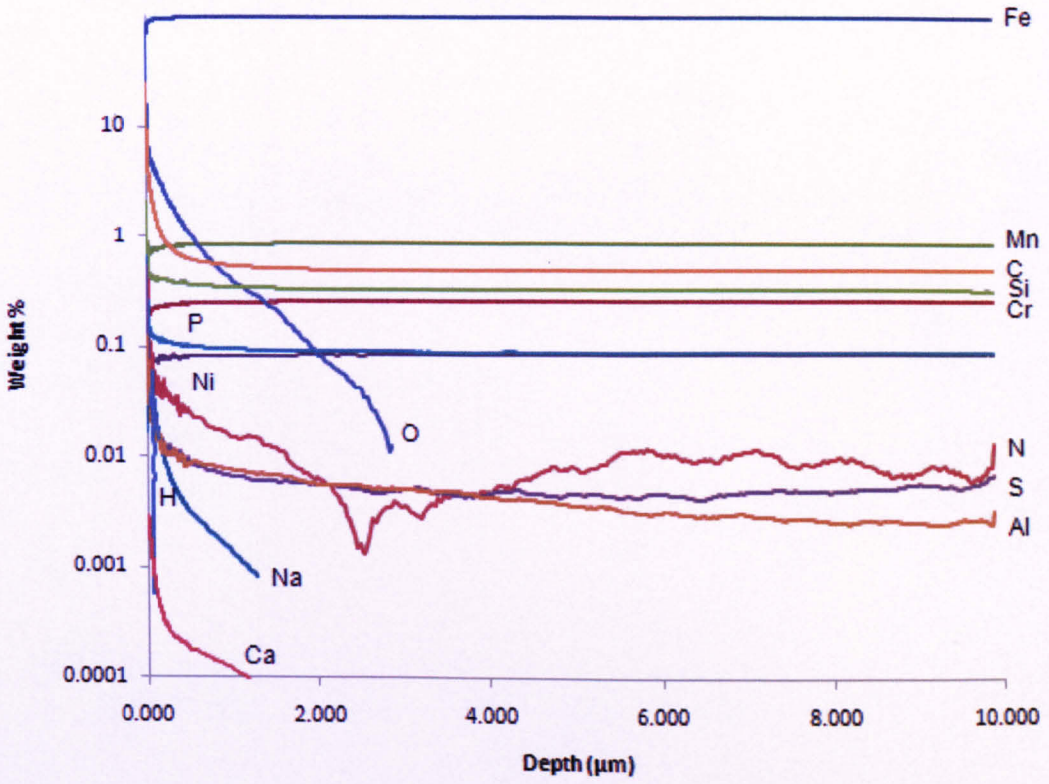

Figure 92 GDOES results for red-FM test performed at 40% RH and 10°C

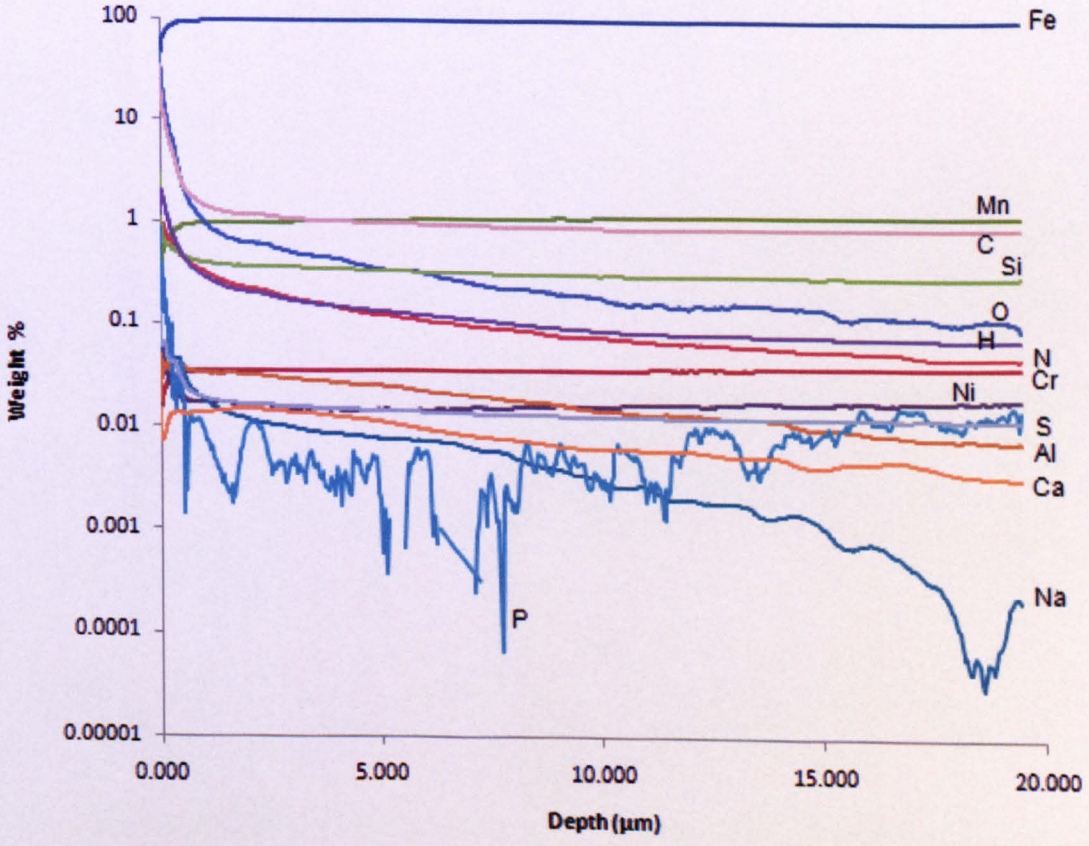

Figure 93 GDOES results for red-FM test performed at 70% RH and 10°C

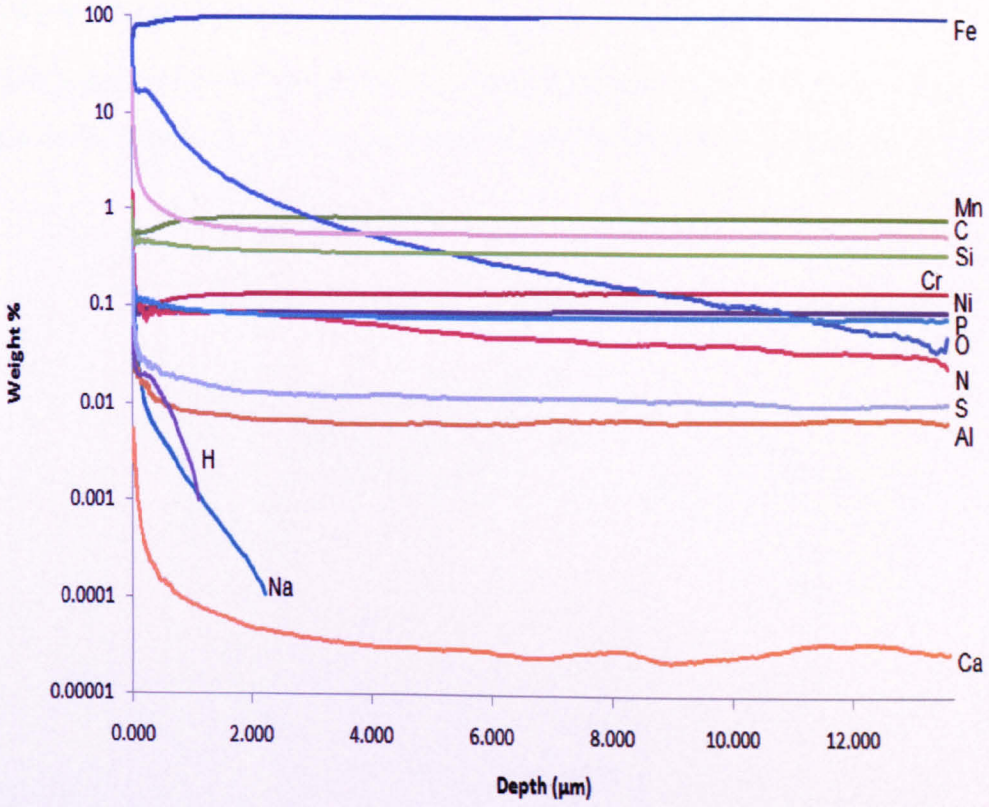

Figure 94 GDOES results for black-FM test performed at 40% RH and 10°C

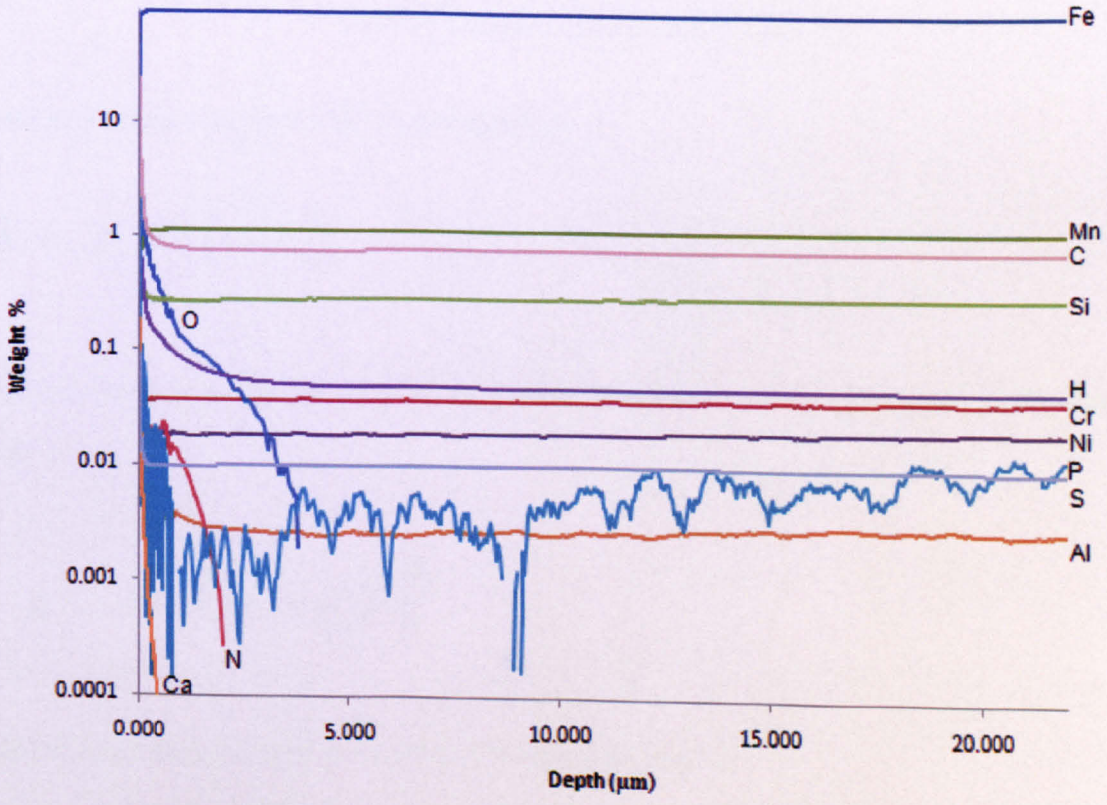

Figure 95 GDOES results for black-FM test performed at 70% RH and 10°C

6.3.5 Wear Results

Wear volumes from each test were calculated by measuring the diameter of the wear scar on each pin as in Figure 96. Equations 9 and 10 can be used to calculate the volume of material lost.

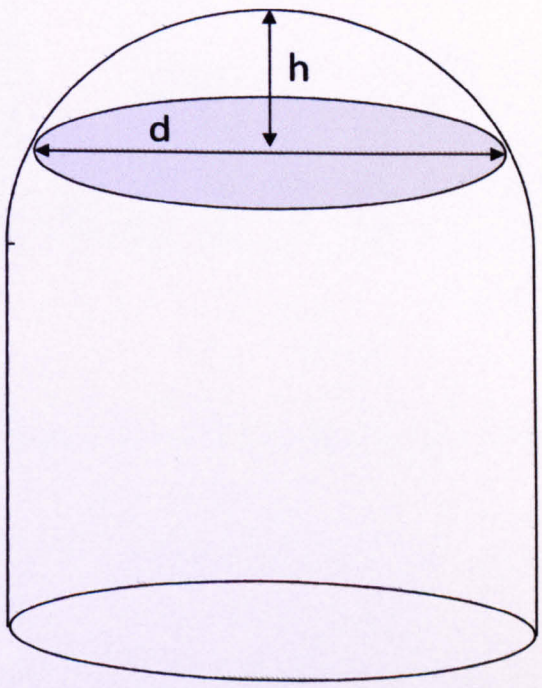

Figure 96 illustration of pin wear volume

The volume of material lost (V) is calculated by:

$$V = \pi . h^2 . \left(r - \frac{h}{3}\right) \quad (9)$$

Where h is the height between the worn surface and pre-worn pin apex and r is the radius of the pin

$$h = r - \left(r^2 - \left(\frac{d}{2}\right)^2\right)^{\frac{1}{2}} \quad (10)$$

Results of wear calculations are shown in Figures 97 and 98.

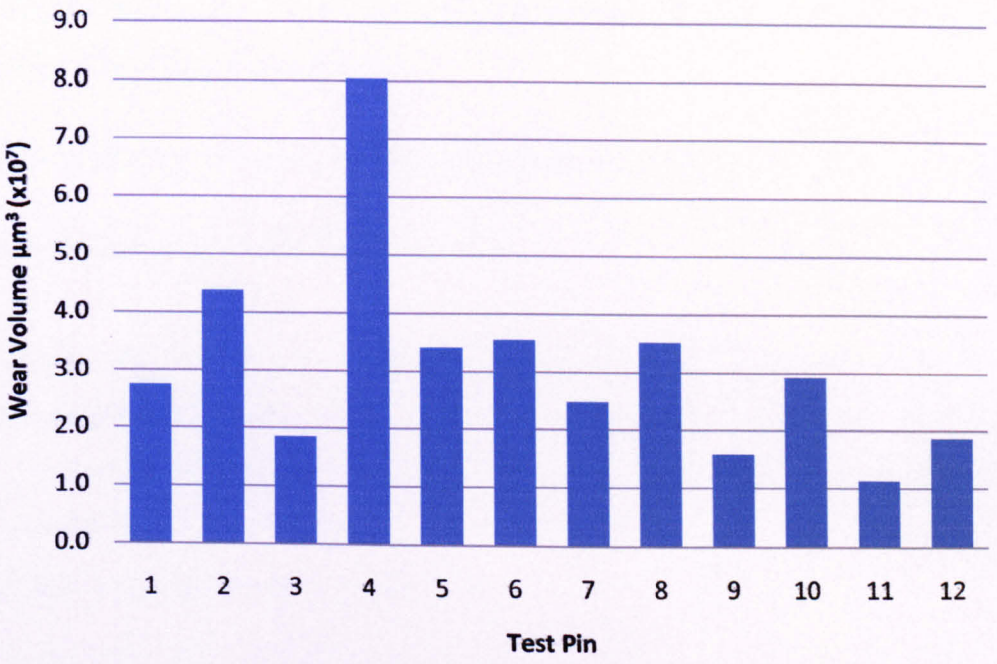

Figure 97 wear data for test series 1 test numbers refer to those in Table 10

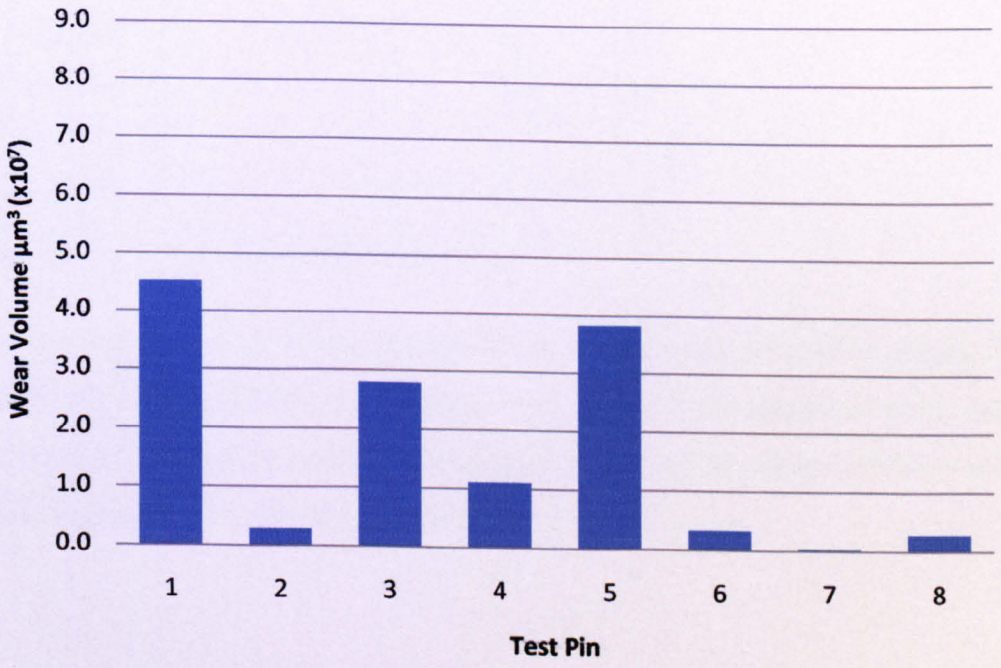

Figure 98 wear data for test series 2 test numbers refer to those in Table 11

The measurement of the wear scars was difficult even with the aid of a microscope. Some of the scars were not perfectly circular and it was often difficult to identify the boundary between worn and un-worn metal. There is always a certain element of error when

calculating wear and this combined with the extremely small wear volumes has resulted in the above data with no correlation.

6.3.6 Exploration of Temperature and Humidity Transitions

6.3.6.1 Investigation of Humidity Transition

A series of tests were designed to explore the humidity transition seen in series 1. Table 13 shows these tests. The transition was seen to be somewhere between 40 and 70% relative humidity. To explore this, three humidity levels which were evenly spaced in between this range namely 45, 55 and 65% were used. This would allow a more accurate identification of the transition to a smaller range of humidity's.

Test	Condition	Concentration %	Temp °C	RH %
1	Red FM	35	10	45
2	Red FM	35	10	55
3	Red FM	35	10	65
4	Red FM	35	10	45
5	Red FM	35	10	55
6	Red FM	35	10	65

Table 13 test matrix to explore humidity transitions

Friction results are shown in Figure 99 and it can be seen that friction is staying low at all three humidity's. In conjunction with results from series 1 the transition point can now be said to lie within a more accurate range of 40-45% RH. (i.e. in series 1 friction increased at 40% RH but will stay low at humidity's above 45%).

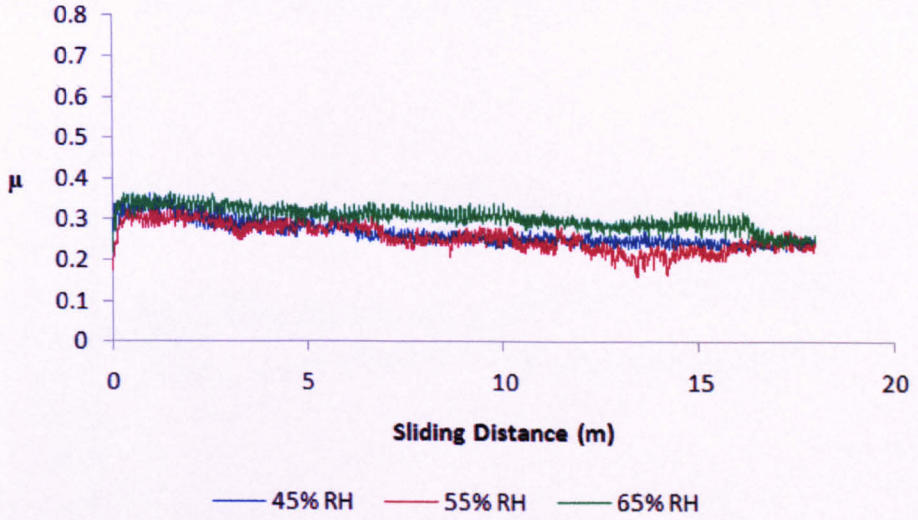

Figure 99 friction plots for test H1, H2 and H3 at a concentration of 35%, 10°C and varying humidity

6.3.6.2 Investigation of Oxide Transition

Series 1 and series 2 data was combined and revealed an oxide dependant transition. A series of tests were designed to explore this further and more accurately locate the transition point. Table 14 shows a matrix of the tests.

Test	Condition	Concentration %	Temp °C	RH %
1	Red FM	37	10	40
2	Red FM	40	10	40
3	Red FM	43	10	40
4	Red FM	37	20	40
5	Red FM	40	20	40
6	Red FM	43	20	40
7	Red FM	37	10	40
8	Red FM	40	10	40
9	Red FM	43	10	40
10	Red FM	37	20	40
11	Red FM	40	20	40
12	Red FM	43	20	40

Table 14 tests to explore the oxide transition seen in the initial tests

Figures 100 and 101 show the friction plots of the oxide investigation at 10 and 20°C respectively.

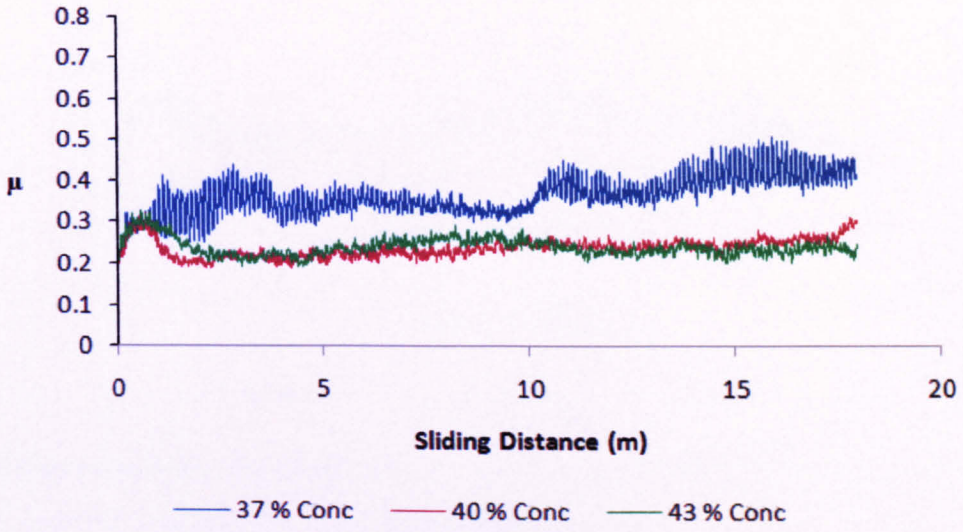

Figure 100 friction plots for test O1, O2 and O3 at a humidity of 40%, 10°C and varying iron oxide concentration

Results from series 1 and series 2 showed a transition in FM performance between oxide concentration levels of 35% and 45% at 10°C whereby the friction stayed low at 45%. Figure 100 shows that the friction also stayed low at 40 and 43% concentration, but started to rise at 37%. The oxide transition at 10°C can now be more accurately identified at being between 37 and 40% of red iron oxide concentration. No transition had been seen, however, at 20°C during the initial tests, even though there was a large range between the concentration levels (25 and 45%). It was decided to explore further within this range. Results shown in Figure 101 show that the friction stays low at approximately 0.25 throughout the entire range of concentrations tested at 20°C. Test results at 10°C show that friction starts to rise at lower concentrations of iron oxide and thus it can be proposed that at 20°C the friction may start to rise at a concentration below 25%. More tests would be required to show this; however, if this were to hold true then it could be shown that the effect of increasing temperature would be to decrease the concentration at which oxide transition occurs.

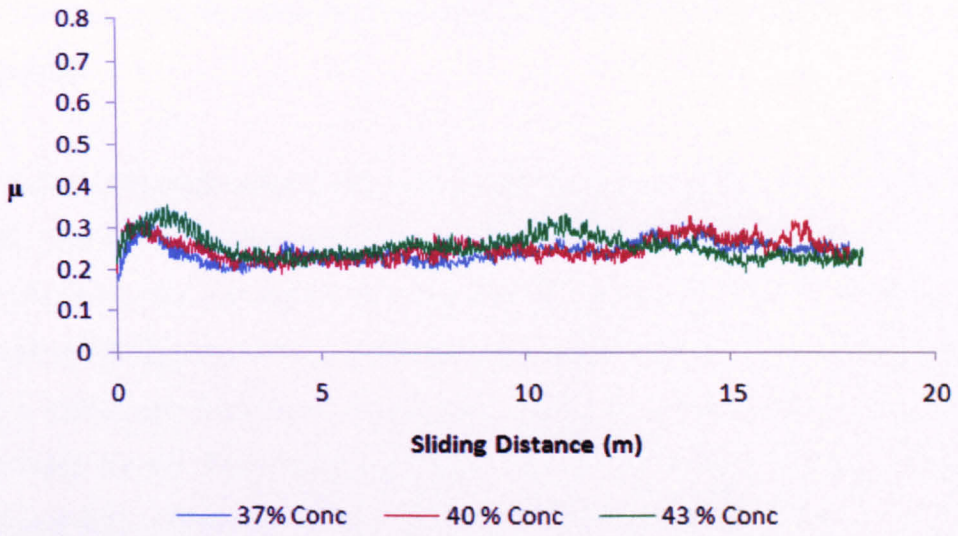

Figure 101 friction plots for test O4, O5 and O6 at a humidity of 40%, 20°C and varying iron oxide concentration

6.4 Discussion

A large amount of data has been generated in these tests and their results are discussed in the sections below. It should be noted that generally the friction coefficients seen in these POD tests are lower than those seen in the field [Harrison, 2002]. This has been seen with previous POD tests [Lu, 2005] and was attributed to the lower speeds, pure sliding and lower roughness's used in the POD tests.

6.4.1 Friction Data

The reference tests were done to accompany and validate the original tests (series 1 & 2). They show the difference between a dry (i.e. 100% Oxide) and a pure friction modifier contact at the 3 different humidity's; 40, 70 and 90%. Humidity has the largest effect on the 100% oxide case as can be seen in figures 81-83 showing an inverse relationship between friction and humidity. The friction at the end of the test is 0.7 at 40% RH, 0.55 at 70% RH and 0.50 at 90% RH. This relationship also correlates with the original data. Pure FM cases do not seem affected by humidity and stay steady at approximately 0.2, rising in the cases of 40 and 90% to 0.3 at the end of the tests. Figure 79 shows how the pin has worn straight through the oxide layer. It was observed during the testing that this happened as soon as the test was started meaning that what is being observed in these tests is a steel on steel contact

not steel on iron oxide. In this case the iron oxide may not have adhered to the disc surface as it was too smooth.

Tests from series 1 were all carried out at a fixed temperature of 10°C and iron oxide to FM ratio of 35%. The most obvious trend from these charts is the effect which humidity has on the friction. For both the red and black oxide the friction would remain steady at the higher humidity's (70 & 90%) yet would rise for tests at the lower humidity. Figures 84 and 85 also highlighted a difference between red and black oxide. Results for black oxide tend to be higher than those for red. For example at higher humidity's friction is in the range of 0.20 – 0.25 for red and 0.25 – 0.30 for black. This represents a significant shift of 0.05. Friction data for pure friction modifier (i.e. friction modifier with no oxide added) was obtained from the GDOES preparation and gave an average value of 0.24 at 70% RH as shown in Figure 102.

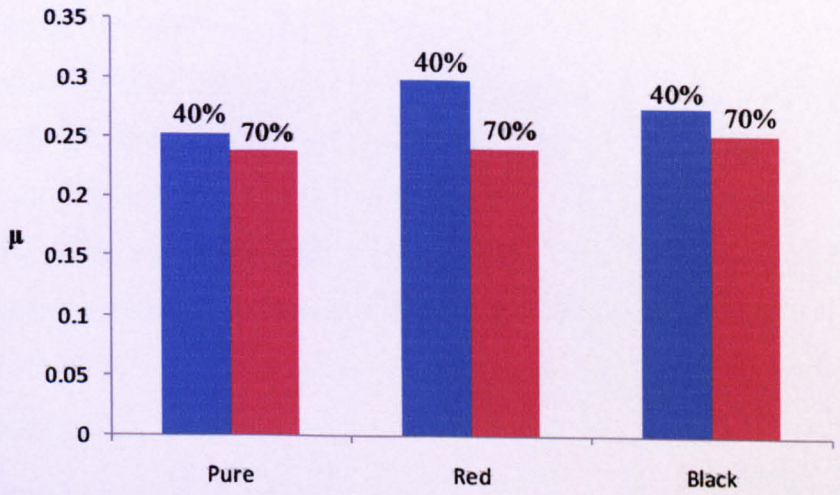

Figure 102 comparison of pure-FM friction (from tests run for GDOES analysis) with red and black-FM data from friction tests under varying humidity and 10°C

Observations showed that the friction modifier would dry out during the tests at 40% humidity, but would remain wet for tests at 70% and 90%. This can explain the difference in behaviour at different humidity's as while the film is still wet it can seep back into the contact and hence it remains effective. Conversely as the film dries no seepage can occur and the film will be worn from the wear track, leading eventually to metal-on-metal contact. This can be seen in Figures 84 and 85 where high friction is reached. Figure 103 shows a chart created using data from a Psychrometric chart which can help explain what we see Figures 84, 85 and 86. The chart shows how the humidity ratio changes with relative humidity, RH, for 10 and 20°C (humidity ratio is the mass (grams) of water vapour in the air per gram of dry air).

Figure 103 shows that there is doubling in the ability of the air to carry water vapour with an increase in its temperature from 10 to 20°C. At the beginning of each test the friction modifier will have a fixed water content which is independent of humidity or temperature. However, the surrounding air's water content will vary with temperature and humidity. It is the ratio between the water in the air and in the friction modifiers which determines if the FM dries or remains wet. At 10°C there is relatively little water in the air compared to that in friction modifier. Hence, water will evaporate to the air, drying the FM/oxide mixture. At the higher temperature there is an effective doubling of the air's water content relative to the fixed amount of water in the FM. Therefore there is a slower evaporation rate from the FM and the film will remain wetted for longer.

This holds true if there is a concentration of iron oxide in the mixture of 35% or less. However, series 2 results indicate that at a concentration of 45% the film does not dry regardless of temperature (see Figure 87). This suggests that iron oxide has the ability to retain water within the FM, slowing the evaporation/drying rate significantly. Figure 88 shows how the rate of increase in friction is inversely proportional to oxide concentration. At a concentration of 45% there is no rise in friction for the duration of the test. This may indicate a turning point where any further increase in iron oxide concentration inhibits the effects of environmental factors on the drying time of the friction modifier.

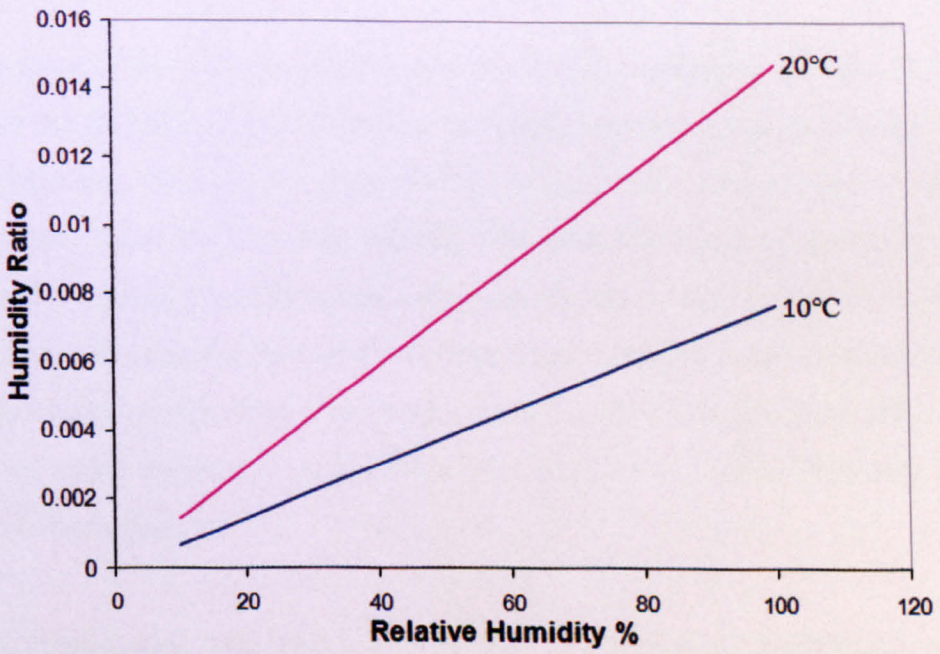

Figure 103 change of humidity ratio with RH data used from a Psychrometric chart

This may not mean, however, that the longer the friction modifier has remained effective in these tests the better it will perform in the field. When applied in the field the friction modifier will only be liquid as it is being spread down the track by a passing locomotive. It is once the friction modifier has dried, forming a thin "re-engineered" third-body on the rail head, that it becomes effective providing a controllable friction coefficient with a desired range of 0.3 - 0.4 [Lu, 2005]. Thus results, shown in Figures 84-88, showing a steady friction coefficient may not be beneficial, as this means the film is remaining wetter for longer and hence, in the field, would not yet be effective. So such conditions where we have a steady friction throughout the duration of the test would actually be detrimental on the friction modifier's performance. For example an FM subject to high humidity and high levels of railhead debris will have a retarded drying rate leading to possible situations where it may be spread over too large an area too thinly or failing to dry at all. In any case it will take longer for the friction modifier to become effective at these conditions.

Results also show that friction levels with black oxide in the mix are generally 0.05-0.1 friction coefficient points higher than those for red oxide at the corresponding humidity. In Figure 85 the 40% line for the black oxide test also rises much faster than red oxide at the same conditions. Black oxide also levels out at a friction coefficient of 0.7, one friction coefficient point higher than red oxide. This is thought to be attributable to the differences in microscopic structure between the two types of oxide particles.

Figure 102 compares from Series 1 and 2 and friction data gathered for pure-FM during the preparation of the GDOES analysis samples. A common theme is that the friction is lower at the higher humidity. This shows that friction is inversely proportional to humidity, a phenomenon also show by Olofsson [2004]. The GDOES sample preparation tests were relatively short in comparison and hence, data from the main friction tests was used from the initial 30 second period at the start of the test and then averaged to give the values in Figure 102; thus allowing a comparison to be made. What is also noticeable from this chart is that the addition of oxide increases friction for a humidity level of 40%. However, at 70% the difference is less obvious.

Part of this investigation was also to investigate the effects of tunnel and underground operating conditions typically 10°C and 70% RH which were replicated in Series 1 tests: 1.3,

1.4, 1.9 and 1.10. Friction data for these tests (see Figures 84 and 85) was relatively low with averages of 0.21 for red oxide and 0.28 for black oxide. However, these values are not reflective of operating friction, but are hence, indicative of drying time. In all tests performed at 10°C and 70% RH the film remained wet for the duration of the test. Thus indicating that Keltrack© may not dry fully under these conditions and hence be less effective.

6.4.2 GDOES Analysis

Data from the GDOES analysis is shown in figures 90-95. The first aspect to be analysed was the depth to which the disc surfaces had been modified from their "before test states". Steel specimens were used in this case and hence, the bulk material was Iron, Fe, with the addition of other chemicals mainly: Manganese, Chromium and Carbon. Six samples were analysed, with the concentration of Fe (bulk material) levelling out at approximately 97%. The depth of surface modification was therefore measured by the depth at which Fe became 97% of the elements detected. This depth is shown in Figure 104 for all six cases.

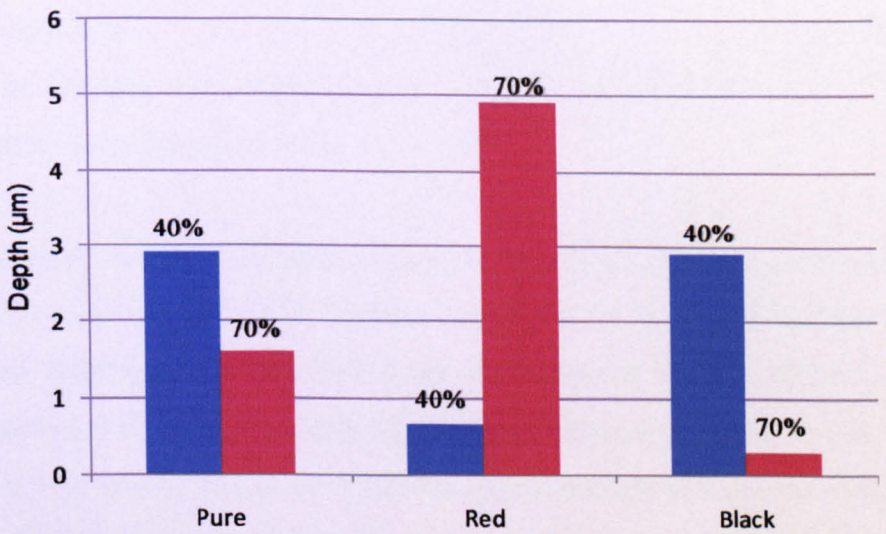

Figure 104 depth from surface modification of test discs for 40 and 70% relative humidity

Almost identical depths of surface modification were observed at the lower humidity for pure FM and FM mixed with black oxide at a depth of just below 3 µm. For the same humidity however, FM mixed with red oxide gave a much shallower depth at just over 0.6 µm below the surface. This pattern however, is reversed for tests at the higher humidity where samples prepared with red oxide give the greatest depth of modification at 4.9 µm. It is interesting to

see how the roles of black and red-FM are reversed with a change in relative humidity. The other main constituents of the base metal (Manganese, Carbon, Silicon and Chromium) all follow a similar pattern to the Iron, and level out early on at values between 1% and 0.1% by weight.

The GDOES charts also show a positive correlation between humidity and the thickness of the oxide layer on the disc surface. The same observation has been made by Olofsson, [2007]. This can be seen in the charts for pure and red-FM, see Figures 90-93. In both cases there is a clear trend for the Oxygen level to tail off at a shallow depth of 12 μm for pure and 3 μm for red-FM for samples prepared at 40% RH. With samples prepared at 70% however, the Oxygen levels out to the end of the test with minimum depths of 22 μm for pure and 20 μm for red FM. The change in depth of oxide layer is greater with the presence of red iron oxide as compared to pure FM. It is in this observation that we witness another trend reversal with black iron oxide. In this case the deepest oxide layer is for the sample prepared at the lower humidity and the shallowest at the higher humidity. Hydrogen also follows a similar pattern to Oxygen, with a positive correlation between humidity and depth of layer for all six samples. The main bulk of Hydrogen and Oxygen will arise from the water content of the friction modifier. Oxygen will also be present in the Iron Oxide and from the natural oxide layer which will have formed on the disc.

Sodium (Na) seemed to follow a general pattern for all the samples except red oxide/FM generated at 70% RH. At 40% RH Sodium started below 0.1% by weight and was not detected beyond depths of 2–5 μm below the disc surface. For the higher humidity, the amount of Na detected at the surface was significantly higher at just over 0.1 for pure and red oxide/FM and 0.7 for black. The level of Sodium at the surface of the discs was much higher for black oxide/FM for both humidity's compared to either pure or red. Both pure and black oxide finished early at 3.4 and 0.3 μm respectively. However, Sodium in the red oxide sample was detected up to 19.5 μm.

A trend was also noticed between levels of Phosphorus detected and humidity. At 40% RH Phosphorus levels at the surface were 0.34 and 0.29 by weight % for pure and black oxide/FM respectively. However, for red oxide/FM this starting level was more than double this at 0.7%. A similar pattern was also observed in the finishing values with 0.03% for both

pure and black oxide/FM, and 0.09% for the red oxide/FM. At 70% the finishing value of each of the samples was almost equal around 0.01%. However, no correlation was seen in the surface values for samples prepared at the lower humidity with values of 0.2%, 0.8% and 1.7% for pure, red and black-FM respectively.

The levels of Nitrogen detected seem to be uninfluenced by the presence or type of oxide for samples prepared at the lower humidity. Surface and end values are very similar for all three FM types. Conversely, at the higher humidity the red-FM there is slightly less Nitrogen detected at 0.9% however, the end value is more than double that seen at 40% RH.

Calcium was present in all of the samples but in much smaller amounts than the other elements. At the low humidity surface Calcium levels started between 0.003–0.006% by weight. Calcium was detected through to the end of the test for both pure and black oxide/FM at depths of 14.3 and 13.6 μm respectively. This was not the case for the red oxide/FM where calcium was detected only to a depth of 1.1 μm. This phenomenon was reversed for the higher humidity with Calcium being detected to only shallow depths for pure and black oxide/FM, but being detected thorough the duration of the test for red oxide/FM.

It is quite clear that surface modification of the disc is strongly influenced by different atmospheric and contamination conditions. Modification of the rail surface is the mechanism by which Keltrack® works. Further investigation is required on the effect of this surface conditioning on the frictional properties of the rail when friction modifiers are not in use, i.e. how does rail that has been conditioned in this way behave when there is contamination (e.g. water, leaves, oil etc) compared to that of a rail which has not been treated with friction modifier. Red oxide is the main constituent of railhead rust and thus it can be assumed that tests with red oxide/FM are the closest representation of a field situation. It has been shown that the depth of surface modification is more than 5 times greater at 70% RH than at the lower humidity. Thus it may be concluded that tunnelled rail treated with Keltrack® has a much different surface compared to a rail which is situated in the open.

6.4.3 Transition Investigation

6.4.3.1 Humidity Transition Tests

Results of the humidity transition tests are shown in Figure 99. These tests were done to explore the transition from low friction at 70% RH and high friction at 40% RH as identified in the initial tests and shown in Figure 84. This range dictated the humidity values used in the humidity transition tests namely 45, 55 and 65% RH. These tests would allow the transition from high to low friction to be more precisely identified. As can be seen in Figure 99 the friction stayed in the low range (0.2 – 0.3) at all three humidity levels. It can now be concluded from these results that the transition lies somewhere between 40 and 45% RH.

6.4.3.2 Oxide Transition

These tests were designed to explore the transition seen in Figure 88. The chart clearly shows a trend of rising friction with lower iron oxide/FM ratios. At a ratio of 45% the friction stays in the low range for the duration of the test. However, at 35% concentration the friction starts to rise during the test. Concentrations of 37, 40 and 43% were chosen to explore this transition further, at two temperatures of 10 and 20°C. Figure 100 shows results at 10°C and it can be seen that at a concentration of 37% the friction rises during the test however, at a slower rate than seen in the initial tests. Figure 88 shows that the rate of increase in friction seems to be inversely proportional to the concentration. This confirms that a transition exists between 37 and 40% concentration at 10°C. Figure 101 shows the tests at 20°C where friction remains low regardless of concentration. This was also seen in the initial tests for the same temperature, but at concentrations of 25 and 45%, see Figure 105.

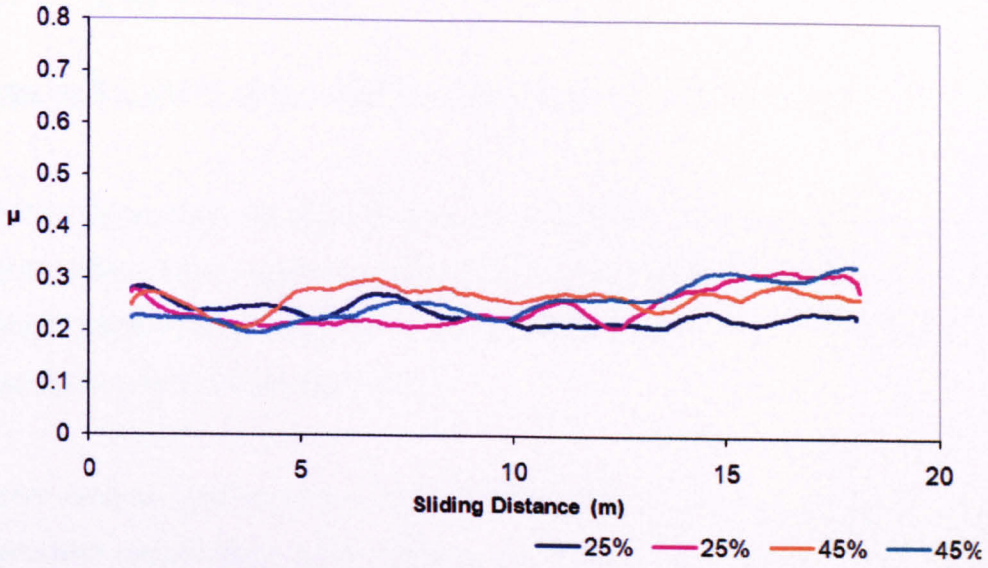

Figure 105 initial series 2 friction plots for tests 2, 4, 6 & 8 at 20°C and 40% RH and varying oxide concentration

This shows that temperature has a stronger influence on the friction modifier than concentration.

Chapter 7: Conclusions

7.1 Effects of Third Bodys within the Wheel/Rail Contact

This review has shown that contamination of the wheel/rail contact can be present in the form of solid particulates, water, grease or oil. There is also an increasing uses of man-made products which are deliberately applied to the wheel/ rail contact to control friction and also combat other issues such as wear and noise.

Solid particles such as sand or ballast can become entrained into the wheel/rail contact. The immense pressure causes them to be crushed into smaller fragments. These pass into the contact and damage the running surfaces either by a process of third body abrasion or fatigue. This can lead to excessive wear. However, sand can restore adhesion to safe operating levels (above 0.1) in situations of low adhesion.

Liquids on the railhead can form a thin separating layer between the wheel and rail when run over. The amount of friction/traction reduction will depend upon the thickness of this layer which will be a function of the speed of the train, the amount of slip in the contact, the combined roughness of wheel and rail and the viscosity of the fluid. It has been seen that water causes a reduction in friction/traction; however it is generally not severe enough to affect operation i.e. above 0.1. The presence of lubricating grease or oil, however, can cause friction/traction to drop to an unsafe level i.e. below 0.1.

The one exception to this observation is the presence of leaves on the track. This solid contaminant can act as a lubricant and reduce friction to unsafe levels (as defined above). It has been shown that there is an apparent chemical reaction between the rail steel and water soluble components of the leaf resulting in a highly durable very low friction solid film on the surface.

Trying to model the effects of these contaminants, in terms of traction, wear, and fatigue is difficult. It is clear from this review that the majority of the available knowledge has been gathered from physical testing either in the field or laboratory.

Friction modifiers have become more widely used as a way to control friction/traction, wear and other wheel/rail related problems. Controlling all of these factors, however, is challenging as they are subject to a great many influencing parameters.

It was clear from reviewing the literature that some gaps in the knowledge of contamination and friction modifiers within the wheel/rail contact exist. Most of the current techniques for the measurement of friction on the railhead can be impractical and can have significant costs. There is also no transferability between the lab and field i.e. there is currently no tool that is suitable for use in both situations.

In the field of friction modifiers there seems to be a lack of scientific knowledge on the workings and effects of these products. These products are increasingly being used by rail networks around the world. However, no study has been performed on how their performance is affected by changes in atmospheric conditions as there will be between different countries.

There has also been no study on how these friction modifiers affect the surface of wheels and rails both chemically and in terms of wear.

There are also new traction enhancing products which are designed to combat low adhesion situations such as leaves on the line. The friction performance of these products has not been studied and the isolation and wear properties of these products are also unclear.

7.2 Development and Testing of an Alternative Technique for the Measurement of Railhead Friction

Testing contained within this chapter has shown that the pendulum can be successfully tested on rail in the laboratory. Testing suggests that the parameters below are adhered to in order to get repeatable data that coincides with other acceptable sources of laboratory based rail testing.

- The pad to be used for testing is the Four-s type rubber.
- Pad strike length needs to be 12.7 cm as specified by the manufacturer

- It is suggested that an area of 12.7 cm length be marked out on the rail head in order to disperse liquid contaminants evenly.
- Difference between Four-s and TRL readings – softer pad able to deflect more hence hydrodynamic lubrication
- TRL pad may be more suitable for liquid contaminants as results are closer to those seen in twin-disc testing
- TRL pad shows friction coefficient of 1.2 for dry tests. This is an order of magnitude higher than values form twin disc and field testing – not suitable for dry tests
- Pad should be frequently replaced in order that a chamfer does not develop on its trailing edge. As this can significantly affect results
- Contaminants should be represented as close as possible to how they are seen in the field i.e. crushed into thin films
- There is a fixed difference between pendulum results and twin-disc results performed under comparable conditions

Results of field testing with the pendulum show very promising results and there is good correlation between laboratory and field data. The data from rail extracted from the field and tested in the lab is also within good agreement. The initial data from the pendulum matches well with corresponding data from the Salient Systems Tribometer. The pendulum is also suited to measurement of localised adhesion spots owing to its relatively short measurement length (12.7 cm). This study has shown that the pendulum rig is a versatile, reliable and practical tool which can be used successfully both in the lab and field. Field trials have also shown that the pendulum is highly suited as a rail maintenance tool.

7.3 Development of a Standard Test Method to Measure Performance of Traction Gels

A technique has been developed for the standard test to measure the performance of traction enhancers in terms of friction. Traction enhancers consist of sand particles suspended in a water based gel and are designed to restore traction levels in cases of adhesion loss. The technique was developed using the University of Sheffield Rolling Sliding (SUROS) tester. Findings of this study are as follows:

- Tests have been carried out to investigate the effect of particle size on the performance of traction enhancers using a twin-disc machine
- Two series of tests were run. Series 1 focused on a fixed mass of traction gel added to the contact; Series 2 aimed to look more closely at the effect of particle size by adding a fixed number of particles to the contact
- A technique has been developed for generating a crushed leaf layer on the twin-disc specimens
- Each traction enhancer's performance was assessed by the rate at which it removed the leaf layer. This was done by monitoring friction rates
- Series 1 results showed that the traction enhancer containing 212 μm particles gave the highest leaf layer removal rate while also showing the least amount of disc surface damage
- Series 1 results showed that 800 μm particles showed the opposite with the lowest rate of leaf layer removal and greatest amount of surface damage caused
- Series 2 results showed that 600 μm particles showed the greatest rate of leaf layer removal with moderate surface damage.
- Series 2 results showed that 212 and 800 μm particles gave almost identical performance in terms of leaf layer removal (less than 600 μm), however , 800 μm again showed a great amount of surface damage

A standard methodology has been developed for the testing and assessment of friction modifiers and traction enhancers.

7.4 Friction, Isolation and Wear Assessment of Traction Enhancers using Standard Test Method

A technique has been developed using the Sheffield University Rolling Sliding (SUROS) test rig to measure the electrical isolation and wear properties of traction enhancing products. These consist of sand particles suspended in a water based gel. Tests were run according to the specification developed in chapter 4. Two variations of test were run: those using a fixed volume of the gel and tests using similar amounts of particles between tests with varying particle size. Specific findings of this study are:

- Lower viscosity gels seem to exhibit poorer traction performance traits as higher viscosity ones such as those tested in the previous chapter.
- Traction increases were almost half of what was seen in the development of the test – this could be due to the lower viscosity of the gel but could also be attributable to the more realistic leaf layer used for the tests in this chapter
- Wear rates measured seemed to show no correlation to particle size. The 600 μm particle gel did show very wide variations in wear rate compared to other particle sizes for both the fixed volume and fixed particle cases. This cannot be explained at the time of writing as it seems isolated to one particular size of particle in the middle of the range tested.
- It is proposed that a third body abrasion wear mechanism is occurring in these tests with evidence shown from wear data and post test observations of the discs. Wear data also confirms that there is a mass transfer process happening during the tests and that these two processes may be occurring simultaneously
- Leaf layer and gel seem to produce significantly lower wear rate over that of sand alone
- It is suggested that tests need to be significantly lengthened so that errors in mass reading are insignificant compared to the resulting increased wear
- The highest level of impedance was seen with a 212 μm gel at approximately 1.5 Ω with the leaf layer showing the next highest at 1.3 Ω. All of the traction enhancers surprisingly gave impedances below this in a range of 0.59 – 1.2 Ω. These levels of impedance are not deemed by the author to be high enough to prevent shunting of this particular simulated track circuit, i.e. with a simulated detector resistance of 10 Ω. Thus if a contaminant/friction modifier presents an impedance lower than this value sufficient current should still be shunted through the axle as to cause a track section to be signalled as occupied
- It is seen that there is significantly higher impedance in the first 5 seconds of the test where the traction curves show dominance by gel as opposed to sand. Between 5 and 10 seconds the impedance falls close to uncontaminated levels. Coincidentally this is the point where the gel starts to evaporate. It therefore may be the case that the gel caused more impedance than the sand
- General impedance levels were not considered high enough for metal shot to be added to the

- No strong correlation was observed between particle size showing that the contact is never completely saturated with sand and there is always sufficient metal-to-metal contact to aid conductance.

7.5 Investigation of Influences of Atmospheric Conditions on Performance of Friction Modifiers

An investigation has been made into how the performance of railhead friction modifiers is affected by changes in atmospheric condition and varying debris levels. This was carried out on a pin-on-disc device with an attached atmospheric chamber. Part of the focus of these tests was also to observe the behaviour of friction modifiers when used in tunnels such as underground networks. Tunnels can provide a very unique set of conditions with low temperatures typically 10°C and high humidity typically 70%.

Glow Discharge Optical Emission Spectroscopy analysis was employed to detect surface modifications of the test specimens as a result of the friction modifier.

Tests were broken down into two series to expand the number of conditions which could be tested.

Series 1 data highlighted an interesting phenomenon. At the higher humidity's the friction would stay low for the duration of the test. However, at 40% humidity the friction started to rise to dry levels at approximately the 4 meter mark. This was due to the greater amount of water vapour in the air at the higher humidity's relative to the amount of water in the friction modifier. This slowed down the rate of water evaporation from the friction modifier (FM) meaning it remained wet and hence could provide a film between the pin and the disc for longer.

Magnetite (Fe_3O_4) (black oxide) in the FM at 40% RH gave higher final friction results and caused a greater rate of friction increase than with Haematite (Fe_2O_3) (red oxide). This could be down to the fact that Magnetite particles are larger than the Haematite.

The presence of both oxide types in the friction modifier raised the friction seen over that of friction modifier alone.

Iron oxide concentrations used in the tests were 25%, 35% and 45%. Series 2 tests explored the effects of oxide content in the FM on its performance. It showed that the influence that temperature has on friction becomes less with an increasing oxide content, i.e. when there was 25% oxide in the friction modifier friction rose to dry levels at 10°C, but remained low at 20°C. However, at a concentration of 45% friction remained low at both temperatures.

Results shown in Figure 101 show that the friction stays low at approximately 0.25 throughout the entire range of concentrations tested at 20°C. Test results at 10°C show that friction starts to rise at lower concentrations of iron oxide and thus it can be proposed that at 20°C the friction may start to rise at a concentration below 25%. More tests would be

shows that the depth of surface modification is much greater at 70% humidity (typical tunnel conditions) than at 40% (typical outdoor humidity) by a factor of more than 7. Thus it can be seen that in situations where friction modifiers are used in tunnels the rail will have a vastly different surface condition than an open air situation. Further investigation is needed to explore this effect of surface modification and how it affects friction in a post-treated state i.e. a rail which has been treated with FM but is then subsequently allowed to run without.

This work has shown that friction modifiers are sensitive to changes in atmospheric condition and railhead contamination. This poses a problem as these products are distributed worldwide. Work here has shown that friction modifiers may need to be chemically tailored to specific operating climates according to the findings here.

Chapter 8: Recommendations

8.1 Recommendations for Rail Operators and Friction Modifier/Traction Enhancer Manufacturers

Work in chapter 3 has shown that the pendulum rig can be reliably used to measure friction on the railhead both in the laboratory and in the field. Data from the pendulum compares favourably with data from alternative methods of friction measurement. The pendulum is also suited for measurement of localised sites of adhesion loss and is therefore recommended for use by rail network operators for investigation of such phenomena.

There are a wide variety of products for use in the wheel/rail contact such as friction modifiers, friction enhancers and lubricants. New products can be used on the railway without having to pass any prior test or receive certification. The first time these products are usually tested is on the railway during active service. This can represent a significant safety issue; as how will the product affect: braking, wear, RCF, isolation, etc. Work in chapters 4 and 5 show that a twin-disc tester can be used for testing of these products. A twin-disc rig can measure the above mentioned parameters and a conclusion as to the track worthiness can be drawn.

It has been shown that the function and performance of friction modifiers can vary greatly due to changes in atmospheric condition. Levels of railhead contamination can also have a profound effect. Use of friction modifiers for management of the wheel/rail contact is becoming accepted worldwide. Temperatures and humidity's will differ from country to country and will be affected by seasonal fluctuations. It is recommended that friction modifiers be tailored for specific working environments and possibly for seasonal changes. Work in chapter 6 also showed that the use of friction modifiers can significantly alter the surface chemistry of the wheel and rail when used under tunnel conditions. This surface modification needs further investigation.

8.2 Further Research

A number of recommendations have been deduced from this study and are also discussed in this section.

8.2.1 Twin-disc Investigation of Various Species of Leaf Layers

It is recommended that there should be a study on creating leaf layers using different species of leaf on the SUROS machine. It would be interesting to see the frictional and isolation properties of these different leaf layers. A catalogue of leaf types and their properties could be collated which may revel which leaves cause the greatest impedance, greatest amount of traction loss or durability, and those which do not pose a problem. This information may be useful in the effort against the "leaves on the line" problem e.g. only problematic species of tree need to be felled or controlled by the line side. In this study Sycamore leaves were used due to the abundance in the local area and convenience to stockpile so they can be used regardless of season. Cann [2006] identified two water soluble components of a leaf which are believed to contribute to their low friction, namely pectin and cellulose. These chemicals were found to chemically react with the rail steel giving the blackish hard wearing layer [Cann, 2006]. It is highly probable that different leaf species will contain different amounts of these chemicals and therefore show different properties.

It is also proposed that a wet leaf layer would present a much lower traction coefficient than seen here. Testing of a dry leaf layer which is then wetted may also cause a significant rise in impedance over a dry leaf layer.

8.2.2 Further Testing of Traction Enhancing Products

The traction enhancers should also be tested on their own i.e. without a leaf layer. This would explore two avenues: 1) the impedance due to the traction enhancers alone and 2) wear solely due to the product. It is estimated from the results of this test that impedance due to the gels alone would be lower than that of leaf and gel combined as it is shown in Figure 67; (for every case excluding the 212 μm fixed particle) the impedance due to the traction enhancers with leaf layer is lower than the impedance for leaf layer alone. The biggest difference may be seen in the wear rates of the discs. This is because (it is proposed) the leaf layer is providing a low friction sacrificial coating on the discs. Hence, a majority of the damage caused by the sand particles could be subjected to the leaf layer rather than the disc surface. This could also partly explain the vast difference in wear rates seen between these tests and similar tests in Lewis [2006b]. An absence of the leaf layer may also affect the third body abrasion process that was witnessed in these tests.

Additional tests with the traction enhancers could also include mixtures with: water, oil and other friction modifiers to simulate cross contamination between natural contaminants and other railway products.

8.2.3 Upgrade of Isolation Rig

It is suggested that an upgrade of the isolation rig and track circuit is made so that phase angle can be measured. In A.C. circuits the phase difference between the voltage and current are affected differently by different components in the circuit. As illustrated in Figure 107, a capacitor will cause the current to lead the voltage. An inductor will have the opposite effect and cause the voltage to lead the current. A resistor will have no effect leaving the voltage and current in phase with each other. The total reactance, X (opposition to current flow due to capacitance and inductance in the circuit) in the circuit is calculated by deducting the reactance due to capacitance from the reactance due to inductance ($X = X_L - X_C$). Both inductive and capacitive reactance is calculated by equations 11 and 12. It can be seen with the aid of figure 106 that the phase angle will be determined by whichever value dominates the circuit either inductance or capacitance. Hence, if the phase angle can be measured, more information can be determined regarding what component is influencing the impedance most. Track products such as greases and friction modifiers could then be chemically tailored to counteract their reactance and hence overall impedance properties.

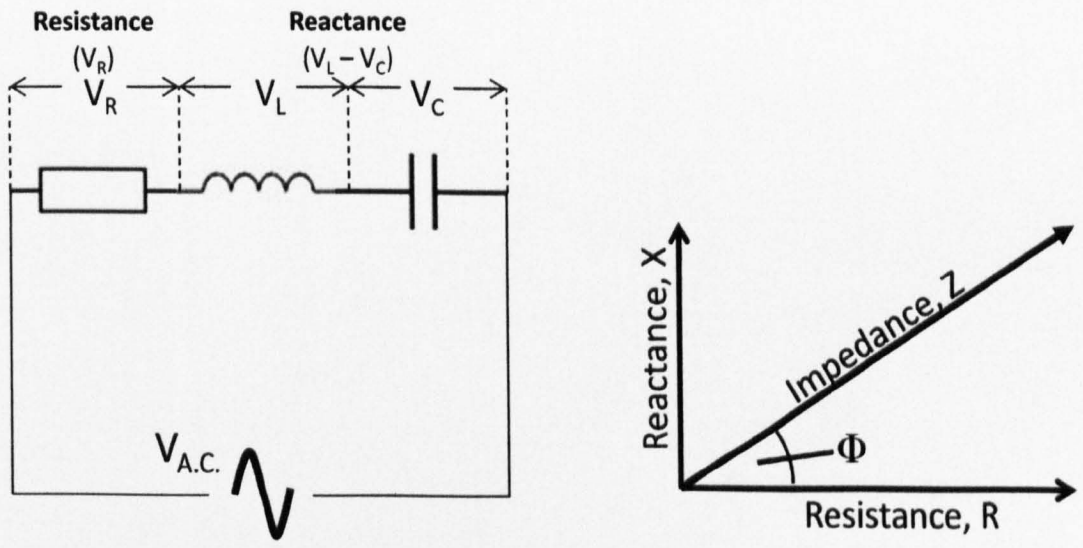

Figure 106 illustration of electrical impedance

$$X_L = 2\pi fL \quad (11)$$

$$X_C = 1/(2\pi fC) \quad (12)$$

Where f is the circuit frequency (Hz), L is the inductance (Henrys) and C is the capacitance in the circuit (Farads).

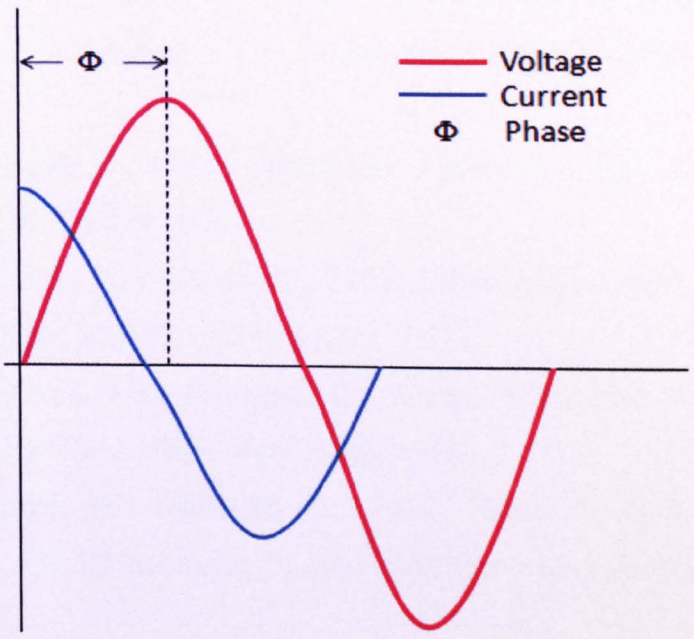

Figure 107 illustration of A.C. current and voltage flowing through a capacitor

References

AS/NZS 4586:2004, Slip resistance classification of new pedestrian surface materials

Arias-Cuevas, O., Li, Z., Lewis, R., Gallardo-Hernandez, E A., 2010a. Rolling–sliding laboratory tests of friction modifiers in dry and wet wheel–rail contacts. Wear, Vol. 268, pp 543-551

Arias-Cuevas, O., Li, Z., Lewis, R., 2010b. Investigating the Lubricity and Electrical Insulation Caused by Sanding in Dry Wheel–Rail Contacts. Tribology Letters, Vol. 37, pp 623-635

Beagley, T M., Pritchard, C., 1975a. Wheel/Rail Adhesion – The overriding influence of water. Wear, Vol. 35, pp 299 -313

Beagley, T M., McEwen, I J., Pritchard, C., 1975b. Wheel/Rail Adhesion – The influence of rail head debris. Wear, Vol. 33, pp 141-152

Beagley, T M., McEwen, I J., Pritchard, C., 1975c. Wheel/Rail Adhesion – Boundary lubrication by oily fluids. Wear, Vol. 31, pp 77-88

Bergseth, E., Torbacke, M., Olofsson, U., 2008, "Wear in Environmentally Adapted Lubricants with AW/EP technology", *Journal of Synthetic Lubrication*, Vol. 25, Issue 4, pp137-158

Broster, M., Pritchard, C., Smith D A., 1974. Wheel/Rail Adhesion – Its relation to contamination on British railways. Wear, Vol. 29, pp 309-321

Bogdanski, S., Olzak, M. and Stupnicki , J., 1998. Numerical modelling of 3D rail RCF squat type crack under operating load. Int. J. Fatigue Fracture Eng. Mat. Struct. 21, pp 923–935

Bolton, P J., Clayton, P., 1984. Rolling Sliding Wear Damage in Rail and Tyre Steels. Wear, Vol. 93, pp 145-165

Bower, A F., 1988. The Influence of Crack Face Friction and Traped Fluid on Surface Initiated Rolling Contact Fatigue Cracks. Trans. ASME, Journal of Tribology, Vol. 110, pp 704-711

Bower, A F., Johnson, K L., 1991. Plastic flow and shakedown of the rail surface in repeated wheel-rail contact. Wear, Vol. 144, pp 1-18

Brookes, R., 2003. Wheel Rail Interface Technology Management; Autumn Performance Trials. Network Rail

BS 7976-1:2002, Pendulum Testers: Part 1 – Specification

BS EN 13036-4:2003, Road and airfield surface characteristics. Test methods. Method for measurement of slip/skid resistance of a surface. The pendulum test

BS ISO 48:2007, Rubber, vulcanized or thermoplastic. Determination of hardness (hardness between 10 and 100 IRHD)

Cann, P M., 2006. The "leaves on the line problem" – a study of leaf residue film formation and lubricity under laboratory test conditions. Tribology Letters, Vol. 24(2), pp 151-158

Descartes, S., Desrayaud, C., Niccolini, E., Berthier, Y., 2005. Presence and role of the third body in a wheel-rail contact. Wear, Vol. 258, pp 1081-1090

Dwyer-Joyce, R S., Lewis, R., 2003. Wear and Fatigue of Railway Track Caused By Contamination, Sanding and Surface Damage. 6th International Conference on Contact Mechanics and Wear of Rail/Wheel Systems, Gothenburg, Sweden 2003

Eadie, D T., Kalousek, J., Chiddick, K C., 2002. The Role of High Positive Friction (HPF) Modifier in the Control of Short Pitch Corrugation and Related Phenomena. Wear, Vol. 253, pp 185–192

Eadie, D T., Santoro, M., Powell, W., 2003a, "Local Control of Noise and Vibration with KELTRACK™ Friction Modifier and Protector® Trackside Application: An Integrated Solution", *J. Sound and Vibration*, Vol. 267, pp761-772

Eadie, D., Kalousek, J., Chiddick, K., 2003b, "The Role of High Positive Friction (HPF) Modifier in the Control of Short Pitch Corrugations and Related Phenomena", *Wear*, Vol 253, pp185 – 192

Eadie, D T., Elvidge, D., Oldknow, K., Stock, R., Pointner, P., Kalousek, J., Klauser, P., 2006. The Effects of Top of Rail Friction Modifier on Wear and Rolling Contact Fatigue: Full Scale Rail-Wheel Test Rig Evaluation, Analysis and Modeling. Wear, Vol. 265, pp 1222- 1230

Egana, J I., Vinolas, J., Gil-Negrete, N., 2005. Effect of Liquid High Positive Friction (HPF) Modifier on Wheel-Rail Contact and Rail Corrugation. Tribology International, Vol. 38, pp 769-774

Fletcher D. I; Beynon J. H., 2000a, "The Effect of Intermittent Lubrication on the Fatigue Life of Pearlitic Rail Steel in Rolling–sliding Contact", *Proc. IMechE Part F: J. Rail and Rapid Transit*, Vol. 214, pp145-158

Fletcher, D I. Beynon, J H., 2000b. Development of a Machine for Closely Controlled Rolling Contact Fatigue and Wear Testing. *Journal of Testing and Evaluation*, Vol. 28 (4), pp. 267–275

Fletcher, D I., Hyde, P., Kapoor, A., 2006. Investigating fluid penetration of rolling contact fatigue cracks in rails using a newly developed full-scale test facility. Proc. IMechE Part F: J. Rail and Rapid Transit, Vol. 221, pp 35-44

Franklin, F J., Widiyarta, I., Kapoor, A., 2001. Computer Simulation of Wear and Rolling Contact Fatigue. Wear. Vol. 251, pp 949–955

Franklin, F J., Kapoor, A., 2006. Modelling Wear and Crack Initiation in Rails. Proc. IMechE Part F: J. Rail and Rapid Transit, Vol. 221, pp 23-33

Fulford, C R., 2004. Review of low adhesion research. Report published by the Railways Safety and Standard Board

Gallardo-Hernandez, E A., Lewis, R., Dwyer-Joyce, R S., 2006. Temperature in a Twin-Disc Wheel/Rail Contact Simulation. Tribology International, Vol. 39, pp 1653-1663

Gallardo-Hernandez, E A., Lewis, R., 2008. Twin Disc Assessment of Wheel/Rail Adhesion. Wear, Vol. 265 (9-10). pp. 1309-1316

Grieve, D G., Dwyer-Joyce, R S., Beynon, J H., 2001. Abrasive Wear of Railway Track by Solid Contaminants. Proc. IMechE Part F: J. Rail and Rapid Transit, Vol. 215, pp 193-205

Halling, J.. 1975. *Principles of Tribology.* London: Macmillan,

Harrison, H., McCanney T., Cotter J., 2002. Recent developments in coefficient of friction measurements at the rail/wheel interface. Wear, vol. 253, pp 114-123

Hoffmann, V., 1993, "Application of Glow Discharge Optical Emission Spectroscopy (GDOES) to the Analysis of PVD- and CVD-Layers", *Fresenius' J. Analytical Chemistry*, Vol 346 (1-3), pp165-168

Hou, K., KalouseK, J., Magel, E., 1997. Rheological model of solid layer in rolling contact. *Wear*, Vol. 211 (1), pp 134-140

[HSE, 2004] The assessment of pedestrian slip risk—the HSE approach, Health and Safety Executive document, 2004 Locomotives. 12th International Wheelset Congress, China, pp 44-52

Jenks C W., 1997. Improved Methods for Increasing Wheel Rail Adhesion in the Presence of Natural Contaminants. Transit Co-operative Research Program (Transportation Research Board National Research Council), No. 17.Research Results Digest: Washington D.C.,

Jin, X S., Zhang, W H., Zeng, J., Zhou, Z R., Liu, Q Y., Wen, Z F., 2004. Adhesion experiment on a wheel/rail system and its numerical analysis. Proc. IMechE Part J, vol. 218(1), pp 293-303

Johnson, T., 2006. Understanding Aerodynamic Influences of Vehicle Design on Wheel/Rail Leaf Contamination. Rail Safety and Standards Board, Research Program report, Project No. T456

Kalker, J J., 1991. Simulation of the Development of a Railway Wheel Profile through Wear. Wear, Vol. 150, pp 355-365

Kalousek, J., Fegredo, D M., Laufer E E., 1985. The wear resistance and worn metallography of pearlite, bainite and tempered martensite rail steel microstructures of high hardness, Wear, Vol. 105, pp 199 - 222

Kalousek, J., Magel, E., 1997, "Optimising the Wheel/Rail System", *Railway and Track Structure*, January

Kaneta, M., Yatsuzuka. H., Murakami, Y., 1985. Mechanism of Crack Growth in Lubricated Rolling/Sliding Contact. ASLE Transactions, Vol. 28 (3), pp 407-414

Kaneta, M., Murakami, Y., 1987. Effects of Oil Hydraulic Pressure on Surface Crack Growth in Rollin/Sliding Contact. Tribology International, Vol. 20 (4), pp 210-217

Kapoor, A., Franklin, F J., 2000. Tribological Layers and the Wear of Ductile Materials. Wear. Vol. 245, pp 204–215

Kapoor, A., Fletcher, D I., Franklin, F J., 2003. The Role of Wear in Enhancing Rail Life, Proceedings of the 29th Leeds-Lyon Symposium on Tribology, pp 331-340

Kumar, S., Krishnamoorthy, P K., Prasanna Rao, D L., 1986. Wheel – Rail Wear and Adhesion With and Without Sand. Transactions of the ASME: Journal of Engineering for Industry, Vol. 108, pp 141-147

Lewis, R., Dwyer-Joyce, R S., Lewis, J., 2003a. Disc Machine Study of Contact Isolation During Railway Track Sanding. Proc. IMechE Part F: J. Rail and Rapid Transit, Vol. 217, pp 11-24

Lewis, R., Braghin, F., Ward, A., Bruni, S., Dwyer-Joyce, R S., Bel Knani, K., Bologna, P., 2003b. Integrating Dynamics and Wear Modeling to Predict Railway Wheel Profile Evolution. 6th International Conference on Contact Mechanics and Wear of Rail/Wheel Systems, Gothenburg, Sweden

Lewis, R., Dwyer-Joyce, R S., 2004. Wear Mechanisms and Transitions in Railway Wheel Steels. Proc. IMechE Part J: J. Engineering Tribology, Vol. 218, pp 467-478

Lewis R., Dwyer-Joyce R S., 2005. Foreign Particles at the Wheel/Rail Interface. Proceedings of the Conference on Excellence in Railway Systems Engineering and Integration, Derby (UK), 25-26 November 2005

Lewis, R., Dwyer – Joyce, R., 2006a. STLE Handbook of Lubrication Chapter - Industrial Lubrication Practice (Wheel/Rail Tribology). Taylor and Francis Group

Lewis, R., Dwyer-Joyce, R S., 2006b, Wear at the Wheel/Rail Interface When Sanding is used to Increase Adhesion. Proc. IMechE Part F: J. Rail and Rapid Transit, Vol. 220, pp 29-41

Lewis, R., Massing, J., 2006c. Static Wheel/Rail Contact Isolation due to Track Contamination. Proc. IMechE Part F: J. Rail and Rapid Transit, Vol. 220, pp 43-53

Lewis, R., Gallardo, E A., Cotter, J., Eadie, D T., 2009a. The Effect of Friction Modifiers on Wheel/Rail Isolation. Proceedings of the 8th International Conference on Contact Mechanics and Wear of Wheel/Rail Systems (CM2009), Firenze, Italy

Lewis, R., Gallardo-Hernandez, E A., Hilton, T., Armitage, T., 2009b. Effect of Oil and Water Mixtures on Adhesion in the Wheel/Rail Contact. Proc. IMechE Part F: J. Rail and Rapid Transit, Vol. 223(3), pp 275-283

Li, Z., Arias-Cuevas, O., Lewis, R., Gallardo-Hernandez, E A., 2009. Rolling–Sliding Laboratory Tests of Friction Modifiers in Leaf Contaminated Wheel–Rail Contacts. Tribology Letters, Vol. 33, pp 97-109

Littmann, W E., Widner, R L., Wolfe, J O., Stover, J D., 1968. The Role of Lubrication in the Propagation of Contact Fatigue Cracks. Trans. ASME, J. Lubrication Technology, Vol. 90, pp 89-100

Lu, X., Cotter, J., Eadie, D., 2005, "Laboratory Study of the Tribological Properties of Friction Modifier Thin Films for Friction Control at the Wheel/Rail Interface", *Wear*, Vol. 259, pp1262 – 1269

Marshall, M.B., Lewis, R., Dwyer-Joyce, R.S., Olofsson, U. Björklund, S., 2004. Ultrasonic Characterisation of a Wheel/Rail Contact, Proceedings of the 30th Leeds-Lyon Symposium on Tribology, pp. 151-158

Mills, R., Dwyer-Joyce, R.S., Loo-Morrey, M., 2009. The Mechanisms of Pedestrian Slip on Flooring Contaminated with Solid Particles, Tribology International, Vol. 42, pp 403-412

Nagase, N., 1989. A Study of Adhesion between the Rails and Running Wheels on Main Lines: Results of Investigations by Slipping Adhesion Test Bogie. Proc IMechE Part F: Journal of Rail and Rapid Transit, Vol. 203, pp 33-43

Olofsson U., and Dizdar S., 1997, "Surface Analysis of Boundary Lubricated Spherical Roller Thrust Bearings", *Wear*, Vol. 215, pp156-164

Olofsson, U., Sundvall, K., 2004. Influence of Leaf, Humidity and Applied Lubrication on Friction in the wheel-rail Contact: Pin-on-disc Experiments. Proc. IMechE Part F: J. Rail and Rapid Transit, Vol. 218, pp 235-242

Olofsson, U., 2007, "A Multi-Layer Model of Low Adhesion between Railway Wheel and Rail", *Proc. IMechE Part F: J. Rail and Rapid Transit*, Vol. 221, pp385 – 389

Rabinowicz, E., Dunn, L A., Russell, P G., 1961. Study of Abrasive Wear under Three Body Conditions, *Wear*, Vol. 4, pp 345–355

Rowe, C N., Armstrong, E L., 1982. Lubricant Effects in Rolling-Contact Fatigue. J. ASLE, Lubrication Engineering, Vol. 38, pp 23-30

Sawley, K J., 2007. Calculation of Temperatures in Sliding Wheel/Rail System and Implications for Wheel Steel Development. Proc. IMechE Part F: J. Rail and Rapid Transit, Vol. 221, pp 455-465

Sinclair, J., 2004, Friction Modifiers, in Vehicle Track Interaction: Identifying and Implementing Solutions, IMechE Seminar, February 17th

Smith, D A., 2003. Rolling Contact Fatigue: A Review of Current Understanding, Rail Safety and Standards Board, Research Program Report

Stanca, M., Stefanini, A., Faccinetti, A., Gallo, R., 2001. Development of an Integrated Design Methodology for a new Generation of High Performance Rail Wheelsets, 16th European ADAMS User Conference, Berchtesgaden, Germany

Suda, Y., Iwasa, T., Komine, H., Tomeoka, M., Nakazawa, H., Matsumoto, K., Nakai, T., Tanimoto, M., Kishimoto, Y., 2005. Development of On-board Friction Control. Wear, Vol. 258, pp 1109-1114

Sundh, J., Olofsson, U., 2009. Relating Contact Temperature and Wear Transitions in a Wheel-Rail Contact, Proceedings of the 8th International Conference on Contact Mechanics and Wear of Wheel/Rail Systems (CM2009), Firenze, Italy

Tomeoka, M., Kabe. N., Tanimoto, M., Miyauchi, E., Nakata, M., 2002. Friction Control Between Wheel and Rail by Means of On-Board Lubrication. Wear, Vol. 253, pp 124-129

Vasić, G., Franklin, F J., Kapoor, A., Lučanin, V., 2008. Laboratory Simulation of Low-Adhesion Leaf Film on Rail Steel. International Journal of Surface Science and Engineering, Vol. 2 (1/2), pp 84-97

Way, S., 1935. Pitting Due to Rolling Contact. Trans. ASME, Journal of Applied Mechanics, Vol. 2, pp A49-A58

Ward, A., Lewis, R., Dwyer-Joyce, R S., 2002. Incorporating a Railway Wheel Wear Model into Multi-Body Simulations of Wheelset Dynamics. Proceedings of the 29th Leeds-Lyon Symposium on Tribology, pp 367-378

Zhang, W., Chen, J., Wu, X., Jin, X., 2002. Wheel Rail Adhesion and Analysis by using Full Scale Roller Rig. Wear, Vol. 253, pp 82–88